UNIVERSITA' DEGLI STUDI DI PARMA

Dottorato di ricerca in Scienze della Terra

Ciclo XXV

Compressional and extensional tectonics inside collisional belts: the case of the western portion of the Northern Apennines

Coordinatore:
Chiar.ma Prof.ssa Giuliana Villa

Tutor:
Dott. Andrea Artoni

Co-Tutor:
Chiar.mo Prof. Massimo Bernini

Dottorando: Mirko Carlini

Index

1. Introduction

The interplay between extensional and compressional tectonics in orogenic belts is a long recognized and debated topic since the '80s (Burchfiel and Royden, 1985; Crespi et al., 1996; Dewey, 1988; Doglioni, 1994; Hodges and Walker, 1992; Houseman et al., 1981; Malavielle, 1993; Malinverno and Ryan, 1986; Molnar et al., 1993; Platt, 1986; Platt and Vissers, 1989; Ratschbacher et al., 1989; Royden, 1993a; Royden, 1993b; Vissers et al., 1995; Waschbusch and Beaumont, 1996). The attempt to constrain the absolute and relative timing and the mechanisms of these processes led to several models aimed to explain the presence of tensional stresses in compressional mountain belts taking into account different geodynamic contexts. In particular, the most common invoked mechanisms are slab retreat, critical wedge spreading, vertical block extrusion associated with mantle wedges, post-orogenic collapse of thickened continental lithosphere and underplating (Willett, 1999 and references therein). Most of the orogenic wedges in the peri-Mediterranean region are characterized by the coexistence of extensional and compressional tectonics, combined with the emplacement of non-metamorphic and far-travelled/allochthonous tectonic units, located mainly in the foreland areas (e.g., Silesian and Subsilesian nappes in the Carpathians, Roca et al., 1995; Balagne nappe in Corsica, Malaveille et al., 2011; Pre-Alpine nappes in the Alps, De Graciansky et al., 2011; Rodgers, 1997 and references therein) (fig. 1.1).

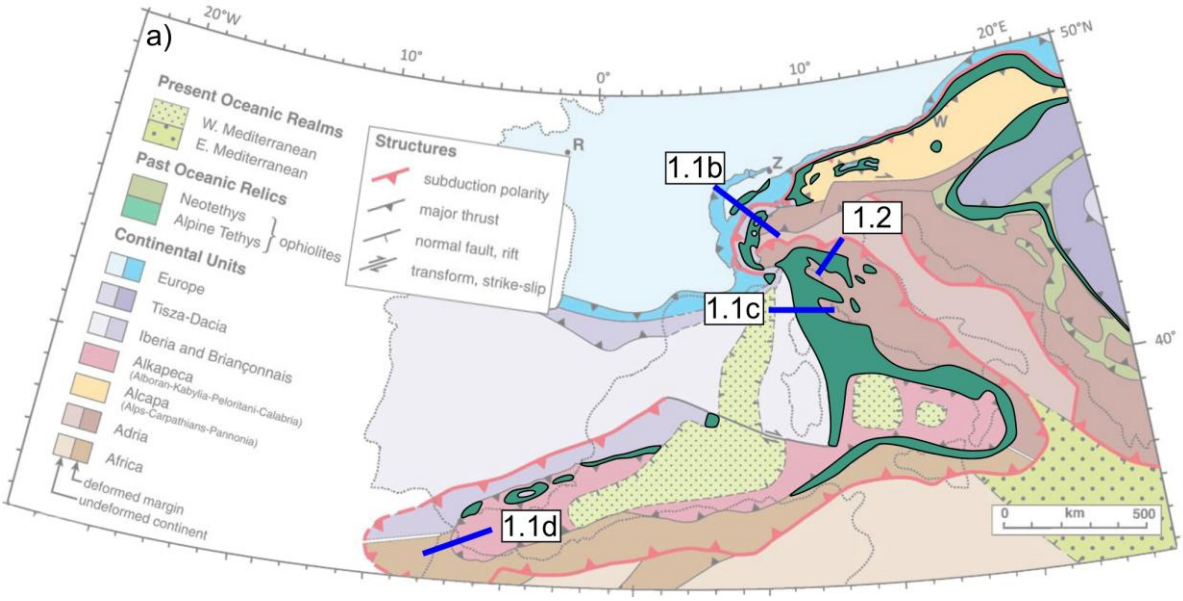

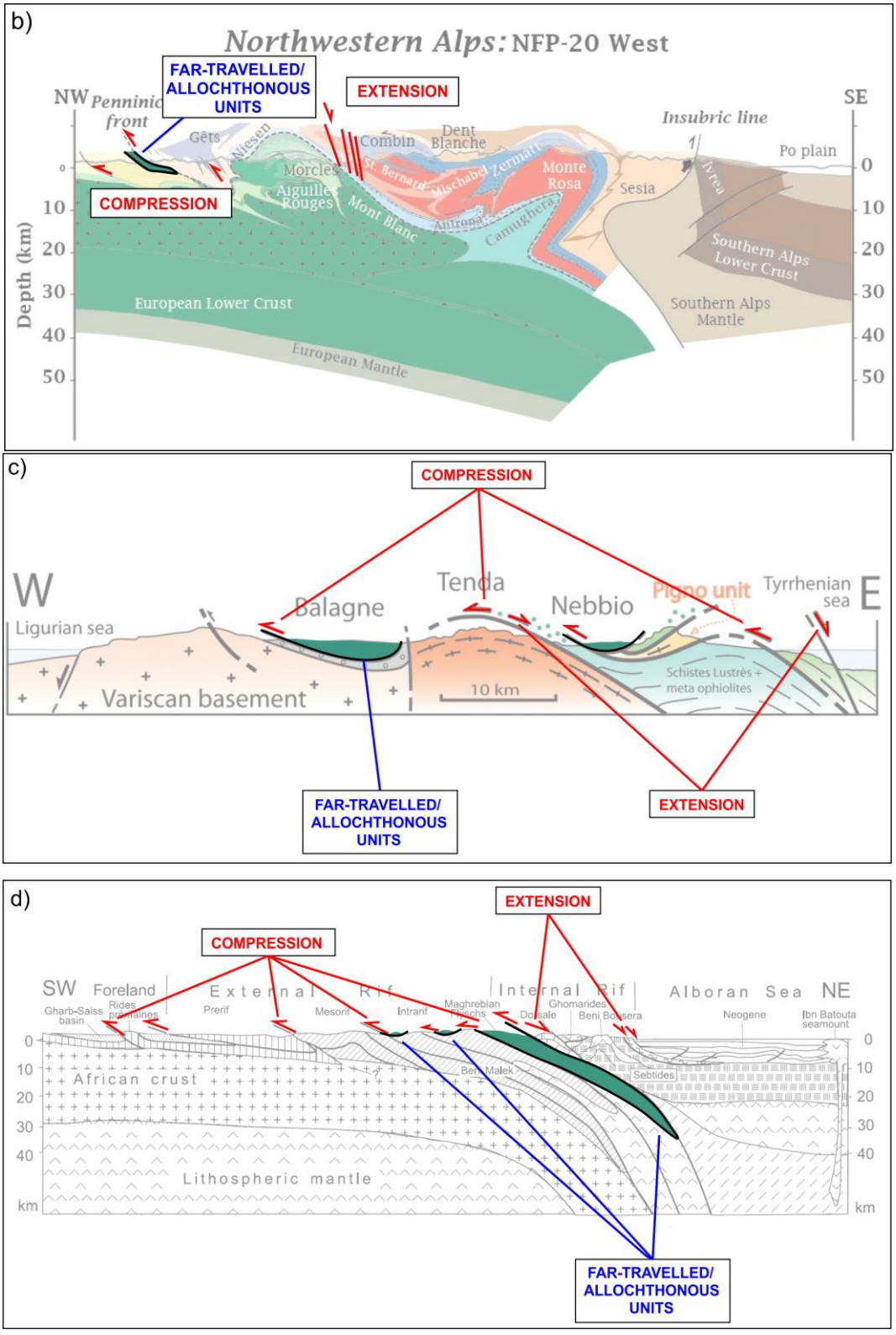

Fig. 1.1 – Examples of geological contexts related to the peri-Meditarranean orogens, in which far travelled/allochthonous units, extensional and compressional tectonics are present. a) map indicating the location of the far travelled/allochthonous units, and the traces of the cross sections drawn in figs. 1.1b, 1.1c, 1.1d, 1.2 (modified after Handy et al., 2010); b) cross section across the north-western Alps (modified after Bousquet et al., 2012); c) cross section across the alpine Corsica (modified after Brovarone et al., 2011); d) cross section across the Rif belt (modified after Michard et al., 2002).

These shallow far-travelled/allochthonous units commonly accomplished their translation, through displacements of several tens of kilometres during many My, while the orogenic processes were still acting. The far-travelled/allochthonous units, thus, are likely to have recorded, in their deformation history, traces of broader orogenic-scale processes, such as the relationships between extensional and compressional tectonics, and their study can give new insights on this relatively poorly delved topic. The Northern Apennines of Italy are not an exception; they form a mountain belt characterized by the concomitant interplay between extensional and compressional tectonics coupled with preserved far-travelled/allochthonous units (fig. 1.2).

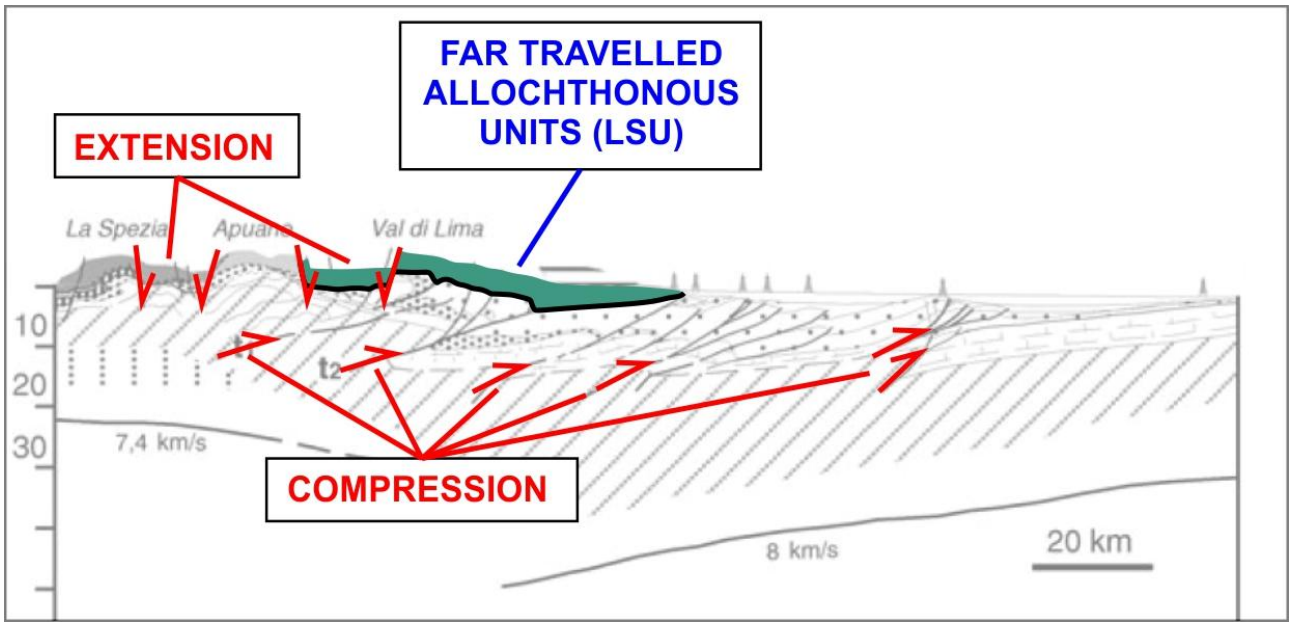

Fig. 1.2 – Geological cross section across the Northern Apennine (see fig. 1.1a for location). The far travelled/allochthonous units (LSU), the extensional and coeval compressional tectonics have been highlighted (modified after Molli, 2008).

These latter are represented by non-metamorphosed, accreted oceanic and ocean-continent transitional units known as Ligurian and Subligurian units (LSU from now on). They offer the unique opportunity to study their emplacement phases in relation to the coupling of compressional and extensional tectonics during the orogenic post-collisional processes.

In the Northern Apennines, the coexistence of extension and compression has been explained through a number of different and partly-contrasting models: critical wedge spreading, slab retreat, lithospheric delamination, slab tearing, and slab breakoff (Argnani et al., 2003; Carmignani and Kligfield, 1990; Gvirtzman and Nur, 2001; Jolivet et al., 1998; Malinverno and Ryan, 1986; Royden, 1993a; Scrocca et al., 2007; van der Meulen et al., 1999; Wortel and

Spakman, 2000). Recent thermochronological and GPS data highlighted how a single model cannot be taken into account in order to explain the variability of these data throughout the orogen (Bennett et al., 2012; Thomson et al., 2010).

This study is aimed at investigating if cause/effect relationships between extensional and compressional tectonics can be constrained in terms of timing and mechanism/s through the investigation of the last emplacement and deformation phases (i.e., since the late Miocene) of the shallow far-travelled/allochthonous units of the Northern Apennines (LSU).

The study has been carried out through the integration of published and newly acquired surface (geological maps, cross-sections), subsurface (seismic lines, boreholes) geological data, low temperature thermal (vitrinite reflectance, clay mineral analyses) and thermochronological (apatite fission tracks) data.

The investigation of the deformation history and, consequently, the record of extension-compression coupling inside the Apenninic far-travelled/allochthonous units allowed us to: 1) build a 3D representation of the LSU present-day geometry; 2) constrain a first thinning of the LSU to the late Miocene and a later reshaping to the Pliocene-Recent; 3) identify the tectonic exhumation and uplift of the deepest foredeep units at the main ridge of the chain as one of the main causes which triggered the thinning processes of the far-travelled/allochthonous units by means of low-angle extensional faults since late Miocene; 4) to relate the later reshaping phase to high-angle extensional faults associated also to increased erosion rates since Pliocene; 5) to recognize lateral variations in the extent of uplift, exhumation and thinning both across (from SW to NE) and along (from NW to SE) the analyzed portion of the Western Northern Apennines.

The main purpose and results of the present study is part of a paper which will be shortly submitted (Carlini et al., in prep.), and constitutes the core of chapter 5, whereas chapters 1-4 present extensively the aim of this work (chapter 1), the geological framework (chapter 2), the methodology and the complete used dataset (chapters 3, 4).

The number of pretty young cooling ages obtained by the AFT analysis (i.e. younger than ~5 Myr) and their possible relationship with the activity of deep Apenninic compressional structures (see § 5) led us to investigate the most recent evolutive phases of these processes through the integration of geomorphological data (Provincia di Parma, 2007), geological surface data, thermochronologic data and a new interpretation of seismic lines crossing the study area (see § 3),

described in a published extended abstract (Carlini et al., 2012, attachment A1), constituting the content of chapter 6.

The processes described in chapters 1-6 are strictly dependent on erosion/exhumation rates and the lack of well constrained estimates of these rates inside the study area led to further investigate the topic through the use of numerical modelling which extract exhumation/erosion rates from thermochronological data. The results of the numerical modelling, discussed in chapter 7, have been obtained using Pecube, a 3D finite element developed by prof. Jean Braun. In order to further explore this topic at a more regional scale, another attempt has been done using G.L.I.D.E., a finite element code developed by PhD Matthew Fox (Fox et al., in preparation), based on the direct inversion of thermochronological data. The results of the G.L.I.D.E. numerical modelling are only preliminary, and, therefore, have been attached at the end of the thesis (attachment A2), without being taken into account in the conclusive remarks of this work.

Finally, the integration of all the results related to chapters 5-7 is presented in the conclusive chapter of the thesis (§ 8). Here the late (i.e., since ~10 Ma) tectonic evolution of the study area is synthesized, in order to explain the relationships existing between extensional and compressional tectonics in the western Northern Apennines. The conclusive remarks contain also insights on the implication of the present work on the regional-scale and geodynamic processes affecting the whole Northern Apennines in their late orogenic evolution.

2. Geological Framework of the Northern Apennines and the study area

The Northern Apennines are a collisional orogenic belt originated from the middle Eocene collision between the European and Adria plates (Boccaletti et al., 1971; Channell et al., 1979; Dercourt et al., 1986; Elter and Marroni, 1991; Faccenna et al., 2004; Kligfield, 1979; Rosenbaum and Lister, 2004) (fig. 2.1). From the late Oligocene times up to the Present, the Apennine orogenic fronts migrated towards E and NE, progressively shortening the foredeep basins turbiditic deposits, while coeval wedge-top basins, the Epiligurian succession, formed on top of the LSU far-travelled/allochthonous units (Argnani and Ricci Lucchi, 2001; Boccaletti et al., 1990; Ricci Lucchi, 1986).

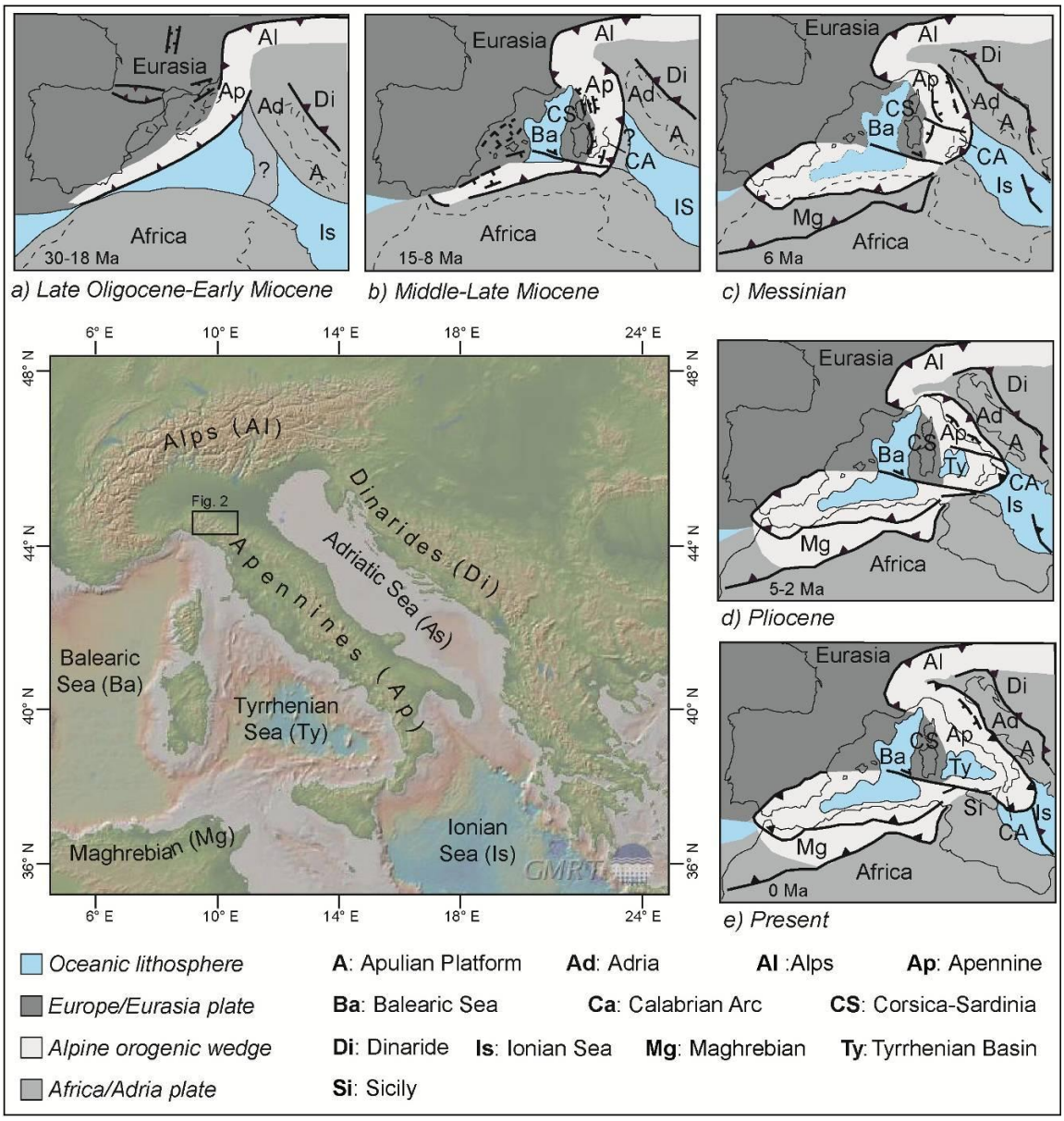

Fig. 2.1: Location of the study area and regional geological evolution of the Mediterranean area. (Modified after Capozzi et al., 2012; Faccenna et al., 2004, Rosenbaum et al., 2004). The location map in this figure is from GMRT Data Portal (http://www.marine-geo.org/tools/maps_grids.php) (Ryan et al., 2009).

The convergence and subsequent collisional processes developed between Europe and Adria plates progressively built up the Northern Apennines orogenic wedge. This latter is formed by two main tectonically superposed structural levels, characterized by different amount of shortening, both along and perpendicular to the tectonic transport direction of the LSU (fig. 2.2). The upper structural level is formed by the allochthonous Ligurian units, which are composed of highly deformed pelagic sedimentary rocks associated with ophiolite fragments, capped by terrigenous or carbonate turbidites deposits. These oceanic units were involved in the accretionary processes related to the subduction of the Ligure-Piemontese portion of the Neo-Tethyan oceanic crust from the Late Cretaceous up to the middle Eocene (Bettelli and Vannucchi, 2003; Marroni et al., 2001; Molli, 2008, Principi and Treves, 1984; Vannucchi and Bettelli, 2002). The Ligurian units translated on top of the Subligurian units, consisting of Paleocene to middle Eocene deep marine sediments unconformably overlain by late Eocene to early Miocene basin plain and turbiditic deposits (Montanari and Rossi, 1982; Plesi, 1975; Remitti et al., 2011; Vescovi, 1998). The Subligurian units, after being partly involved in the oceanic accretionary processes, were possibly removed from the toe of the Ligurian wedge by frontal tectonic erosion processes during the early Miocene (Remitti et al., 2011; Vannucchi et al., 2008). The LSU, constituting most part of the upper structural level, are unconformably overlain by the middle Eocene-late Miocene Epiligurian succession, which consists of hemipelagic, turbiditic and shallow water deposits, sedimented in wedge-top basins (Amorosi et al., 1993; Boccaletti et al., 1990; Mancin et al., 2006; Mutti et al., 1995; Papani et al., 1987; Ricci Lucchi, 1986) (fig. 2.2).

Underneath the far-travelled/allochthonous LSU, the lower structural level consists of a metamorphic basement and an overlying late Triassic to Eocene carbonate and hemipelagic succession passing upward to the Oligocene to Recent foredeep deposits (Argnani and Ricci Lucchi, 2001; Boccaletti et al., 1990; Ricci Lucchi, 1986) (fig. 2.2). The lower structural level can be divided in three major tectonic units: 1) the Apuane Alps metamorphic complex; 2) the Tuscan units, represented by the inner Macigno and Cervarola siliciclastic foredeep sediments (late Oligocene – early Miocene) with related Mesozoic substratum; 3) the Umbria-Romagna unit, formed by the outermost Apenninic Marnoso-arenacea (Langhian-Messinian) and Pliocene-Pleistocene foredeep basin, together with the underlying Mesozoic successions.

Since the Aquitanian, the LSU thrusted over the late Oligocene and subsequently the early Miocene foredeep deposits (Macigno and Cervarola units, respectively), causing the end of sedimentation in progressively younger basins (Argnani and Ricci Lucchi , 2001; Catanzariti et al.,

2003; Cerrina Feroni et al., 2002 and references therein). Since late Oligocene, deformation starts to affect the Apuane Alps and the Tuscan Metamorphic units (e.g., Carmignani et al., 1980), while during middle-late Miocene, the foredeep deposits and the Mesozoic substratum of the Tuscan and Umbria-Romagna units were deformed in a fold-and-thrust belt, which caused underplating at deep crustal levels (Carmignani et al., 1978; Moll2i, 2008), uplift, foredeep depocenter's migration and advancement of the overlaying LSU together with the passively transported Epiligurian succession (wedge-top basins), to form the present-day Apennine orogenic wedge (figs. 2.1, 2.2).

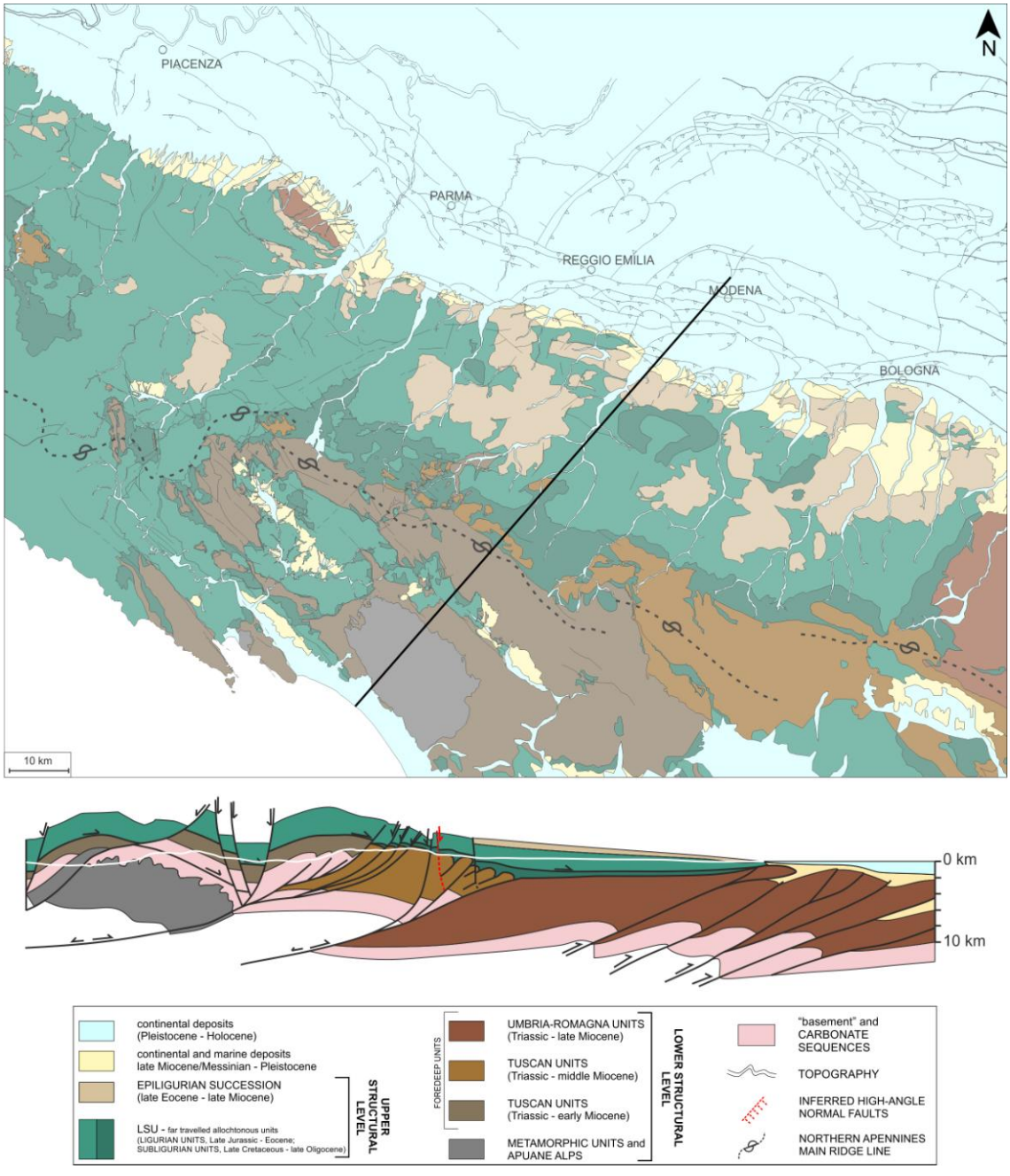

Fig. 2.2 – Synthetic geological map and cross-section of the Northern Apennines from Piacenza to Bologna, as obtained by the collection of data described in chapter 3; a) The solid black line represents the trace of the cross-section in fig. 2.2b; b) geological cross-section through the Northern Apennines, modified after Remitti et al., 2012.

The age of the folding and thrusting of the Tuscan and Umbria-Romagna foredeep deposits and their Mesozoic substratum is not well constrained, and most authors agree that their deformation is subsequent to the translation of the overlying LSU; although locally, thrusting activity might have started before or during the LSU emplacement (Barchi et al., 2001; Bettelli et al, 2002; Botti et al., 2003; Botti et al., 2004; Catanzariti et al, 2008; Chicchi and Plesi, 1991; Pini, 2004; Plesi, 2002; Remitti et al., 2007; Zattin et al., 2000; Zattin et al., 2002).

In the outer portion of the Northern Apennine foothills, both the upper and lower structural levels are presently unconformably overlain by late Messinian (post-evaporitic unit) to Recent deposits (Artoni et al., 2007; Gelati et al., 1987; Iaccarino and Papani, 1979; Ricci Lucchi et al., 1982; Roveri et al., 2001) (fig. 2.2).

At the Tyrrhenian side of the chain, crustal extension related to the exhumation and uplift of deeper portions of the orogen, such as the Apuane Alps metamorphic complex, has been evidenced since middle-late Miocene times (Carmignani and Kligfield, 1990; Fellin et al., 2007; Jolivet et al., 1998), leading to the formation of extensional basins (Bernini et al., 1990; Boccaletti et al., 1990; Molli et al., 2010). Similar extensional tectonic processes might have affected also the westernmost portion of the Northern Apennines during the Quaternary, acting at the same time of the compressional tectonics which characterizes the external sector and the deeper parts of the Apenninic orogenic wedge (Argnani et al., 2003; Boccaletti et al., 2011).

According to seismological studies, recent seismicity analysis and GPS data, the Northern Apennines present extension/transtension regime in shallow portions (0-10km), vertically superposed to a compressive/transpressive regime in deeper portions (>45km) and outermost fronts (Bennett et al., 2012; Eva et al., 2005 and references therein; http://bollettinosismico.rm.ingv.it/). These data testify that, at present and/or recently, the Northern Apennines orogenic wedge is still developing within the kinematic and tectonic context proposed for the late orogenic phases of the chain (i.e., since ~5 Ma, see above), which is characterized by an overall compressional regime coeval to relatively shallow extension.

3. Methods and dataset – surface and subsurface geological data

In order to put new constraints on the timing and mechanism/s of coeval compressional and extensional tectonics, the study area, comprised between the main ridge of the Northern Apennines, the Ceno and Secchia rivers and the Apenninic topographic front (fig. 2.2), has been investigated through a multidisciplinary approach which took into account (fig. 3.1):

1) surface geological data: results from field-based works on the evolution of the external (NE) slope of the chain, collection and compilation of published geological maps and 23 geological cross sections;
2) subsurface geology: a) structural analysis and interpretation of seismic reflection profiles and b) analysis of boreholes stratigraphies.

We integrated all the geological data in a database georeferenced through ESRI ArcMap 10 software.

3.1 Surface geological data

The geological data are constituted by a synthetic geological map of the western portion of the Northern Apennines (figs. 2.2, 3.1), compiled by prof. Massimo Bernini, dott. Andrea Artoni and dott. Paolo Vescovi, from the collection of several published data (Bettelli et al., 2002; Boccaletti and Coli, 1982; Bortolotti et al., in press; Cerrina Feroni et al., 2002; Di Dio et al., 2005; Elter et al., 2005; Martini and Zanzucchi, 2000; Plesi, 2002; Puccinelli et al., in press (a); Puccinelli et al., in press (b); Vescovi et al., 2002; http://www.isprambiente.it/Media/carg/index.html), and 23 geological cross-sections passing through the study area (see figs. SM1.1a, SM1.1b in Supplementary material 1).

fig. 3.1: Geological sketch map of the study area, scale 1:250.000, resulted from the collection of several published data, compiled and georeferenced with ESRI ArcMap 10 software. Traces of the geological and seismic cross-sections represented in fig. 5.3; traces of the three swath profiles and location of the boreholes represented in fig. 5.4; A_L, B_L and C_L indicate the low angle extensional contacts, B_H and C_H indicate the more recent high angle extensional faults cross-cutting the older low angle ones (B_L and C_L, respectively); blue squares indicate tectonic windows cited in the text: I) Valdena; II) M.te Zuccone; III) Pracchiola; IV) Ghiare di Berceto; V) Gova; VI) Salsomaggiore; VII) M.te Staffola; VIII) Coscogno. Zone 1, 2 and 3 indicate the three portions in which the study area has been subdivided for clearness sake and similarity of data (see § 5).

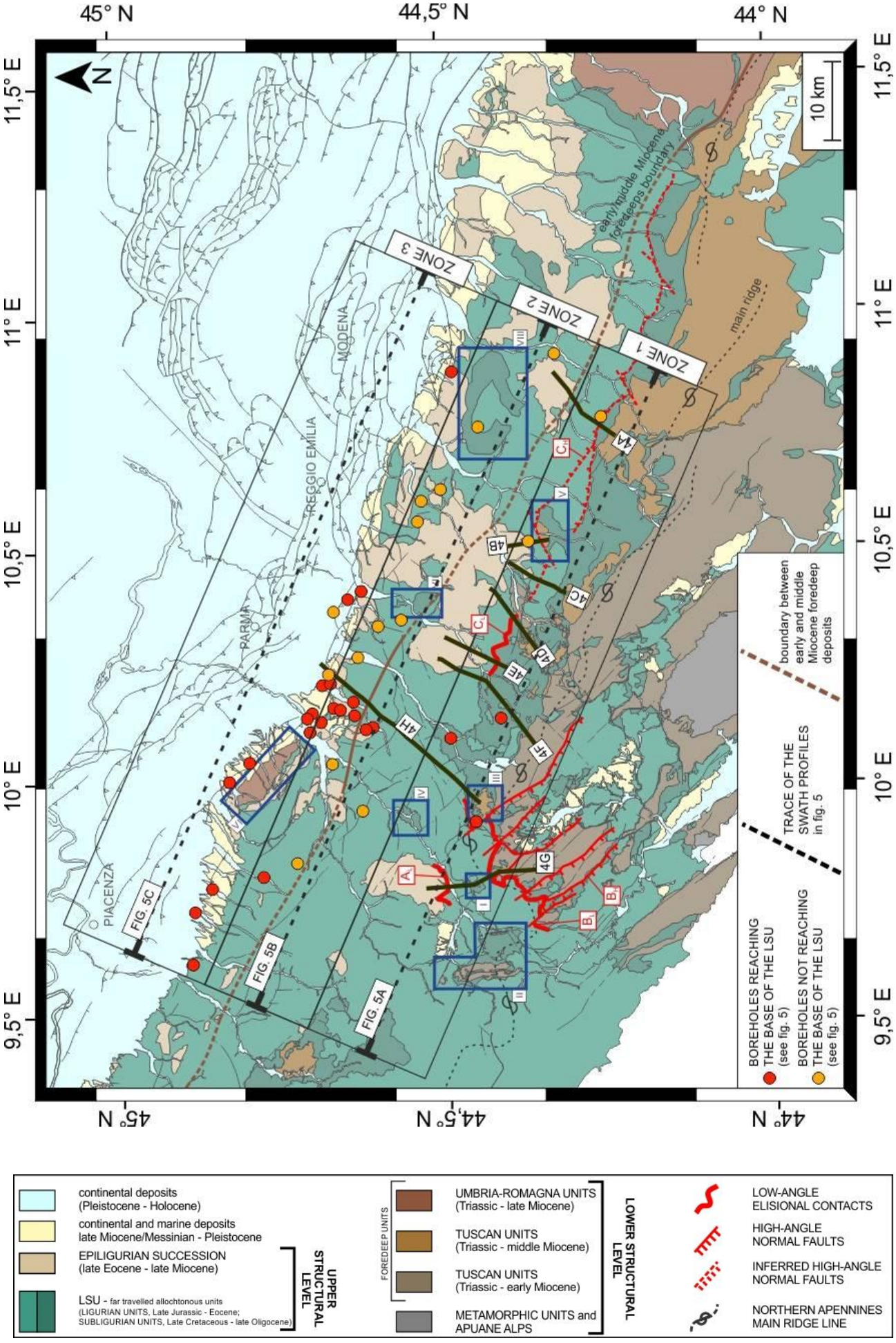
45° N
44,5° N
44° N
11,5° E
11° E
10,5° E
10° E
9,5° E
N
10 km
ZONE 3
ZONE 2
ZONE 1
MODENA
REGGIO EMILIA
PARMA
PIACENZA
early/middle Miocene foredeeps boundary
main ridge
FIG. 5C
FIG. 5B
FIG. 5A
boundary between early and middle Miocene foredeep deposits
TRACE OF THE SWATH PROFILES in fig. 5
BOREHOLES REACHING THE BASE OF THE LSU (see fig. 5)
BOREHOLES NOT REACHING THE BASE OF THE LSU (see fig. 5)
continental deposits (Pleistocene - Holocene)
continental and marine deposits late Miocene/Messinian - Pleistocene
EPILIGURIAN SUCCESSION (late Eocene - late Miocene)
LSU - far travelled allochtonous units (LIGURIAN UNITS, Late Jurassic - Eocene; SUBLIGURIAN UNITS, Late Cretaceous - late Oligocene)
UPPER STRUCTURAL LEVEL
FOREDEEP UNITS
UMBRIA-ROMAGNA UNITS (Triassic - late Miocene)
TUSCAN UNITS (Triassic - middle Miocene)
TUSCAN UNITS (Triassic - early Miocene)
METAMORPHIC UNITS and APUANE ALPS
LOWER STRUCTURAL LEVEL
LOW-ANGLE ELISIONAL CONTACTS
HIGH-ANGLE NORMAL FAULTS
INFERRED HIGH-ANGLE NORMAL FAULTS
NORTHERN APENNINES MAIN RIDGE LINE

3.2 Subsurface geological data

Subsurface geological data consist mainly of 39 deep boreholes stratigraphies and 47 commercial 2D seismic reflection profiles (for a total length of 1191 km), made available by ENI S.p.A (fig. 3.1). The analysis of the seismic reflection profiles has been integrated with previously published interpretations of subsurface data (Argnani et al., 2003; Camurri, 2000; Camurri et al., 2001).

Stratigraphies of the boreholes were obtained from well logs freely available and downloadable from the VIDEPI Project website (http://unmig.sviluppoeconomico.gov.it/videpi/). The well logs used in this work are collected in fig. SM1.2 (Supplementary material 1), where the tectonic contacts between the LSU and the foredeep units and between the upper and lower portion of the LSU have been marked (for the interpretation see fig. 5.4 and § 5).

The interpretation of the seismic reflection profiles data has been carried out in collaboration with dr. Luca Clemenzi (PhD student in Earth Sciences at the University of Parma), using Halliburton's SeisWorks® PowerView software, mounted on DELL workstations, made available by ENI S.p.A. by their offices in San Donato Milanese. The interpreted data have been subsequently elaborated through Midland Valley's Move software, available by the University of Parma Physics and Earth Sciences department.

The structural interpretation has focussed on two main points: 1) a more precise definition of the deep (i.e. involving the "basement" units) Apenninic tectonic structures; 2) a more clear definition of the shallower portions of the chain, where Epiligurian Succession, LSU and foredeep Tuscan and Umbria-Romagna units are present. While the investigation of the Apenninic chain deeper portions is still in progress, the shallower portion has been well constrained, as shown in figs. 3.2 and 3.3. Fig. 3.3 shows a portion of a profile belonging to the dataset presented by Camurri et al., 2000; in the present study, the shallower portion of the seismic profile has been detailed (where the foredeep units-LSU contacts are present) and a partly different interpretation has been proposed.

Within the shallow portion, particularly relevant for the aim of this work, the basal contact of the LSU over the foredeep units has been defined almost in every analyzed section, while only in some cases the recognition of the Epiligurian succession and other important contacts inside the LSU has been possible.

The different Apenninic tectonic units have been distinguished on the basis of the character of the seismic signal, which, deeply affected by the lithology and other physical (acoustic) properties of rocks, is quite recognizable throughout the shallowest portion of the Apenninic nappe stacking, in particular:

- the foredeep units together with their Mesozoic carbonate substratum are always characterized by poorly- to no-reflective seismic signature, which is distributed over large areas, preferentially in the central portion of the seismic profile; locally high amplitude reflectors appear, but they are extremely short and without lateral continuity. Foredeep units and Mesozoic carbonate successions have been interpreted as cut by thrust faults whose presence and displacement become evident only where the upper contact of these units with the base of the LSU is imaged;
- the LSU are characterized by strong reflective seismic signals with high amplitude and low frequency, which form clearly distinguishable portions displaying discrete lateral continuity; the distinction between the lower and upper portion of the LSU (Subligurian and Ligurian units, respectively) has been possible only thanks to the local presence of more reflective signals, linked to the surface outcropping geology;
- the Epiligurian succession is often represented by quite reflective signals that, even if locally similar to the LSU, are characterized by a good lateral continuity of reflective horizons and their consistency to depth allows to quite easily define their lower contact of over the LSU; also in this case the link to surface outcropping geology has been important for the interpretation.

The seismic reflectors have been calibrated, where possible, with the aid of stratigraphies of boreholes located close to the traces of the seismic lines. The depth of the horizons in well logs (expressed in m) has been converted in seconds according to the velocities suggested by Barchi et al., 1998.

The most relevant results obtained from these data and methodologies have been the definition of the contact between foredeep and far travelled/allochthonous units (LSU) and the geometry of these latter in their innermost (SW) outcropping zone. These results can be synthesized as follows: a) the LSU basal contact shows indications of involvement in the thrusting and folding processes affecting the underlying foredeep units; b) the present-day geometry of Subligurian and Ligurian Units in their inner (SW) outcropping portions is characterized by a low

thickness, which increases towards NE. These two major results, important for the reconstruction of the tectonic evolution of the Apennines far travelled/allochthonous units, will be discussed in chapter 5.

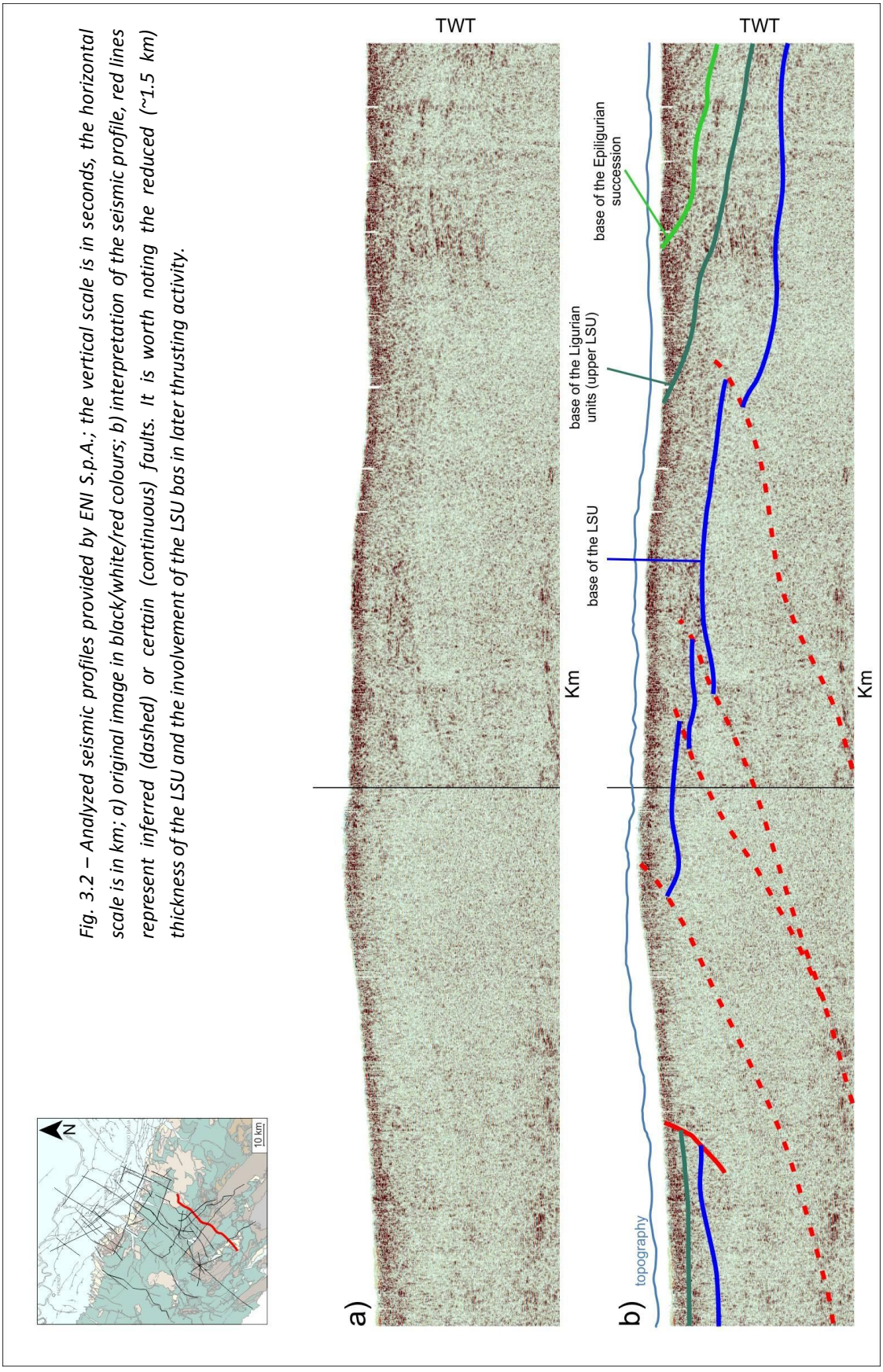

Fig. 3.2 – Analyzed seismic profiles provided by ENI S.p.A.; the vertical scale is in seconds, the horizontal scale is in km; a) original image in black/white/red colours; b) interpretation of the seismic profile, red lines represent inferred (dashed) or certain (continuous) faults. It is worth noting the reduced (~1.5 km) thickness of the LSU and the involvement of the LSU bas in later thrusting activity.

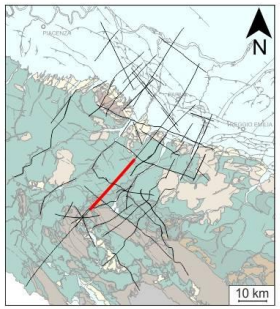

Fig. 3.3 – Analyzed seismic profiles provided by ENI S.p.A.; the vertical scale is in seconds, the horizontal scale is in km; a) original image in black/white/red colours; b) interpretation of the seismic profile, red lines represent inferred (dashed) or certain (continuous) faults. The interpretation of this profile is based and modified after the interpretation proposed by Camurri, 2000. It is worth noting the involvement of the LSU bas in later thrusting activity.

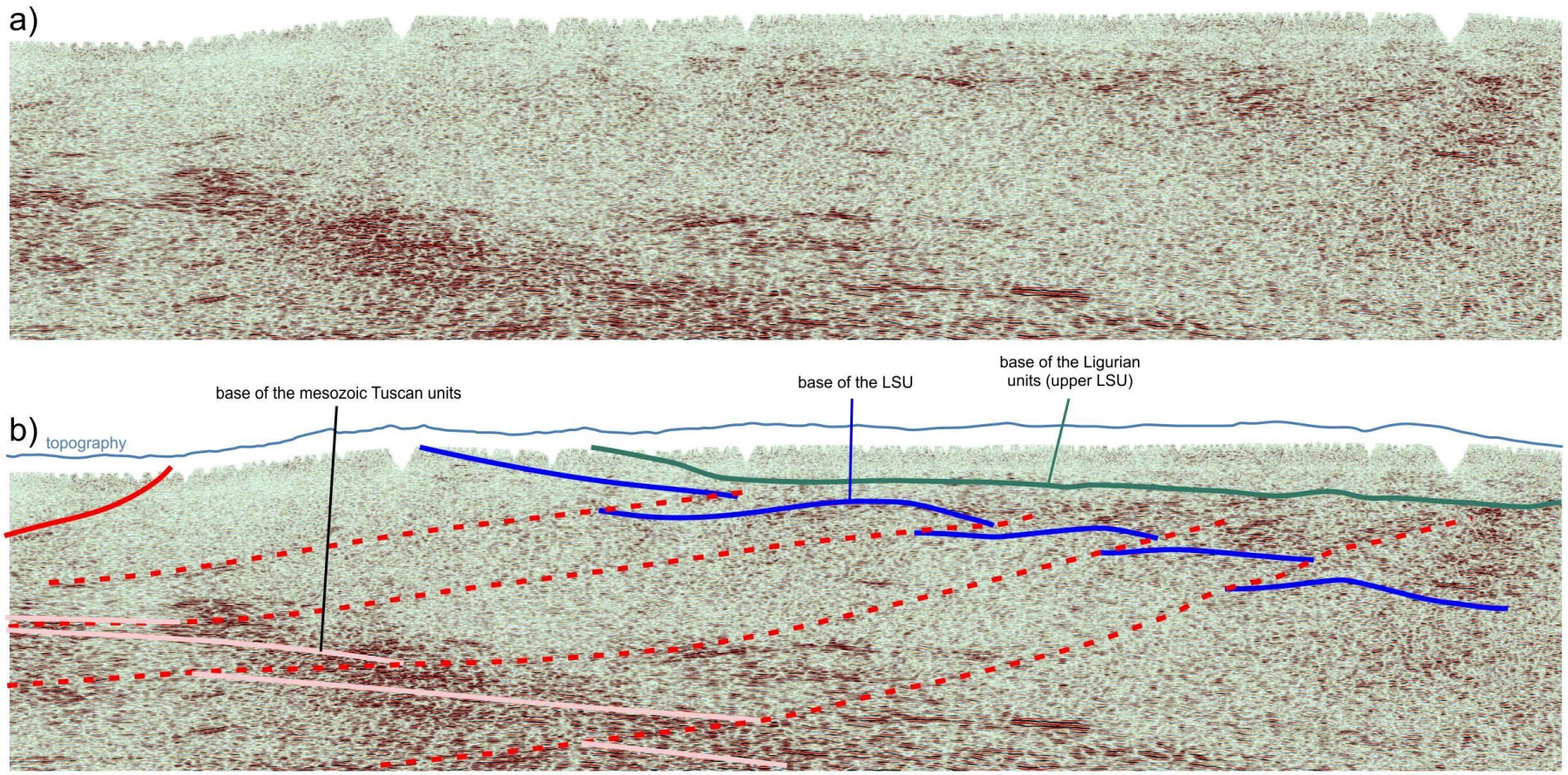

4. Methods and dataset – paleothermal and thermochronological data

In order to study the late evolution of the far travelled/allochthonous LSU within the study area, the afore mentioned geological data (see § 3) have been integrated with paleothermal and thermochronological data. This kind of data, widely used in the study of the evolution of mountain belts, give important information about the evolution of rocks in terms of load, unload, thermal evolution and dating of these processes. As already highlighted in the literature (Bray et al., 1992; Corrado et al., 2010; Green et al., 2002; Green et al., 2003; Japsen et al., 2005; Ventura et al., 2001), the integration of thermal and thermochronological data provides important constraints on the thermo-tectonic evolution of rocks, such as maximum paleo-thermal gradients and timing of cooling processes. The multi-method approach allows us to get information about timing and entity of exhumation relative to: 1) each tectonic unit; 2) eventual coupling/decoupling events of the units during the exhumation processes.

The analyses were performed in collaboration with prof.ssa Sveva Corrado (vitrinite reflectance, University of Roma Tre), PhD Luca Aldega (clay mineral-based geothermometers, Sapienza Università di Roma), and PhD Maria Laura Balestrieri (AFT, IGG-CNR Firenze).

4.1 Thermal maturity in sedimentary rocks

The sedimentary and/or tectonic burial of sediments leads to a series of mostly irreversible reactions and processes which leave structural imprints on the organic matter and clay minerals of the burial and, thus, of the reached maximum temperature. These reactions, fundamental in coal and hydrocarbons generations, are indicative of sedimentary basins' maturity which depends on burial timing, thermal maturity, maximum burial depth and the tectonic events affecting the basin's history; thus, they are commonly employed in basin analysis. The most common parameters used to determine the thermal maturity are vitrinite reflectance (based on the optical reflectance of dispersed organic matter in sediments) and clay mineral analyses (related to the study of the "crystallinity" and expandability of phyllosilicates).

The thermal maturity analyses of organic matter and clay minerals are complementary, because vitrinite is much more reactive to low temperature processes, but also much less abundant in sediments compared to clay minerals; clay minerals, even if less reactive, are almost always present and allow to study thermal maturity even in red-beds sequences (where organic

matter is completely oxidized or absent) or in successions which are older than the evolution of plants on the earth.

Nonetheless correlations between these two analyses aren't always free of complications because in situations affected by particularly high geothermal gradients clay minerals are more sensitive to long-lasting heating events compared to organic matter. On the other hand, rapid heating events such as magmatic intrusions and hydrothermal fluids accelerate maturation processes in organic matter more than smectite illitization reactions (Bevins et al., 1996). Moreover high burial rates can inhibit organic matter maturation (Carr and Williamson, 1990; Dalla Torre et al., 1997) and deformational events can increase both organic matter maturity and illite crystallites dimensions (Bonazzi and Costa, 1989; Teichmüller, 1987).

In order to correlate the two afore-mentioned parameters we adopted the correlation chart proposed by Merriman and Frey, 1999 (fig. 4.1), in turn resulted from modifications of the one proposed by Merriman and Kemp in 1996, and considered suitable for geothermal gradients of ~30 °C/km, which are common in many fold-and-thrust belts (Merriman and Kemp, 1996; Merriman and Frey, 1999).

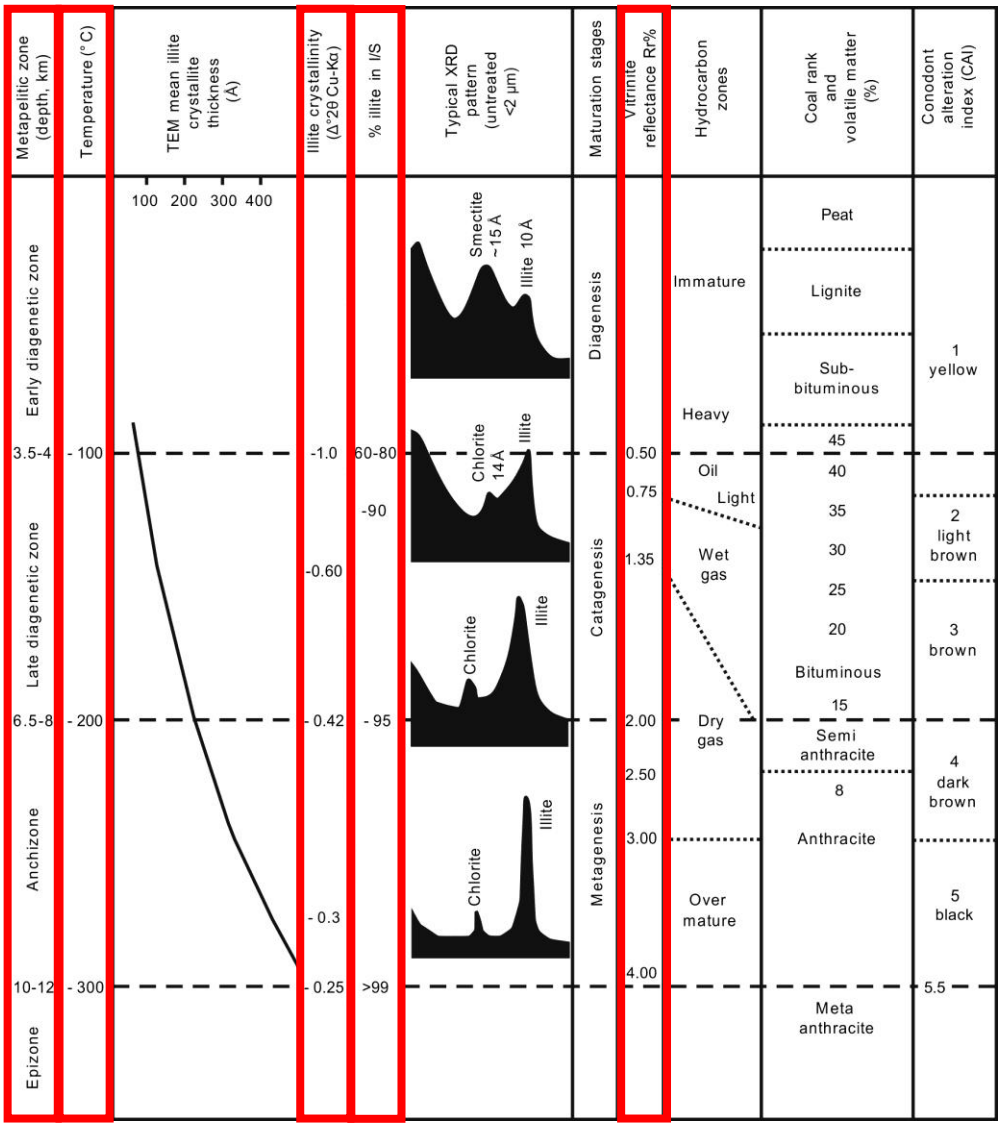

4.2 Paleotemperatures derived from clay mineral analyses

The most common analyses in studies of thermal maturity made through the analysis of clay minerals rely on three parameters which can give information about the maximum paleotemperatures reached by the sediments: the composition of a) illite-smectite (I-S) mixed-layers, and b) chlorite-smectite (C-S) mixed-layers in clay minerals reaction series; c) the Kübler Index (KI, i.e. the old concept of illite "crystallinity").

During low- and very low-grade metamorphism clay minerals are affected by structural and compositional variations related to the thermo-baric conditions at which the minerals re-equilibrate, and the general trend of the reactions inside the minerals indicate a gradual decrease of structural disorder, reached through a series of metastable phases (mixed-layers).

Two main reaction series considered in this kind of studies:

- Dioctahedral clay minerals: smectite → illite-smectite (I-S) mixed-layers → illite → muscovite;
- Trioctahedral clay minerals: smectite → chlorite-smectite (C-S) mixed-layers → chlorite.

The abundances of the two series depend mainly on the composition of the starting rocks, so that pelitic sediments are usually dominated by the presence of dioctahedral minerals series, while in Fe-Mg-rich sediments it is possible to observe a predominance of the second series.

The calculations of percentages of illite and smectite inside an I-S mixed-layers is made by comparing a glycolized and an air-dried diffractograms of the same sample (see § 4.2.4). The comparison is made calculating the difference between Δ°2θ angles in peaks illite 002/smectite 003 and illite 001/smectite 002. Then the obtained angular value is inserted in reference tables which indicate a range of illite-smectite content percentages related to this difference.

In order to obtain a temperature value from clay minerals analyses the afore-mentioned angular difference, which take into account the structure of mixed-layers, indicated by the "R" parameter, is then inserted in Merriman and Frey's correlation chart (Merriman and Frey, 1999, fig. 4.1). This parameter assumes values of 0, 1 and 3 (the existence of R2 structures is still a matter of debate), increasing as a direct function of temperature, and indicates the level of order in the repetition of single clay minerals layers and illite-smectite mixed-layers.

Fig. 4.1 – Correlation chart for different paleothermal indicators proposed by Merriman and Frey, 1999. The red boxes highlight the parameters we adopted in this study (see text for explanation), and the corresponding temperatures and depths at which the main reaction in clay minerals and organic matter occur, adopting a geothermal gradient of 30°C/km.

Value 0 refers to cases of disordered structures, 1 when the illite content raises to 50%, 2 should be relative to an illite content of 67%-80% and 3 refers to structures in which the illite content is higher than 90%.

The passage from R0 to R1 structures occurs at temperatures of ~100-110 °C, while R3 structures can be found at temperatures higher than ~170-180°C, with a geothermal gradient of 25-30 °C/Km (Hoffman and Hower, 1979; Pollastro 1990).

Finally the third type of clay mineral analysis takes into account the concept of "crystallinity", which, in this context, acquires the meaning of thickness, and thus dimension, of clay mineral crystallites (single crystals or mineral fragments). With increasing temperatures and pressures, crystals become thicker and acquire larger surfaces; therefore, crystallinity is a function of the prograde reactions affecting the minerals, and represent a state controlled by pressure-solution and recrystallization processes, related, in turn, to fluid activity, temperature and tectonic strain.

The Kübler Index, first born from studies aimed to define the limits between diagenesis, anchizone and epizone (Kisch, 1990, 1991; Kübler, 1967), measures shape variations of the first illite basal reflex (interplanar spacing ~10 Å), in air-dried and glycolized diffractograms realized with the <2µm fraction. The width measurement is made at half height of the peak (*full width at half maximum, FWHM*), and variations of this parameter are expressed in Δ°2θ. As illite crystallites become thicker in metapelitic sequences, the 001 peak profile at 10 Å becomes narrower and the Kübler Index decreases; the FWHM value is associated to temperature values which are reported once again in Merriman and Frey's chart (Merriman and Frey, 1999, fig. 4.1).

4.2.1 X-ray powder diffraction: sample preparation and instrumental conditions

The afore-mentioned parameters (% illite in I-S mixed layers, % chlorite in C-S mixed layers and Kübler Index) are measured through X-ray diffraction (XRD) and each sample is subjected to two different analyses, one on a sample with random orientation of the crystallites and the other with crystallites preferential orientation (e.g., Giampaolo and Lo Mastro, 2000). While the random-oriented samples analysis give a semi-quantitative estimate of the mineralogical composition, the oriented samples analysis results in precise information about composition and content of clay minerals.

4.2.2 Random-oriented sample preparation

After a first crushing and exsiccation inside an oven at 40°C for 24 hours, 2-3 g of the sample are comminuted to an impalpable powder with agate mortar and pestle. Half gram of material is inserted in a sample holder, covered by rough filter paper, and put under a compressed air press at 5 bar. The advantages of this kind of preparation are (Giampaolo and Lo Mastro, 2000):

- "infinite" thickness (~2 mm) to X-ray diffraction;
- corrugated surface, assures clay minerals random orientation;
- same standard deviation in the crystallites inclination angle with respect to the mean orientation of crystallites in the aggregate;
- repetitivity of sample preparation;
- possibility to compare different samples, analyzed through XRD in different times;
- possibility to quantify different minerals inside the same aggregate.

4.2.3 Oriented samples preparation

In order not to alter too much phyllosilicates structures in these samples the material has to be left as undisturbed as possible, therefore, it is necessary to generate a clay minerals crystallite-rich suspension, avoiding intense mechanic actions.

20 g of the finest sample fraction are dispersed in 150 ml of distilled water, inserted in 500 ml Erlenmeyer flasks and treated in a stirrer running at 200 oscillations per minute; each sample for a total time of 60 minutes. Subsequently 50 ml of suspension are extracted and put inside test tubes destined to centrifuge. Centrifugation is necessary in order to make the coarser material to deposit on the bottom of the tube, while the < 2 μ fraction remains suspended inside the water, in the upper half of the test tube. The centrifuge is run at 1000 rpm (revolutions per minute), for 2'10", according to reference tables which specify the duration of the operation as a function of the interested granulometric fraction, temperature of the water and velocity of the centrifuge. This operation is also aimed to check the eventual presence of soluble salts (chlorides and sulphates), which have to be removed from the suspension, in order not to disturb the XRD analysis.

At the end of this step ~25 ml of suspension are extracted and dropped in 30 ml sterile holders and successively extracted with a pasteur dropper in order to be placed, as a suspension

bubble, on previously cleaned and weighted glass slides. The slides are characterized by a diameter of 25 mm and a thickness of 1.3 mm. It is important to make the bubble as big as possible, in order to make deposit as much material as possible on the glass slides, because higher density of material plays a fundamental role in the results of the analysis.

Once the prepared sample is dry, in order to obtain the sample density it is necessary to weigh the slides once again and to apply this formula:

$$\rho = \frac{w_2 - w_1}{a},$$

where ρ represents the density of the sample, w_2 the weight of the glass slide with the powder, w_1 the weight of the clean glass slide, and a the area of the slide.

At this point the air-dried samples are ready for the diffraction, after which, they are placed in an ethylene glycol-saturated desiccator which produces an expansion (reversible) of the expandable clay minerals crystalline lattice. The glycolized samples have to be treated for at least 17 hours, and then analyzed within 8 hours from the end of the glycolization process.

4.2.4 Diffractograms interpretation

In the random-oriented samples, where no granulometric separation has been done, the quantity (as a percentage) of each single mineralogical phase is obtained through the measure of the FWHM, and thus of the area of each peak (fig. 4.2).

Then the percentage of each phase with respect to the total is given by:

$$c_i = \frac{\frac{A_i}{F_i} \times 100}{\sum_{i=1}^{n} \frac{A_i}{F_i}},$$

where c_i is the content of the i phase, A_i is the area of the i phase peak, F_i is the PIF (Peak Intensity Factor) of the i phase, i represent each single phase, while n is the total number of mineralogical phases present in the sample. In these samples phyllosilicates are considered as a unique phase.

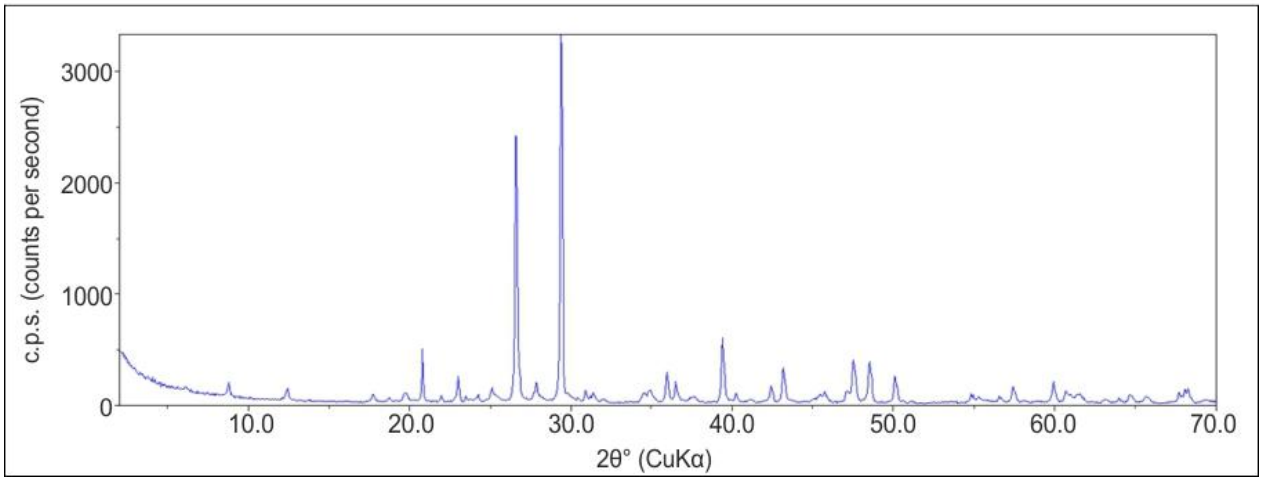

Fig. 4.2 – Random-oriented sample diffractograms related to sample PR 3 CM.

In the samples with granulometry < 2 µm, on the contrary, the same formula is used to obtain the percentage of each clayey fraction over the total of the present phyllosilicates (fig. 4.3).

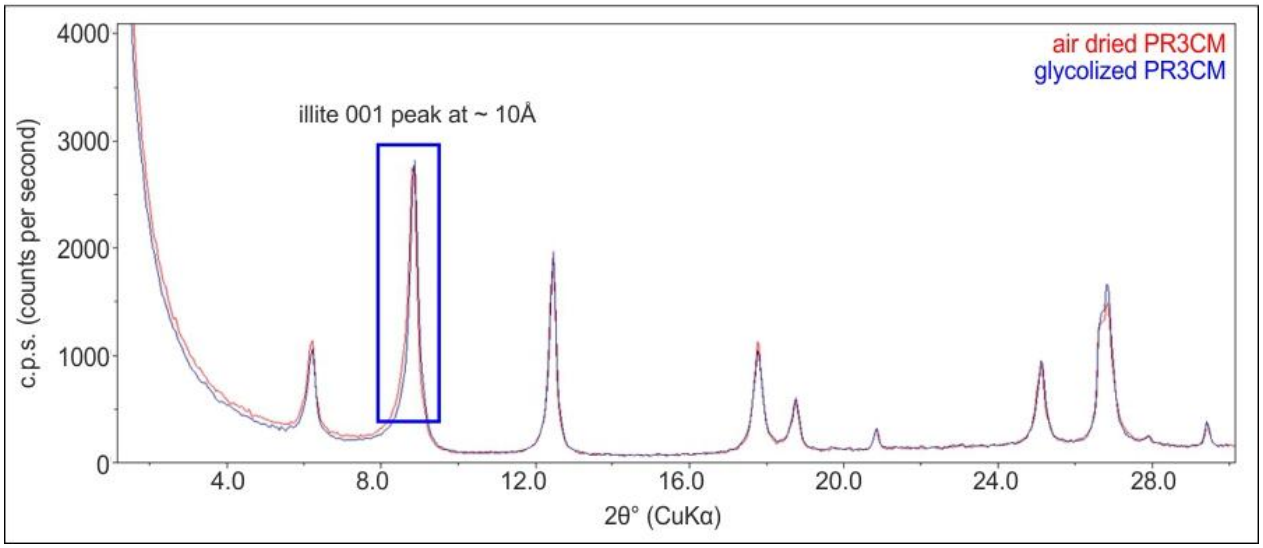

Fig. 4.3 – Air-dried and glycolized samples diffractograms, related to the analysis of < 2 µm granulometric fraction in sample PR 3 CM.

4.3 Paleotemperatures derived from analysis of dispersed organic matter

Organic matter dispersed within sediments has a wide range of different compositional and genetic characteristics, and is composed mainly by carbohydrates, proteins, lignin and lipids. The term kerogen indicates the fraction of organic matter resisting to the attack of organic acids which affect the first centimetres of basin floor sediments.

Among the main constituents of dispersed organic matter the huminite-vitrinite group occupies a relevant position because the reflectance of its components is strongly dependent on the basin maturity grade, and vitrinite-rich host rocks can generate gaseous hydrocarbons.

The quantity of dispersed organic matter of terrigenous origin depends on many factors, such as distance of deep basins from emerged continents or islands (covered with vegetation), pelagic sedimentation rates versus turbiditic sedimentation and mass-flows emplacement, primary productivity of marine plankton and its chemical stability, activity of bacteria and oxidizing agents, velocity and direction of marine currents (Littke et al., 1994).

Organic matter, while transported through the water column, is altered by biologic, chemical and physical processes, and can be characterized through petrological and geochemical studies, in particular through the definition of the percentage of total organic carbon and the hydrogen index (HI) (Bordenave, 1993; Espitalié et al., 1977; Katz, 1983; Wakeham and Lee, 1993).

The most used parameter for the study of sedimentary rocks thermal maturity is vitrinite reflectance (Ro%), i.e. the capacity of dispersed organic matter to reflect light, which varies as a function of thermal maturity, or maximum reached temperature, represented mainly by volatile loss and progressive graphitization.

Organic matter maturation is subdivided in three groups, in relation to oil and gas production:

- Ro% ≤ 0.5: chemical and physical processes fall inside diagenesis field, affecting mainly the quantity of oxygen present in the first centimetres of sediments. In this phase organic matter is transformed in kerogen, and bacterial processes prevail on the effects of temperature and burial;
- 0.5 < Ro% ≤ 2.0: catagenesis, temperature effects become the most relevant, kerogen becomes thermodynamically unstable and starts a physical-chemical reorganization which leads to the expulsion of products such as: H_2O e CO_2 (initially), oil (in the main phase, called “oil window”, fig. 4.4), and wet gases in the most advanced phases;
- 2.0 < Ro% ≤ 4.0: metagenesis, temperature and pressure rise until only dry gases are expelled (mainly methane). Kerogen loses H, O, N and S, and progressively transforms in graphite.

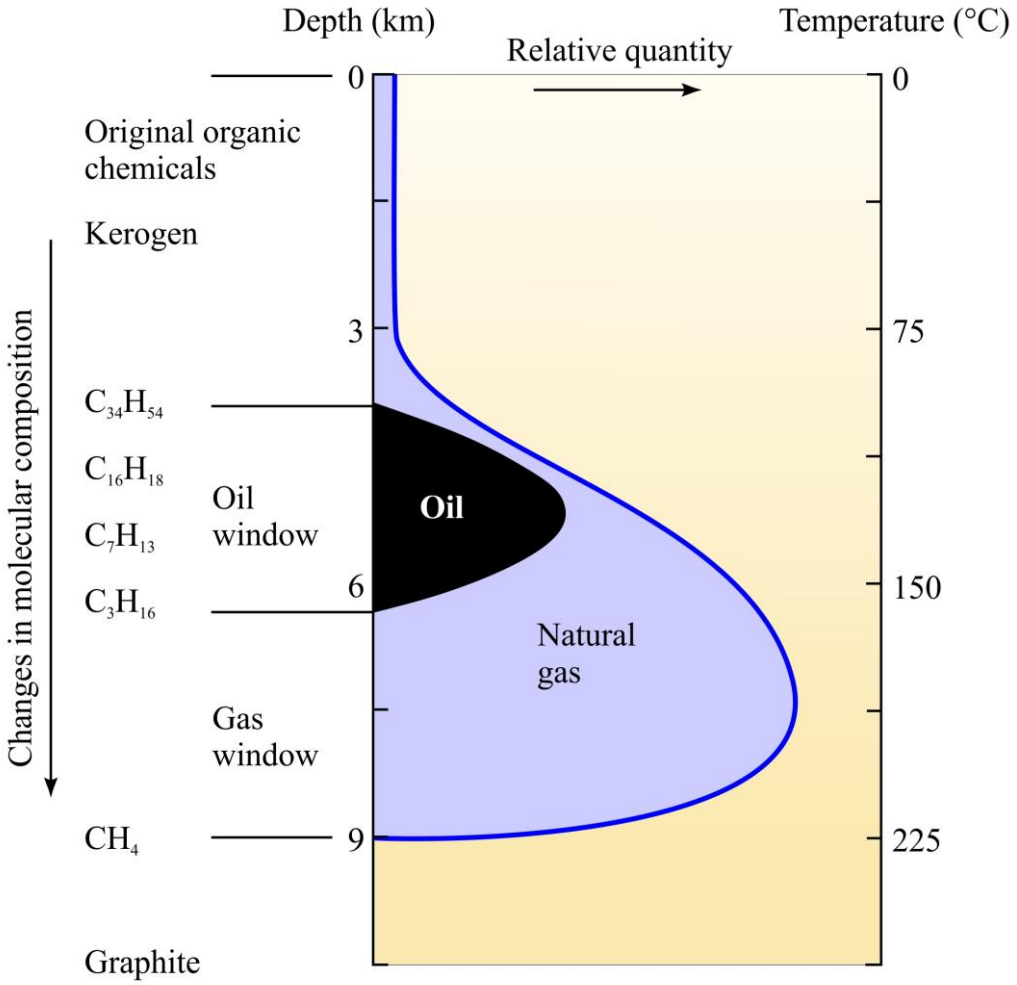

Fig. 4.4 – Chart representing the progression of reactions and modes of hydrocarbons generation with increasing depth and temperature (modified after Marshak, 2001).

4.3.1 Vitrinite reflectance sample preparation and analysis

Samples are prepared crushing the collected rock, leaving a coarse granulometry, in order to avoid a too long or intense mechanic action, which would lead to the destruction of the vegetal material, much weaker than the detritic components of sediments.

It can be useful, in particularly organic matter-poor samples, to do a manual picking, with optical microscopes, in order to concentrate the organic matter in the sample. Selected material is then incorporated in epoxy resin and left to dry for some hours.

The preparation ends with three steps of honing and three steps of polishing; honing phase is characterized by the use of sandpaper with progressive finer granulometry (in the range 60-600) and water, while polishing is made with progressively finer aluminum oxide paste, from 0.3 to 0.05 µm.

Vitrinite reflectance analysis is accomplished through a common petrography optical microscope, upon which it's mounted a vertical illumination system.

Measurement conditions are standardized, and are referred to an ideal atmospheric temperature of 23 °C, made through oil immersion (with refraction index = 1.518) and a light filter of thickness 546 nm; the microscope is set with a magnifier of 50x (Bustin et al., 1990). Since daylight affect the conditions at which the measurements are performed, it is suitable to recalibrate the instrument more than once through the day.

After setting various parameters related to the microscope light emitter and receiver system the calibration continues with the measurement of three standard samples (with refraction index 0.426, 0.595, 0.905) and after each measurement the correlation line is controlled to be always as close as possible to 1. Each standard sample with at least 10-15 measures (from which an arithmetic mean is then obtained) accomplished on each vitrinite fragment (fig. 4.5).

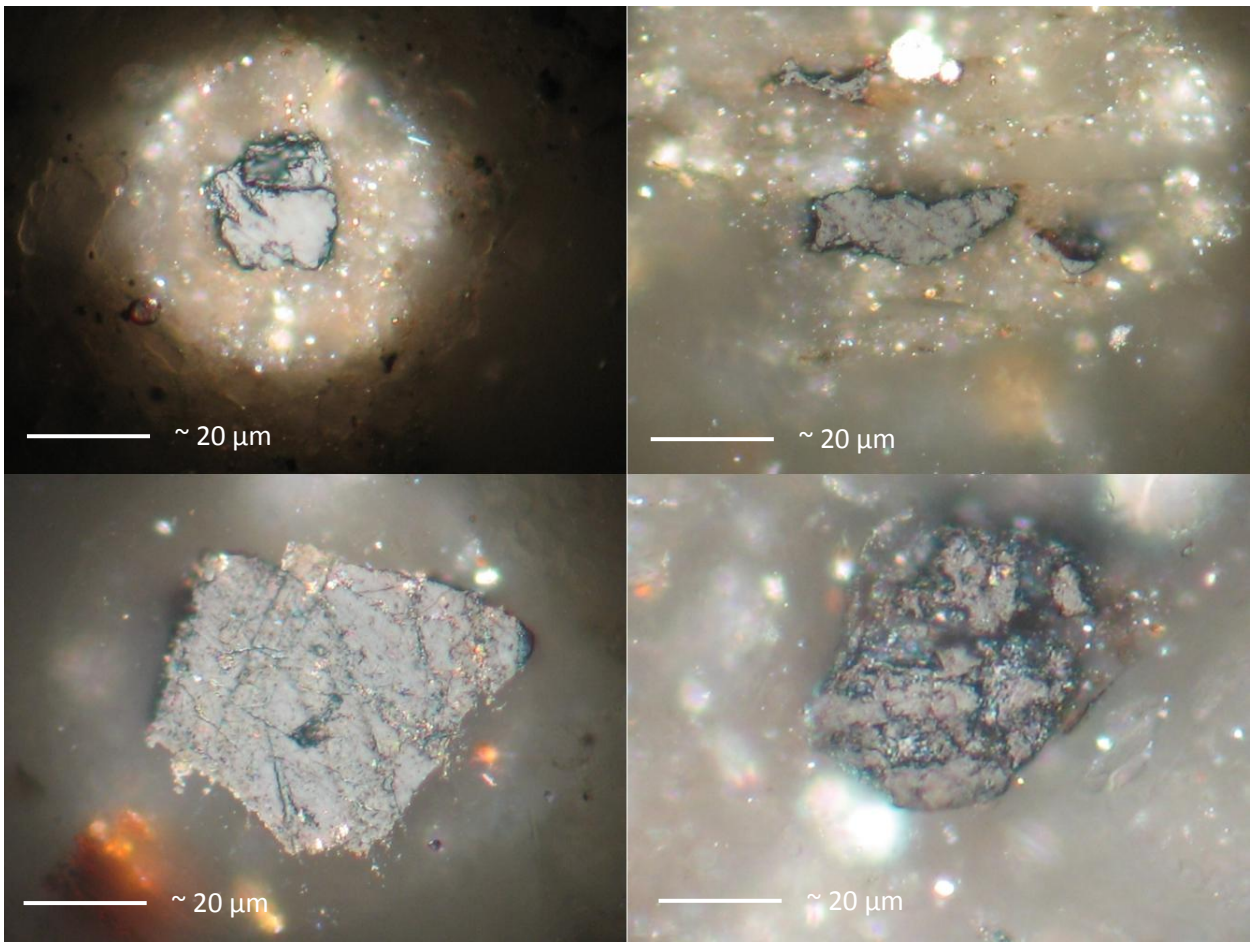

Fig. 4.5 – Examples of microscope photos of vitrinite fragments analyzed in the new data.

Paleotemperatures values are obtained from vitrinite reflectance values adopting Barker and Pawlewicz's equation (1994):

$$T = \frac{\ln(Ro \pm s) + 1.68}{0.0124},$$

where *T* is temperature, in °C, *Ro* is the vitrinite reflectance value and *s* is the standard deviation value.

4.4 Apatite fission track dating

Fission track analysis is a method of determining mineral ages which uses geochronologic dating to give information about both age and temperature of the samples, in particular, as other thermochronologic methods, it is a widely diffused technique adopted to determine the thermal history (T-t paths) of rocks (Gallagher, 1995). The basic difference between apatite fission track dating (AFT dating) and classic geochronologic methods (e.g. U-Pb dating) is that AFT age isn't related to the age of the apatite crystal formation, but it is related to the age at which thermal events affected the crystal at specific moments of the geological history of a rock.

The fission track dating method was born in the '60s of the past century and applied mainly first to apatite and successively also to zircon minerals (Tagami et al., 1999); apatite minerals are characterized by many fundamental characteristics which make them a very suitable mineral fission track dating, such as their nearly ubiquitous natural occurrence in rocks, their physical properties, the chemistry of their major, minor and trace elements, their ability to retain fission tracks in geological environments and the ease of reproduction of many apatite characteristics in labs (Donelick et al., 2005).

The basic principles of the method are related to the fact that the age constraint can be obtained thanks to the radioactive decay occurring in natural unstable isotopes (parent isotopes) which loose particles in order to reach a stable nuclear configuration (daughter isotope). In the described method, in particular, it's taken into account the spontaneous decay of ^{238}U, which occurs at a known rate and it's proportional to the number of parent atoms left at any time, N_p:

$$\frac{dN_p}{dt} = -\lambda N_p,$$

where λ is the decay constant (time^{-1}) and t is time.

^{238}U radioactive decay is achieved mainly through emission of α particles (α-decay) which lead to a stable ^{206}Pb nucleus. Nonetheless for every about two million ^{238}U nuclei undergoing α-decay, one ^{238}U nucleus will experiment spontaneous nuclear fission, whose effect is the formation of tracks, or trails of disrupted atoms inside the crystal lattice.

Therefore in the AFT dating method the measured parent and daughter are the spontaneous and induced fission tracks (fig. 4.6).

Fig. 4.6 – Photomicrograph of a polished and etched prismatic section through an apatite crystal. The arrow indicates the intersection between an etched surface and a horizontal confined track (after Gallagher et al., 1998).

The isotopic age equation, which take into account, thus, spontaneous and induced fission tracks, for the AFT method is the following (Gallagher et al., 1998):

$$t = \frac{1}{\lambda_d} \ln\left(\lambda_d \frac{\rho_s}{\rho_i} \rho_d \zeta g + 1 \right),$$

where t is the age, ρ_s and ρ_i are spontaneous and induced track densities, ρ_d is the track density in a dosimeter (a glass of known Uranium concentration), λ_d is the α-decay constant for ^{238}U, g is a geometry factor, ζ is a constant of proportionality.

The thermochronometric age determined in the AFT dating, therefore, is based on a comparison between spontaneous (i.e. already present before the analysis) and induced (produced in lab) fission tracks (reviews in Gallagher et al., 1998; Gleadow and Brown, 2000; Hurford, 1991; Ravenhurst and Donelick, 1992; Flescher et al., 1975; Wagner and Van den Haute, 1992).

During the cooling history of a rock, when the temperature is still higher than ~120 °C all the tracks formed in apatite crystals are annealed ("repaired") at rates strongly influenced by the apatites chemistry and the tracks crystallographic orientation; thus, the mineral doesn't record anything of the rock thermal history and its age is equal to 0 (Green et al., 1986; Carlson, 1990; Donelick et al., 1999; Barbarand, 2003). Only once the temperature drop under this temperature the system starts to retain fission tracks, which are only partially annealed, until the temperature decreases under ~70 °C, when the system can be considered almost "closed", allowing the crystals to entirely preserve the tracks (fig. 4.7). The field comprised between ~70-120 °C is thus called Partial Annealing Zone (PAZ) (Naeser, 1979; Wagner, 1979), a concept that is analogous to the partial retention zone in other isotopic systems (e.g. U-TH-Sm/He in apatite and zircon).

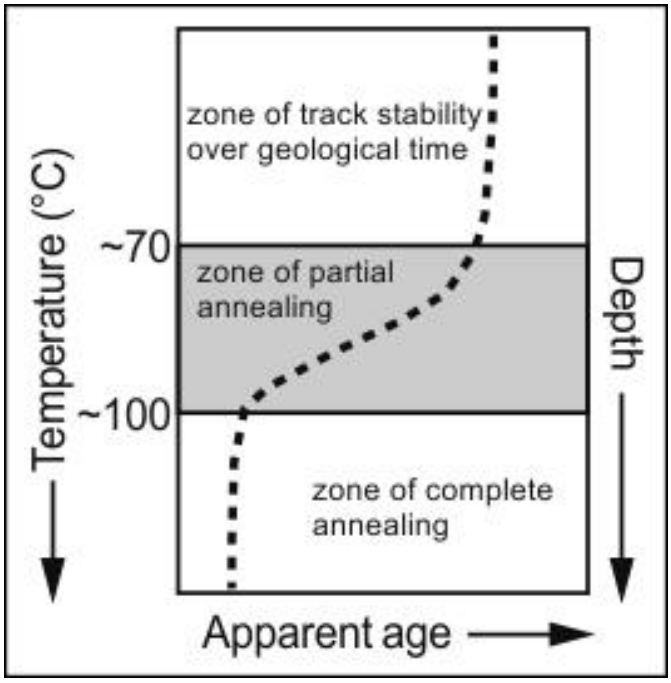

Fig. 4.7 - An apatite age profile with a distinctive shape within the partial annealing zone because of its characteristics of track annealing. Here a partial annealing zone (PAZ) has formed in a relatively stable thermotectonic environment over some time. Thermochronological ages decrease rapidly in the PAZ. The depth of the system base depends on the geothermal gradient (modified after Fitzgerald et al., 1995).

Apatites in a rock sample at surface, consequently, preserve a mix of tracks which are partly annealed and partly fully preserved, related to the last thermal event responsible for the rock cooling down under 120 °C, which might not coincide with the last thermal event, and above all with the last geological/exhumational event affecting the history of the rock. In this last case, the preserved fission tracks would hold the record of more than one events in the evolution of the sample.

4.4.1 AFT dating sample preparation and analysis

Apatite grains are usually separated through a series of phases, in most part common to separation processes of other heavy minerals.

After a first reduction of the rock samples to a granulometry of about ~200-300 μm in a jaw crusher, the apatites are separated, together with other heavy minerals such as zircons, in a water shaking table. Then the use of heavy liquids and magnetic separation techniques coupled with a final manual microscope check allow to obtain the apatite grains which are subsequently mounted on holders. At this point the samples are polished and etched with HNO_3, in order to reveal and highlight the grains spontaneous tracks. Next the samples are covered by standard CN-5 glass dosimeter (with known U-content) and a low-U muscovite external detector, and together irradiated by thermal neutrons which induce the formation of new fission tracks. After another phase of track etching in the external detector through HF, the samples are ready for the optical analysis, which basically compare the length of the spontaneous tracks in the apatite grains (partially shortened by annealing processes) and the induced tracks in the muscovite external detector which preserve their maximum length according to the grain chemical and physical properties. In each sample 20 randomly encountered grains and 100 randomly encountered tracks are usually measured (where present), and this approach provides a reasonable results both in terms of statistics and economy of the analysis (Donelick et al., 2005). For each sample, finally a central age from the logarithmic mean of the single-grain ages and the associated age dispersion is calculated.

4.5 Paleothermal and thermochronologic data in the Northern Apennines

The Northern Apennines are characterized by a large dataset of paleothermal (vitrinite reflectance and clay mineral analyses) and thermochronological (AFT, ZFT, U-Th/He in apatite and zircon) data related to all the main tectonic units, and the main regional-scale trends regarding burial, exhumation and timing of the related tectonic processes have been long-recognized and highlighted in literature (Corrado et al., 2010 and references therein; Thomson et al., 2010 and references therein, see also § 5).

In order to understand what was the state of the art of the afore-mentioned analyses inside the study area, all previously published paleothermal and thermochronological data have been collected in the afore mentioned GIS-referenced dataset (figs. 4.8, 4.9).

Paleothermal analyses have been performed since the end of the '70s of the last century, also inside the study area (fig. 4.8) (Bonazzi et al., 1982, 1984, 1987, 1989; Cerrina Feroni et al., 1983, 1985; Reutter et al., 1980, 1983, 1991; Venturelli and Frey, 1978), but the evolution of lab methods, standards, reference scales and the uncertainty of old samples location didn't allow to directly compare the published results with paleothermal data produced today. Thermochronological data, on the contrary, were almost totally lacking inside the area investigated in this study (fig. 4.9).

These observations and results derived from literature, thus, led us to conclude that a new set of samples was needed in order to investigate the thermo-tectonic evolution of the study area.

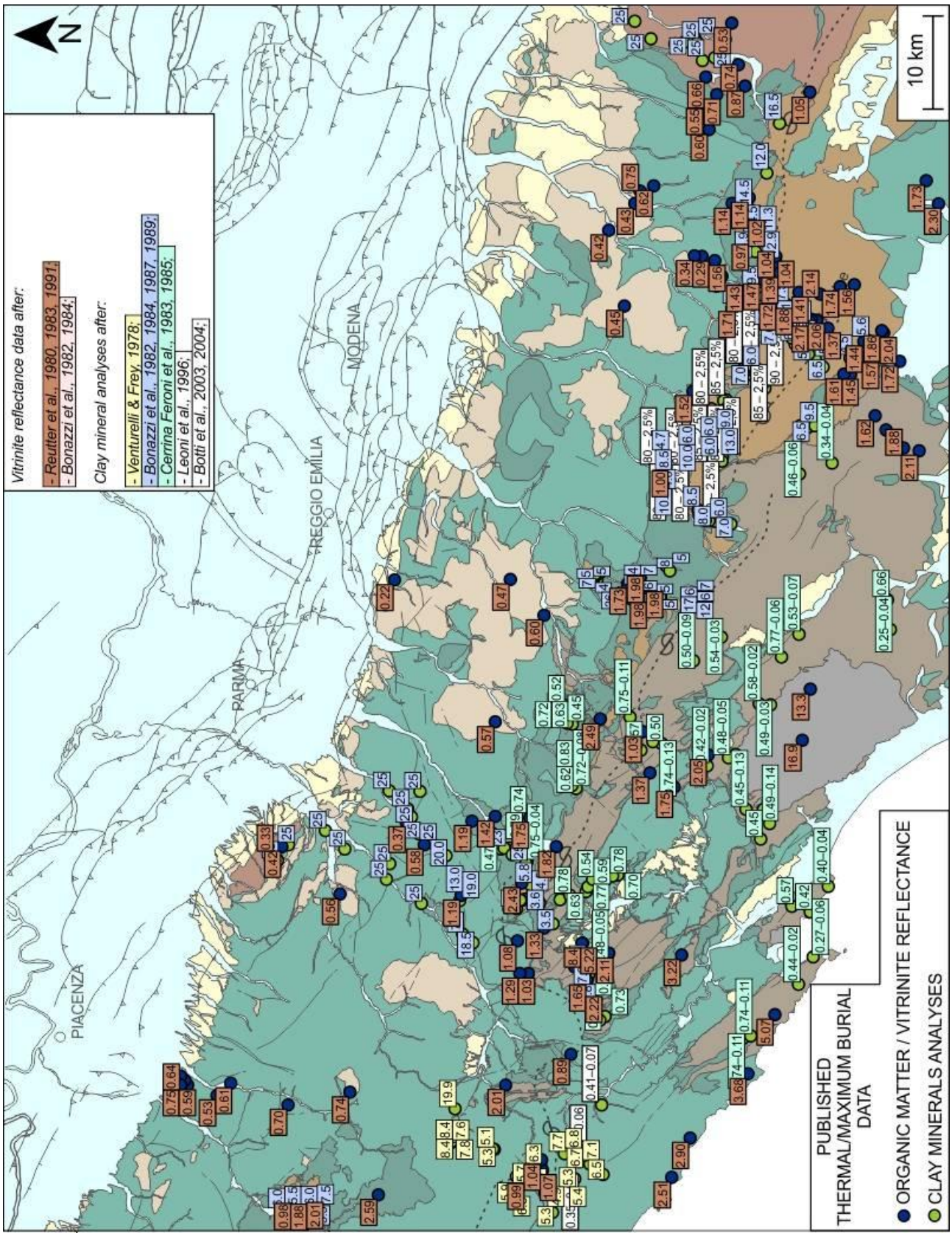

4.8 – Synthetic geological map of the Northern Apennines with previously published paleothermal data; values are referred to analyses of vitrinite reflectance and clay mineral based geothermometers (KI and illite content in mixed layer I-S). The white labels refer to the only data produced with modern lab procedures, directly comparable with the new data shown in this work (see § 5).

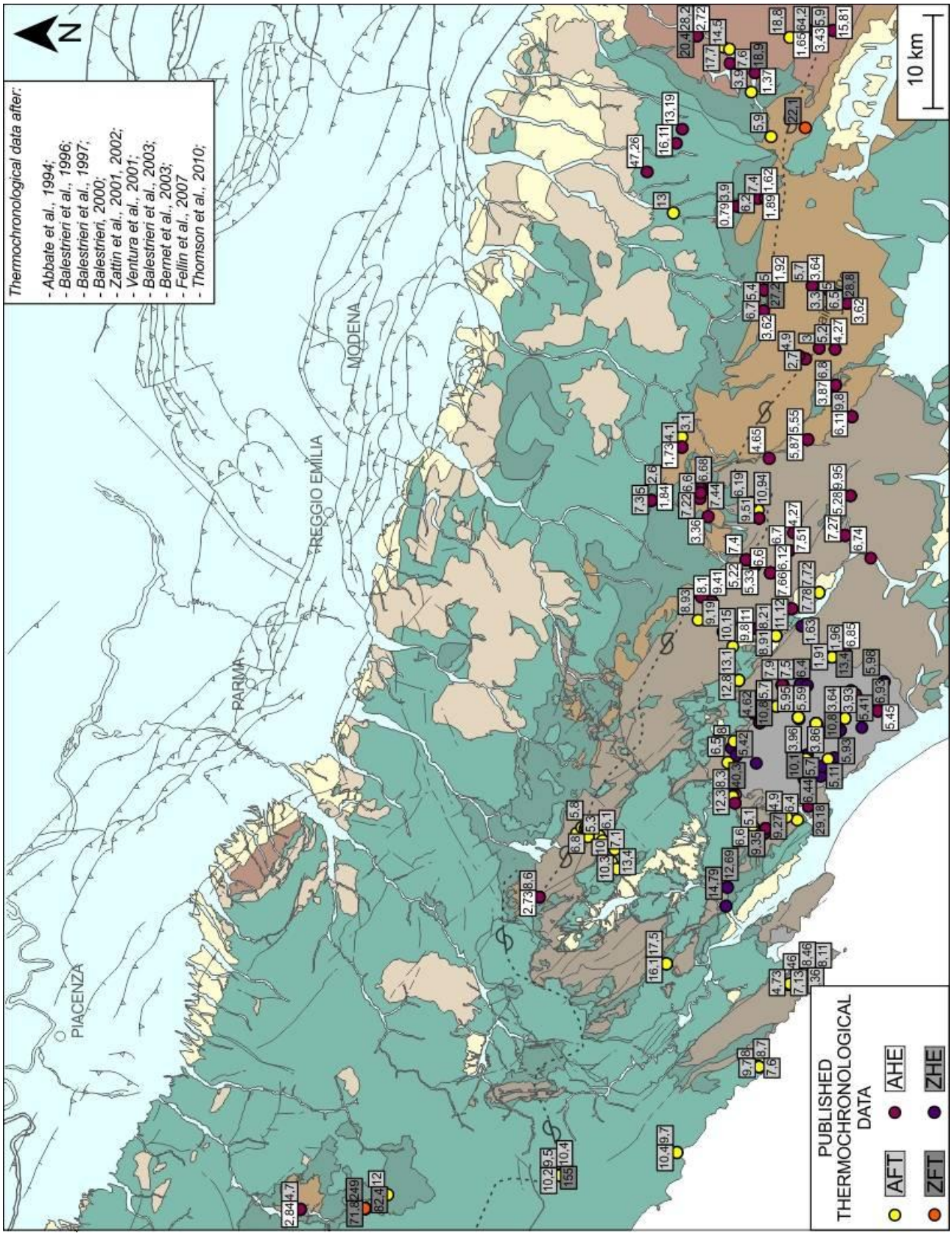

4.9 – Synthetic geological map of the Northern Apennines with previously published thermochronological data; values are referred to analyses of fission tracks and U/Th-He diffusion in both apatites and zircons; the new data shown in this work have been fully integrated with this previously published dataset (see § 5). AFT: apatite fission track; AHE: U/Th-He in apatite; ZFT: zircon fission track; ZHE: U/Th-He in zircon.

4.5.1 New paleothermal and thermochronological data: sampling strategy and methods for temperature-depth conversion

The new samples have been collected following in each sampling site, where possible, these two criteria: 1) sampling for all of the three afore listed methodologies; 2) sampling all the main tectonic units occurring within the study area. We collected and analyzed 21 new samples for vitrinite reflectance, 22 for clay minerals analyses (Kübler Index and % illite in I-S mixed layer clay minerals) and 15 for apatite fission track datings, in areas located near the main ridge of the chain and in four tectonic window, where all the major tectonic units crop out and paleothermal/thermochronological data were lacking (table 1, fig. 4.10).

	Sample	Latitude	Longitude	Elevation (m)	Domain	Ro%	KI	%I in I-S	AFT ages (My)
1	PR 10	44,509	9,792	458	Epil.	0,482			
2	PR 12	44,353	9,776	668	Tusc.	0,855	0,48	94%	8,70
3	PR 3	44,446	9,943	600	Tusc.	1,010	0,55	94%	6,20
4	PR 5	44,456	9,804	718	Lig.	0,827	0,77	84%	7,80
5	PR 6.1	44,456	9,783	600	Sublig.	0,658	0,67	92%	4,30
6	PR 6.2	44,456	9,783	602	Sublig.		0,84	87%	
7	PR 25.1	44,320	9,995	248	Tusc.	1,695			7,00
8	PR 27	44,525	9,824	618	Epil.	0,735			4,70
9	PR 30	44,755	10,037	224	Umbria-R.	0,200			
10	PR 31	44,751	10,031	243	Umbria-R.	0,255			
11	PR 32	44,755	10,022	269	Epil.	0,333			
12	PR 4	44,439	9,919	535	Tusc.	1,700			
13	PR 7	44,550	11,239	301	Sublig.	1,110			4,90
14	PR 1	44,468	9,937	973	Lig.		0,74	85%	
15	PR 2	44,465	9,941	929	Sublig.		0,8	80%	
16	PR 8	44,549	9,940	310	Sublig.		0,67	68%	
17	PR 9	44,561	9,927	326	Lig.		0,71	78%	
18	PR 11	44,463	9,930	880	Sublig.				8,70
19	R 15	44,472	9,966	1085	Lig.				7,30
20	PR 17	44,379	10,196	860	Lig.				4,10
21	PR 18	44,380	10,194	780	Sublig.				4,60
22	PR 26	44,463	9,602	1135	Tusc.				5,40
23	PR 33	44,755	9,975	550	Lig.				76,90
24	PR 28.1	44,522	9,931	710	Lig.				3,20
25	PR 28.2	44,522	9,931	702	Lig.				4,10

Table 1 - New samples collected for the present study. The location of the sample is indicated in fig.4.10. Epil.: Epiligurian succession; Tusc.: Tuscan foredeep units; Lig.: Ligurian units (upper LSU); Subl.: Subligurian units (lower LSU); Umbria-R.: Umbria-Romagna foredeep units.

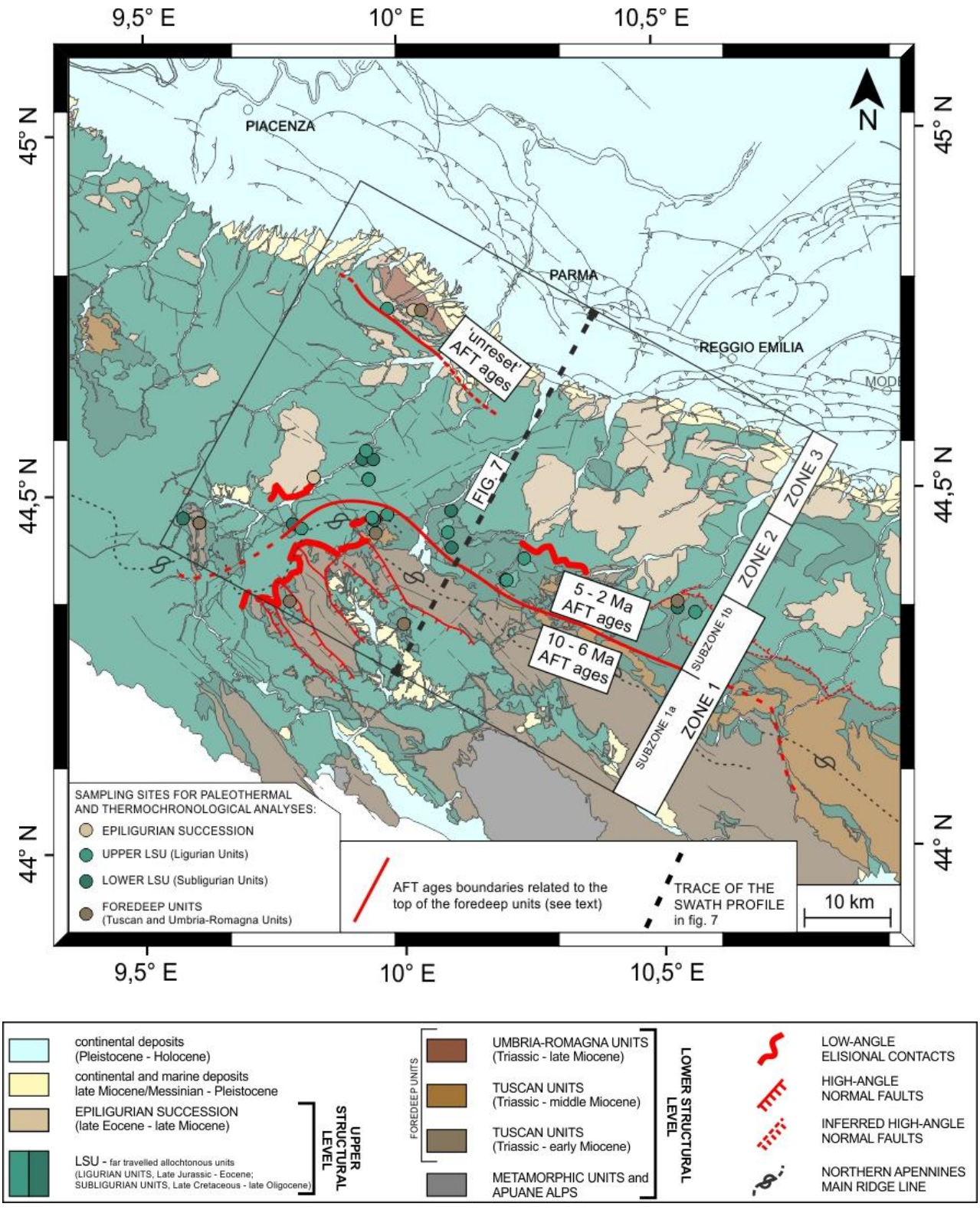

Fig. 4.10 - Synthetic geological map of the study area with location of the new samples collected for paleothermal and thermochronological analyses (see § 5 for further explanations).

5. Uplift and reshaping of far-travelled/allochthonous tectonic units in the western Northern Apennines (Italy)

The content of this chapter constitutes the core of a paper which will be shortly submitted (Carlini et al., in preparation), as mentioned in § 1.

In order to simplify the presentation of the data and results, the study area has been subdivided in three zones and two subzones in which boreholes, thermal and thermochronological data and LSU geometry have similarities (Zone 1 with Subzones 1a and 1b, Zone 2 and Zone 3, fig. 3.1). These zones cover, from SW to NE, the main ridge and higher slope area (Zone 1), the mid-slope area (Zone 2), and the Apenninic external (NE) margin (Zone 3); as it will be see, they also roughly correspond to portions of the LSU which experienced a common evolutionary history.

5.1 The far-travelled/allochthonous LSU in the western Northern Apennines

The far-travelled/allochthonous LSU are the remnants of a Late-Cretaceous – middle Eocene oceanic accretionary wedge. Since the late Oligocene, the orogenic processes, related to the continental collision, caused the translation of the LSU above the foredeep units over a distance of ~100 km, from the present-day Tyrrhenian coastline to the Apennine foothills, south of the Po Plain (fig. 2.2 and previous chapter § 2). The translation occurred at various steps as testified by the progressively younger age of the foredeep deposits underneath the LSU (fig. 3.1) (Boccaletti et al., 1990; Ricci Lucchi, 1986).

During the middle Miocene, the LSU leading edge was placed in a not well defined position SW of the Serravallian Marnoso-arenacea foredeep; LSU-derived mass-transport deposits inside this foredeep deposits are witnesses of the proximity of the LSU to the basin (Pini, 1999; Camerlenghi and Pini, 2009 and references therein). This testifies that from middle to late Miocene the LSU moved further NE, towards the position they occupy at present close to the outer (NE) margin of the Northern Apennines foothills; in fact, here the LSU are unconformably overlain by late Messinian to Recent deposits (see above, fig. 2.2). Within the study area, the boundary between the early and middle Miocene foredeep deposits (approximately traced in fig. 3.1) can be located underneath the LSU ~12 km SW of the topographic front, as derived from available surface and subsurface borehole stratigraphies. This measure (~12 km) represents an estimate of the distance covered by the LSU since the middle Miocene in the investigated area.

The timing and amplitude of the LSU translation, however, is strongly influenced by the varying width and morphology of the Apennine foredeep basins along the NW-SE direction (Mutti et al., 2002; Ricci Lucchi, 1986). In fact, SE of the study area, the LSU leading edge during the middle Miocene was placed ~30 km SW of the present-day Apennine topographic front, and covered most of this distance during the Serravallian-Tortonian time interval (Landuzzi, 1994; Zattin et al., 2002).

During the early collisional phases (late Oligocene-early Miocene), the LSU belonging to the NE slope of the Northern Apennines (fig. 2.2) were characterized by a geometry which tapered out towards the foreland area, (i.e., to the NE; Principi and Treves, 1984; Remitti et al., 2011; Vannucchi et al., 2008; Zattin et al., 2002). As it will be shown later (see chapter § 5.2), the late collisional phases (mainly of late Miocene to Recent age) caused the LSU to be strongly reshaped and to acquire a double tapered wedge geometry, with thinner edges both towards SW and NE.

Although it is commonly agreed that the external (NE) portion of the LSU wedge was deeply reshaped by surface sedimentary mass-wasting processes (Artoni et al., 2010; Papani et al., 1987; Remitti et al., 2011), there is still poor agreement about the mechanisms responsible for the reshaping of the LSU wedge in its inner (SW) portions. There, the anomalous reduced thickness of the LSU has been mainly ascribed to tectonic elision processes related to shallow low angle normal faults (Artoni et al., 2006; Bettelli et al., 2002), or folding and doubling of the underlying basement and foredeep units (e.g., Boccaletti et al., 2011; Molli et al., 2010). Moreover, it is not yet clear whether one of the afore-mentioned processes could have predominated or they mutually exclude each other, and what is their precise timing. However, it is remarkable that the reshaping of the LSU occurred when the Apenninic orogenic wedge was affected by coeval extensional and compressional tectonics (see § 2).

5.2 The present-day geometry of LSU derived from integrated surface and subsurface geological data

The present-day geometry of the LSU has been constrained by integrating surface and subsurface data; the compiled geological sketch map shows that the LSU are present over most of the study area, sealed by the middle Eocene to Tortonian Epiligurian succession and the late Messinian to Holocene deposits at the Apennine foothills (fig. 2.2). The LSU were translated over

the foredeep units which crop out along the main divide of the mountain chain and in tectonic windows (fig. 2.2).

5.2.1 Surface geological cross sections

Within Zone 1, the present-day geometry of the LSU and their relationships with all the major tectonic units are shown by the 7 most relevant of the 23 collected geological cross sections (figs. 3.1, 5.1, SM1.1 - Supplementary Material 1). In this area, in fact, the lower (over the Tuscan units) and upper (beneath the Epiligurian succession) main contacts of the LSU crop out.

The present-day geometry of the basal contact and other main tectonic discontinuities in the lower portion of the LSU (e.g., the contact between the Ligurian and the underlying Subligurian units) are represented by NE-dipping low- and high-angle surfaces (figs. 3.1, 5.1).

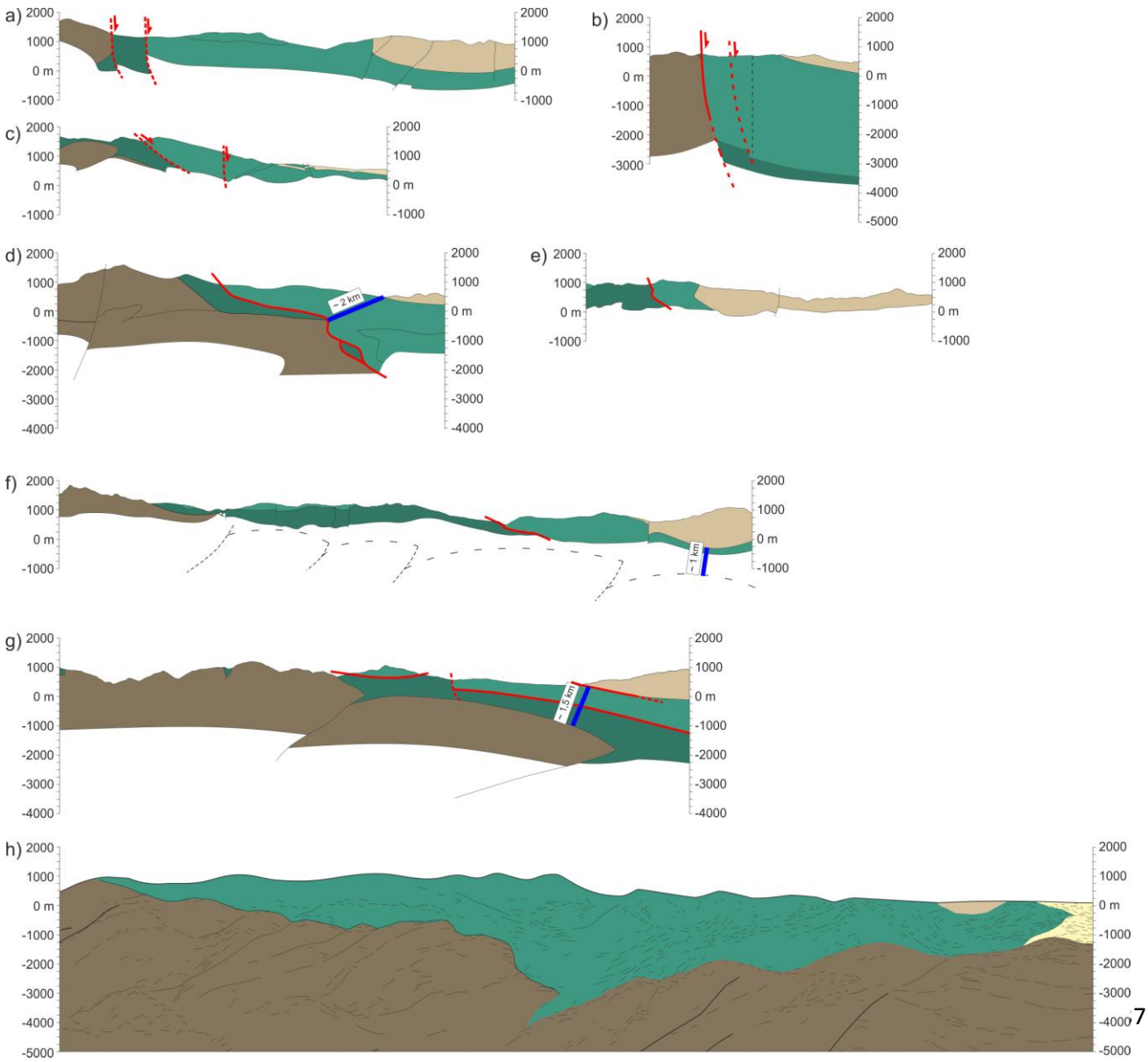

Some of these NE-dipping contacts are located ~1000 m above the LSU basal contact with the Tuscan Unit (fig. 5.1). According to the literature, the basal contact of the LSU has not been reactivated but it has been passively deformed by the thrusting and folding affecting the underlying Tuscan foredeep units during late Miocene - early Pliocene times. On the other hand, the possible reactivation of pre-existing weakness surfaces within the LSU, above their basal contact, is still a matter of debate. As a matter of fact the low and high-angle NE-dipping surfaces inside the LSU (figs. 3.1, 5.1) have been interpreted in basically two different ways:

1) as a NE gentle tilting (low-angle) or folding and verticalization (high-angle) of the older overthrust contacts inside the LSU, in response to the tilting and folding of the underlying foredeep units (Boccaletti et al., 2011; Cerrina Feroni et al., 2002; CNR, 1980);

2) as late Miocene low-angle normal faults delaminating and reactivating older overthrust surfaces inside the lower portion of the LSU, cut by younger high-angle normal faults (Bettelli et al., 2002; Plesi et al., 2002; Vannucchi et al., 2008).

In the seven cross-sections we analyzed (fig. 5.1), the upper boundary of the LSU is represented by the basal contact of the overlying Epiligurian succession or is under erosion at the topographic surface. Because the preserved Epiligurian succession is much less deformed compared with the underlying LSU (Bettelli et al., 1987), it can be argued that the contact between the two units (i.e., LSU-Epiligurian succession) was not been significantly deformed after the beginning of the deposition inside the wedge-top basins (i.e., after the middle-late Eocene § 2). Nonetheless, locally low-angle extensional and compressional tectonic features affect the upper portion of the LSU, in proximity of the base of the Epiligurian succession (e.g., the extensional fault in the M.te Barigazzo area – a) in fig. 3.1, Artoni et al., 2006; overturned fold of Ranzano area – b) in fig. 3.1, Cerrina Feroni et al., 2002).

Fig. 5.1: Geological cross-sections across the study area. See fig. 3.1 for locations. a) modified after Bettelli et al., 2002; b) modified after Plesi et al., 2002; c) modified after Plesi et al., 2002; d) modified after CNR, 1980; e) modified after Cerrina Feroni et al., 2002; f) modified after Puccinelli et al., in press (a) and Cerrina Feroni et al., 2002; g) from this work; h) modified after Camurri, 2000.

Within Zone 1, low-angle extensional faults affecting the whole LSU are very common (A_L, B_L and C_L in fig. 3.1); these faults put in contact units belonging to different structural levels within the LSU wedge. They locally involve the overlying Epiligurian succession, implying the removal of several kilometres of LSU which are presently missing (Artoni et al., 2006; Bernini et al., 1997; Cerrina Feroni et al., 2002; Elter and Schwab, 1959; Papani et al., 1987; Puccinelli et al., in press (a); Vescovi, 1991; Vescovi et al., 2002;). In particular, A_L brings the Epiligurian succession directly on top of the lower portion of the LSU, while B_L and C_L downthrows the very upper portion of the LSU (Ligurian Units) onto the bottom portion of the LSU (Subligurian Units) or upon the Macigno foredeep deposits (B_L).

The seven cross-sections (fig. 5.1) allowed to estimate that within Zone 1 the LSU are ~1000-2000 m thick. This thickness corresponds to the distance between the base of the Epiligurian succession and the top of the Tuscan/foredeep units (figs. 3.1, 5.1). The field evidences and the non-reactivation of both the basal an upper contacts of the LSU imply that the reshaping processes acted predominantly inside the LSU wedge, leaving undisturbed its top and basal tectonic boundaries. This is an important constrain as it will be discussed later (see § 5.6).

The present-day LSU geometry has been constrained also by a regional-scale seismic line, depth converted and crossing the study area between the Taro and the Parma rivers (fig. 5.1h) (Camurri et al., 2001) and confirmed in newly analysed seismic profiles (figs. 3.2, 3.3). This regional scale cross-section depicts the LSU as a SW and NE out-tapering body, characterized by the highest thickness of ~4000 m in its central portion, i.e., within Zone 2 (fig. 5.1h); within Zones 1 and 3 the LSU are ~1000-2000 m and ~1000 m thick, respectively.

5.2.2 Boreholes data

The thickness of the LSU calculated by the well stratigraphies has been correlated along three strike-oriented transects, with respect to the main NW-SE trend of the chain axis (S1, S2 and S3), which correspond to the three zones shown in fig. 3.1.

Section 1 (fig. 5.2a) comprises the wells located in the innermost part of the outcropping LSU, close to the basal contact of the LSU lying over the Tuscan units (Zone 1). The three westernmost wells (Lama dei Cerri, Corniglio, Monchio delle Corti) intercept the base of the LSU at a depth between ~1000 and 1700 m below the surface, while the two

eastern boreholes (Quara and Sestola), on the contrary, were drilled down to more than 3000 m without reaching the top of the Tuscan units. This important thickness lateral variability is related to the fact that the SE portion of the study area was locally affected by post-Miocene high angle extensional tectonics downthrowing the base of the LSU (Bettelli et al., 2002; Plesi et al., 2002; Vannucchi et al., 2008) (see § 5.2.1).

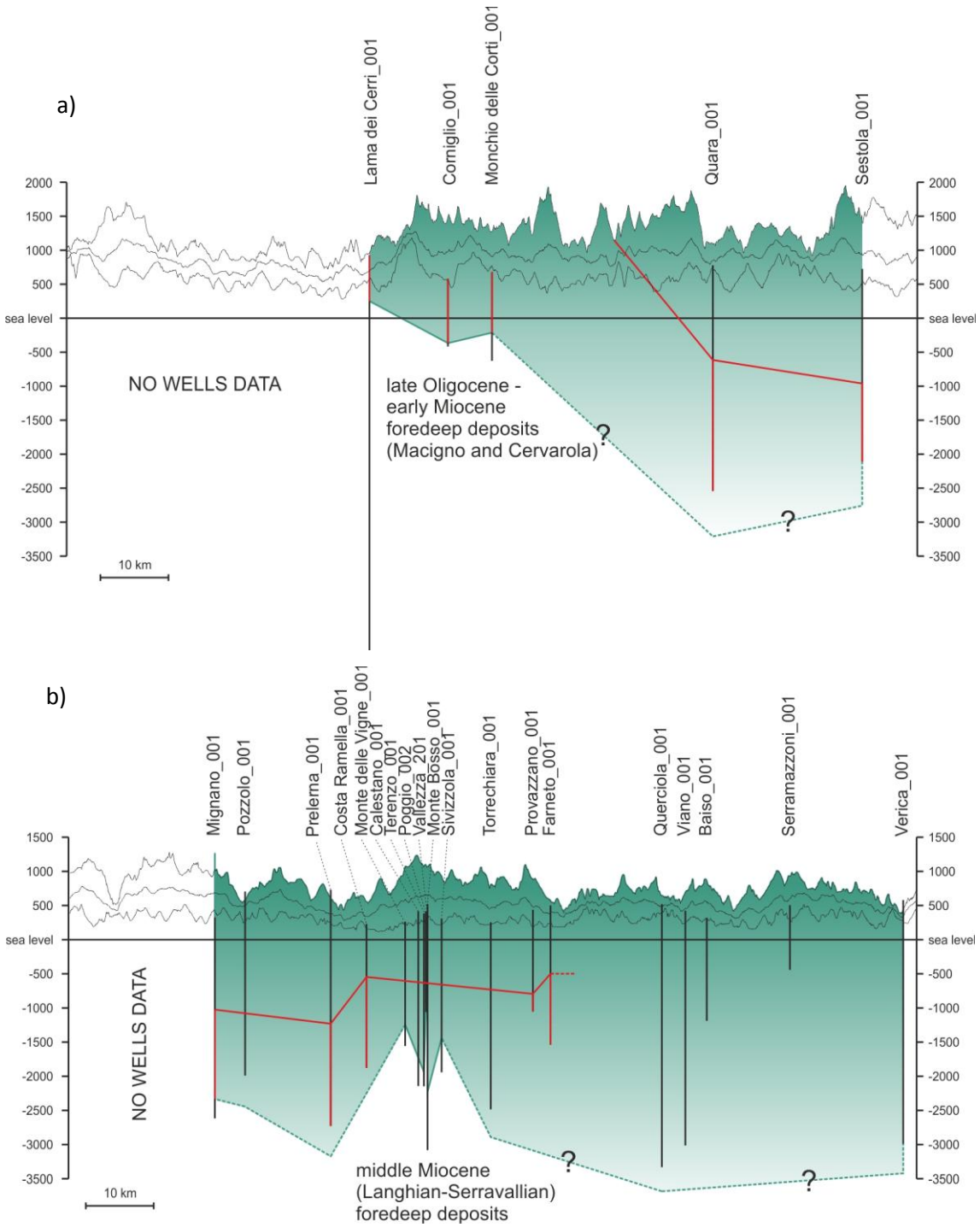

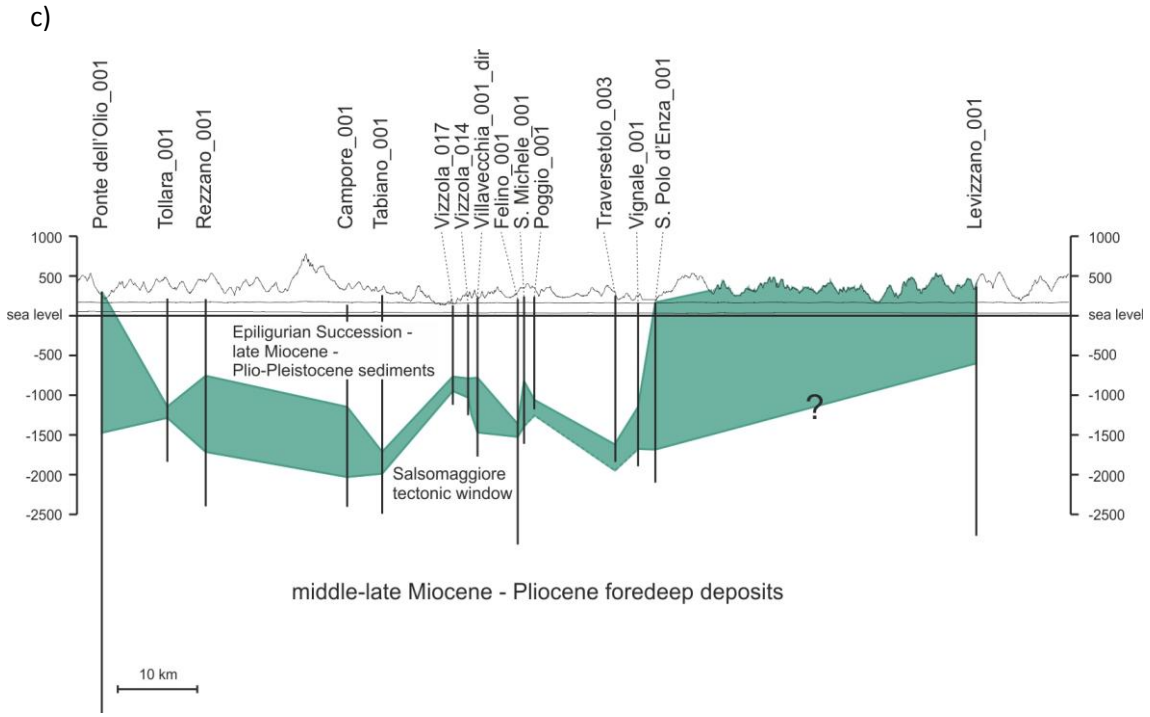

fig. 5.2: Boreholes correlations. a) Section 1 within Zone 1 – higher slope area; b) section 2 within Zone 2 – mid-slope area; c) section 3 within Zone 3 – lower slope area. The green areas represent the thickness of the LSU, the horizontal red lines indicate the boundary between Ligurian (above) and Subligurian (below) units inside the LSU, the vertical redlines indicate the portion of the boreholes in which the Subligurian units are found. Boreholes data and stratigraphies come and are freely downloadable from http://unmig.sviluppoeconomico.gov.it/videpi/.

The correlation between the wells in section 2 (fig. 5.2b) shows an increase of the LSU thickness up to more than ~3000 m in this mid-slope area (Zone 2). Even if most of the wells in this section did not reach the base of the LSU, a minimum thickness of ~4500 m can be estimated. The seven central wells of the section (namely Monte delle Vigne, Calestano, Terenzo, Poggio, Vallezza, Monte Bosso, Sivizzola) reached the top of the foredeep units and highlight an average thickness for the LSU of ~3000 m. The anomaly in the central portion of this section can be explained by the presence of SW-NE-oriented tectonic discontinuities which affect the base of the LSU between the Parma and Taro rivers (e.g., the "Taro Line", Argnani et al., 2003 and references therein).

Section 3 (fig. 5.2c) shows the thickness of the LSU along the external margin of the chain (Zone 3). Despite the irregular geometry, the thickness of the LSU ranges from a couple of hundreds of meters (mostly in the western portion) to a maximum of ~1000 m, with local maxima of ~2000 m (in Ponte dell'Olio, S. Polo d'Enza and Levizzano boreholes). Thickness changes, occurring within distances lower than 10 km, are related to: 1) the original shape of the LSU (e.g., between Campore and S. Polo d'Enza boreholes), 2) the late Messinian mass-transport deposits departed from the top of the LSU (Artoni et al., 2010 and references

therein), 3) the proximity to subsurface structures related to the underlying foredeep units (e.g., Salsomaggiore anticline close to Vizzola and Tabiano wells), and 4) the discontinuous occurrence of the Epiligurian succession and/or the Quaternary deposits, which locally seal the top of the LSU wedge (e.g., San Michele, Felino and Poggio boreholes).

Summarizing, the boreholes data indicate that the LSU are characterized by maximum thickness values in the mid-slope area (Zone 2) and minimum thickness values moving towards both the LSU inner (SW, Zone 1) and outer (NE, Zone 3) tips (fig. 5.2).

5.3 Surface and sub-surface geological data analysis: geometry and lateral variability of the LSU

Despite uncertainties and the occurrence of irregular features, the geological cross sections, seismic line interpretations and boreholes data are consistent and allowed a reconstruction of the present-day geometry of the LSU wedge.

This geometry can be visualized on the isopach map of figure 5.3a, showing the LSU thickness. The depth of the LSU base has been calculated by integrating all the subsurface and surface geological data (comprised the LSU SW outcropping boundary and the NE extension of the mass-wasted bodies) and interpolated through a cubic algorithm from Mathworks Matlab 7.10. Then, the present-day upper surface of the LSU (used to construct the isopach map but not represented in fig. 5.3a) has been obtained by subtracting the thickness of the preserved Epiligurian succession from the topography. The isopach map, finally, has been obtained through the use of the ESRI ArcMAP 10 Spatial Analyst's "Plus" tool which added both the depth of the basal surface and the elevation of the upper surface at each point of the map. The resulting total estimated thickness of the present-day LSU body has been contoured with isolines ranging between ~4100 m (in the central portion) and 0 m (by the inner and outer edges).

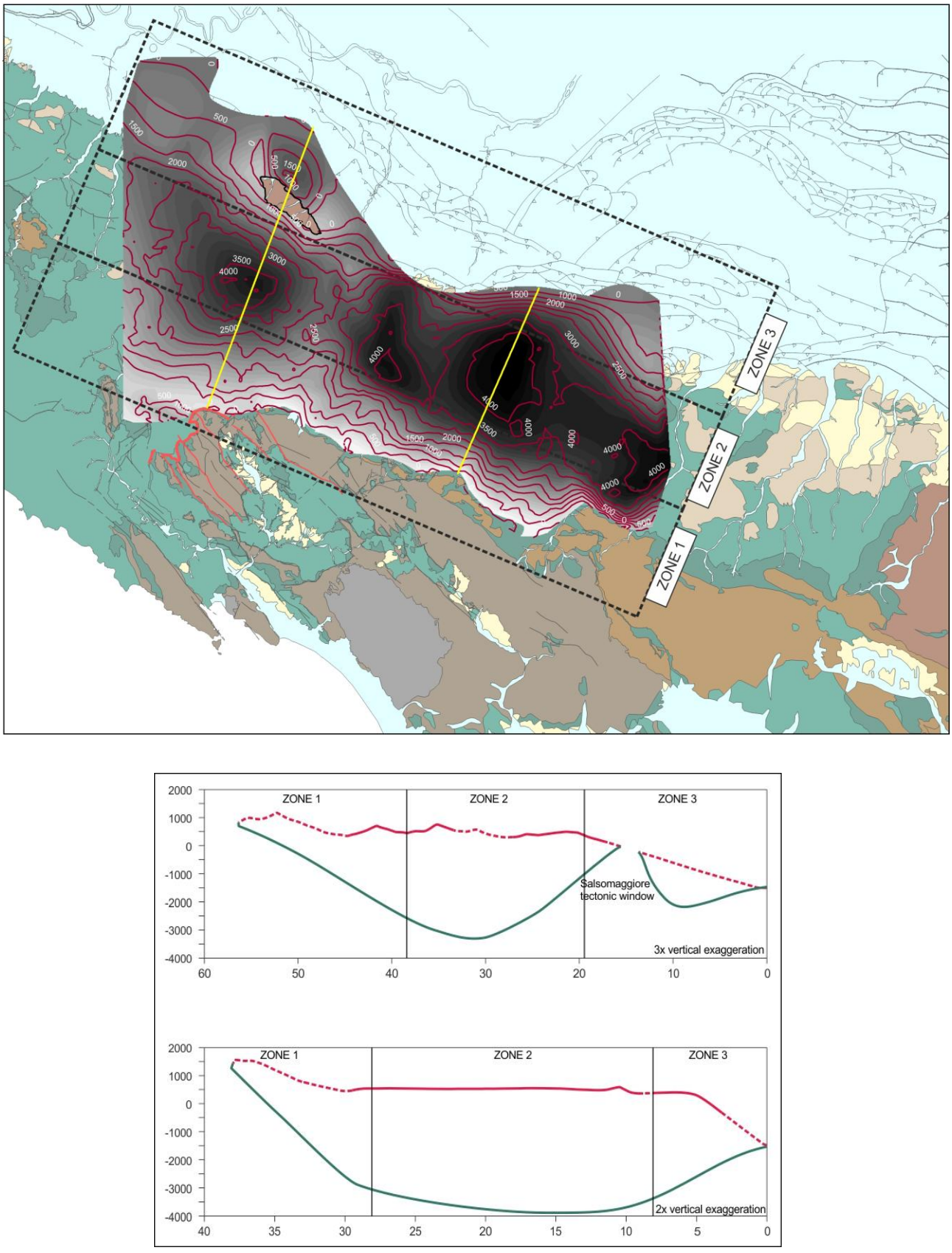

Fig. 5.3: present-day geometry of the LSU inferred from surface and subsurface geological data. a) 3D shaded map of the LSU basal trend, isopachs of the LSU and boundaries of Zones 1, 2 and 3; yellow lines represent the traces of the profiles depicted in fig. 5.3b. b) Profiles A and B traced across the upper (not represented) and basal (3D shaded map in fig. 5.3a) surfaces of the LSU; the red lines represent the LSU upper boundary (solid when constrained by the Epiligurian Succession, dashed where constrained by topography), the green lines represent the trend of the basal surface.

Two cross-sections, A and B (fig. 5.3b), visualize the double tapered wedge geometry of the LSU in the two portions where the LSU are thicker. Within both inner Zone 1 (SW) and outer Zone 3 (NE) the LSU basal trend shows a high variability in dip angles, ranging from values < 25° to > 45°. This variability, highlighted also by the geological cross sections and the boreholes sections (figs. 3.1, 5.1 and 5.2), can be related to:

- the discontinuous presence of high angle extensional features cross-cutting former low-angle NE-dipping faults along the inner zone (see § 5.2.1);
- the presence of tectonic discontinuities affecting the base of the LSU and of structural highs at the top of the foredeep units along the outer zone. The most prominent structure is the Salsomaggiore tectonic window, where Umbria-Romagna foredeep units crop out.

5.4 Vitrinite reflectance, clay minerals and AFT results

We collected new samples for each tectonic unit outcropping within the study area favouring techniques crosschecking in each sampling site (tab. 1).The multi-method approach (see § 4) allows us to get information about timing and entity of exhumation relative to: 1) each tectonic unit; 2) eventual coupling/decoupling events of the units during the exhumation processes.

Maximum temperatures and cooling ages are from Zone 1 and Zone 3, and correspond to section 1 and section 3 of the boreholes correlation (fig. 5.2, table 1). The lack of foredeep units exposure within Zone 2, related to the fact that in this area only the shallower portion of the LSU crops out, led us to favour the sampling within zones 1 and 3.

Fig. 5.4: thermal and thermochronological data newly collected in the study area; maximum temperatures and cooling ages are plotted with error bars, versus the samples distance from the NE front of the chain; the solid black lines represent the general trend of the data related to the top of the sampled foredeep units, see § 5.2 for explanation. a) Vitrinite Reflectance values; b) clay mineral analyses (square and triangles represent the two different clay minerals analyses); c) AFT ages; the horizontal black dashed line inside Zone 1 represent the boundary between Subzones 1a and 1b; the red ovals represent two tectonic windows in which the second younging trend is observable; the blue box represent the Valdena tectonic window (see fig. 3.1 for location).

a)

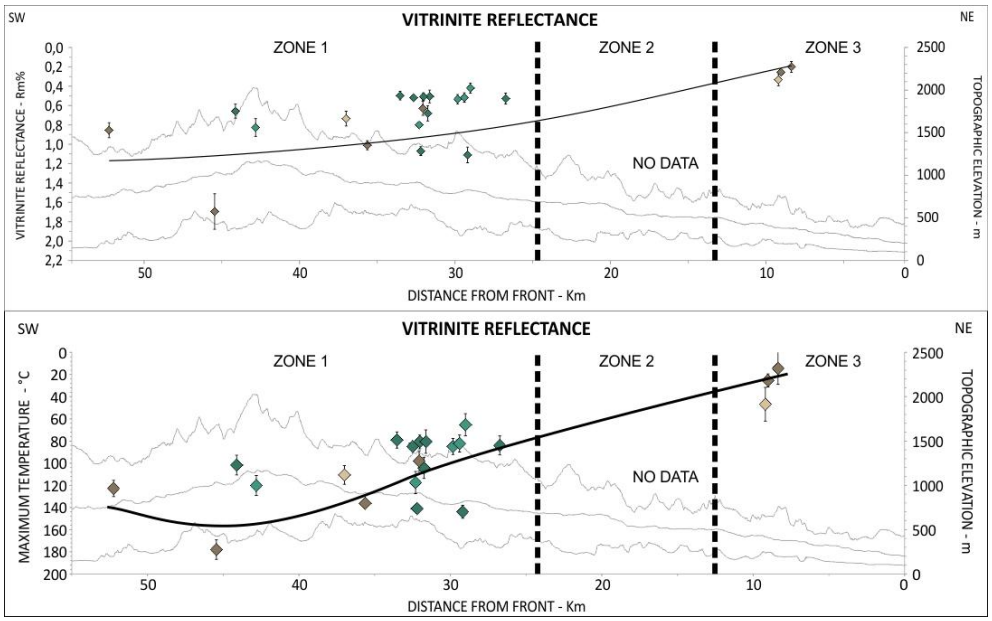
SW
VITRINITE REFLECTANCE
NE
ZONE 1
ZONE 2
ZONE 3
NO DATA
VITRINITE REFLECTANCE - Rm%
TOPOGRAPHIC ELEVATION - m
DISTANCE FROM FRONT - Km
SW
VITRINITE REFLECTANCE
NE
ZONE 1
ZONE 2
ZONE 3
NO DATA
MAXIMUM TEMPERATURE - °C
TOPOGRAPHIC ELEVATION - m
DISTANCE FROM FRONT - Km

b)

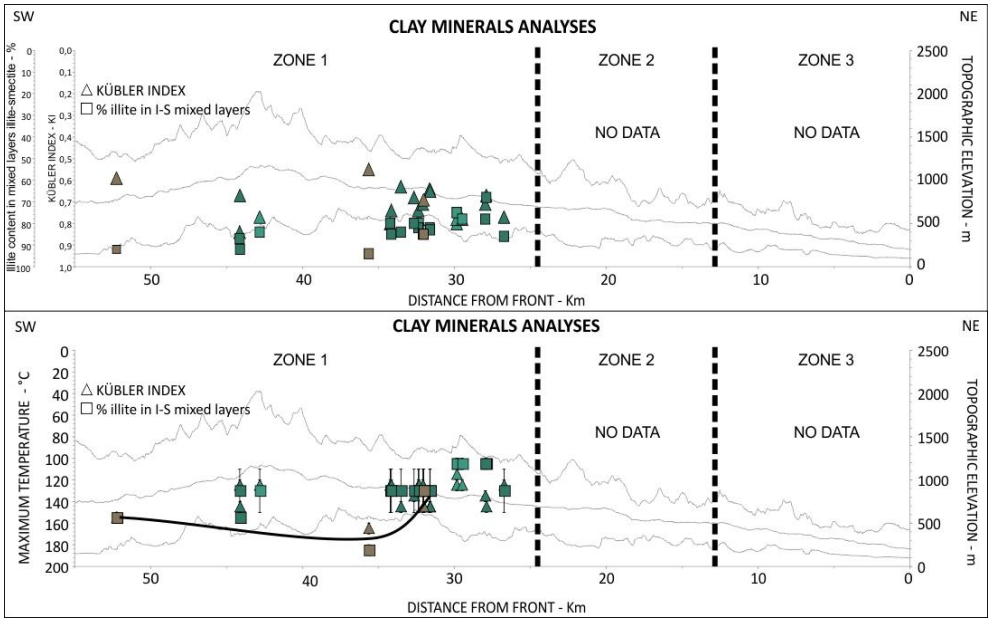
SW
CLAY MINERALS ANALYSES
NE
ZONE 1
ZONE 2
ZONE 3
△ KÜBLER INDEX
□ % illite in I-S mixed layers
NO DATA
NO DATA
illite content in mixed layers illite-smectite - %
KÜBLER INDEX - KI
TOPOGRAPHIC ELEVATION - m
DISTANCE FROM FRONT - Km
SW
CLAY MINERALS ANALYSES
NE
ZONE 1
ZONE 2
ZONE 3
△ KÜBLER INDEX
□ % illite in I-S mixed layers
NO DATA
NO DATA
MAXIMUM TEMPERATURE - °C
TOPOGRAPHIC ELEVATION - m
DISTANCE FROM FRONT - Km

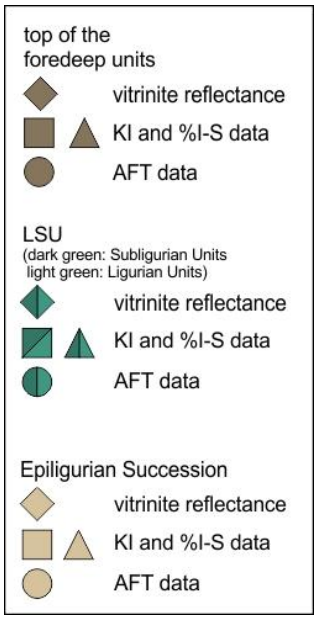
top of the foredeep units
vitrinite reflectance
KI and %I-S data
AFT data
LSU
(dark green: Subligurian Units
light green: Ligurian Units)
vitrinite reflectance
KI and %I-S data
AFT data
Epiligurian Succession
vitrinite reflectance
KI and %I-S data
AFT data

c)

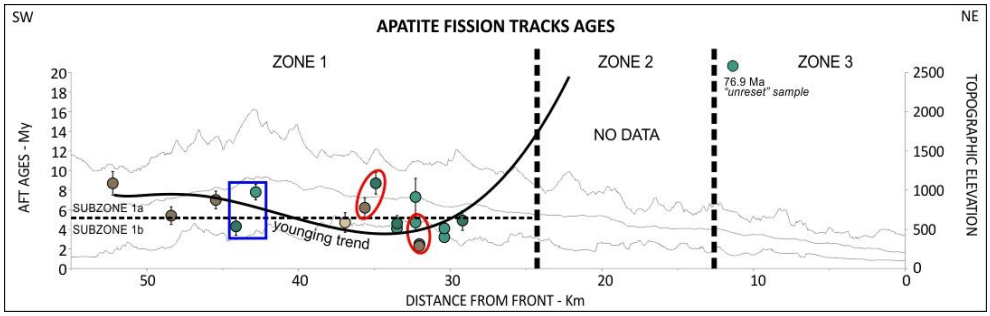
SW
APATITE FISSION TRACKS AGES
NE
ZONE 1
ZONE 2
ZONE 3
76.9 Ma
"unreset" sample
NO DATA
AFT AGES - My
SUBZONE 1a
SUBZONE 1b
younging trend
TOPOGRAPHIC ELEVATION
DISTANCE FROM FRONT - Km

5.4.1 Vitrinite Reflectance

Vitrinite eflectance (VR) data (fig. 5.4a) related to the foredeep units display values decreasing from 1.695±0.18% - 0.629±0.072%, within Zone 1, down to values of 0.255±0.019%-0.200±0.056%, almost at the lower resolution limit of this analytic technique, within Zone 3. Because of the low reliability of Zone 3 samples, only Zone 1 samples have been converted into paleotemperatures, and their values range from ~178°C to ~98°C.

VR data for the LSU, collected only within zone 1, range from 1.110±0.081% to 0.419±0.052%, corresponding to paleotemperatures spanning from ~144°C to ~65°C.

The two samples belonging to the Epiligurian Succession display VR values of 0.735±0.076% (Zone 1) and 0.333±0.062% (Zone 3), corresponding to paleotemperatures of ~111°C and ~47°C.

The general paleotemperature decreasing trends, moving from SW to NE and from deeper units (foredeep units) to shallower units (LSU and Epiligurian Succession), reflect the maximum burial variability across the Apennine chain previously highlighted in literature (Reutter et al., 1980, 1983, 1991; Bonazzi et al., 1982, 1984; Corrado et al., 2010) (see § 4).

5.4.2 Clay mineral-based geothermometers

Samples for this technique have only been collected within Zone 1 (fig. 5.4b). The Tuscan foredeep units display an illite content in mixed layer I-S (squares in fig. 5.4b) ranging from 94% to 85% (mainly R3 stacking order) and KI values (triangles in fig. 5.4b) from 0.55 to 0.69. According to the mixed layer I-S, the paleotemperature estimates are between ~190°C and ~110°C, while the KI parameter indicates paleotemperatures ranging from ~170°C to ~140°C.

The LSU illite content in mixed layer I-S ranges between 92% and 68% (R3 and R1 stacking order), while the KI value is comprised between 0.63 and 0.84. Mixed layer I-S indicate paleotemperatures ranging from ~150°C to ~100°C and the KI parameter indicate paleotemperatures from ~150°C to ~120°C.

The two inorganic parameters indicate that maximum temperatures are fairly regularly distributed within Zone 1, decreasing from SW to NE and from samples belonging to the deeper Apenninic units (Tuscan units) up to samples related to the shallowest portion of the LSU. Only two data at ~ 35 km from the Apenninic front (PR3IS and PR3KI, see § 4) fall out of the main

decreasing trend because of the presence, in a relatively external (NE) position, of a tectonic window in which the Tuscan units crop out. Previously published data for this zone are fully consistent, in terms of main trends, with the new results, highlighting both the same regional decreasing SW-NE trend, and the maximum burial decrease moving from deeper to shallower units (Bonazzi et al., 1982, 1984, 1987, 1989; Cerrina Feroni et al., 1983, 1985; Corrado et al., 2010) (see § 4).

5.4.3 Apatite fission track data

All the samples collected within Zone 1 for the apatite fission track analysis (fig. 5.4c) have been completely reset, meaning that they were heated up to more than 120 °C before the last cooling event. This event has been recorded by the Tuscan foredeep units between 8.7±1.2 and 2.3±0.3 Ma, and similarly by the LSU between 8.7±1.1 and 2.5±0.5 Ma. The sample collected at the base of the Epiligurian Succession displays an AFT cooling age of 4.7±1.0 Ma, falling inside the same time interval indicated by the deeper units.

The AFT sample (PR33FT in fig. 4.10) collected within Zone 3 is the only unreset sample of our whole new dataset and it belongs to the LSU outcropping at the NE external margin of the chain (fig. 5.4c). This sample shows an AFT age of 76.9±5.9 Ma and a reduced mean track length of 10.84±0.20 μm. This AFT age isn't related to any Apenninic tectonic phases, and implies that during the Neogene Apenninic orogenesis this sample has never been heated at temperatures higher than ~70°C (see § 4).

Two younging trends can be observed from the data, one SW-NE oriented and the other one related to the relative depth of the sampled tectonic units inside the Apenninic stacking. The first trend is highlighted by two groups of cooling ages located within the Zone 1 close to the main ridge of the Apennine; one ranging from 8.7 to 6.2 Ma (Subzone 1a), and the other ranging from 4.9 to 3.2 Ma (Subzone 1b). The two groups as a whole define a younging trend from SW to NE (fig. 5.4c) and they correspond to areas in which two different foredeep depocenters belonging to the Tuscan units crop out: Subzone 1a is related to the Macigno foredeep, while Subzone 1b is related to the Cervarola foredeep. This first tendency is a long-recognized trend in the Apennines which has been interpreted as related to the main SW-NE direction of migration of the orogenic processes and foreland basins (e.g., Boccaletti et al., 1990; Cavinato and DeCelles, 1999; Doglioni, 1991; Thomson et al., 2010).

The second trend, instead, is observed especially inside tectonic windows (red circles in fig. 5.4c) and it is characterized by cooling ages which become progressively younger from the shallower (LSU) to the deeper units (foredeep units) (fig. 5.4c). This observation implies that the tectonic stack constituted by the foredeep units and LSU moved through the 120°C isotherm as a single crustal block.

In the case of the Valdena tectonic window (I in fig. 5.4c) this second trend is confirmed once again, but the difference in cooling age between two samples collected in the upper and lower portion of the LSU ranges from a minimum of 0.1 My to a maximum of 6.9 My (considering 2σ error), not justifiable by the little difference in the structural position of the two samples, and possibly indicating the lack of a certain amount of LSU (whose thickness depends on the assumed exhumation rate).

Previously published data in the study area are partly related to the Macigno foredeep succession and partly to the shallower overlying LSU (Thomson et al., 2010 and references therein) (see § 4), all falling inside our Subzone 1a. The published cooling ages related to the Macigno succession span from 9.6 to 5.3 Ma, highlighting once more the same time interval related to the exhumation of the main ridge observable in our new data. The published AFT ages related to the LSU range from 13.4 to 10 Ma and together with the underlying Tuscan units ages they highlight the same second trend observed in our new data, related to the denudation of progressively deeper units (Thomson et al., 2010).

5.5 Maximum burial and cooling ages

Within Zone 1 the maximum temperatures recorded by clay mineral thermal indicators and apatite fission track are in good agreement, and indicate a general temperature decrease towards NE because progressively shallower units have been sampled (fig. 4.10). VR data distribution is much more scattered, even among samples belonging to the same structural level. Nonetheless, a general decreasing trend can be envisaged taking into account the limit of the methodology applied (see § 4).

The maximum paleotemperatures recorded inside the outer Zone 3, are in good agreement as well, and indicate that since the middle-late Miocene the maximum burial of the sampled units occurred at a temperature never exceeding ~40-50°C.

In order to better constrain how the LSU geometry evolved through time we focussed our analysis on the thermal and thermochronological evolution of the underlying foredeep units (i.e., the Tuscan and Umbria-Romagna units), whose maximum loads in the study area have been constituted by the LSU and the Epiligurian succession. The conversion of the maximum paleotemperatures into thickness values has been made assuming a geothermal gradient of 30°C/Km, considered reasonable in areas of active thrusting (Botti et al., 2004) (see § 4).

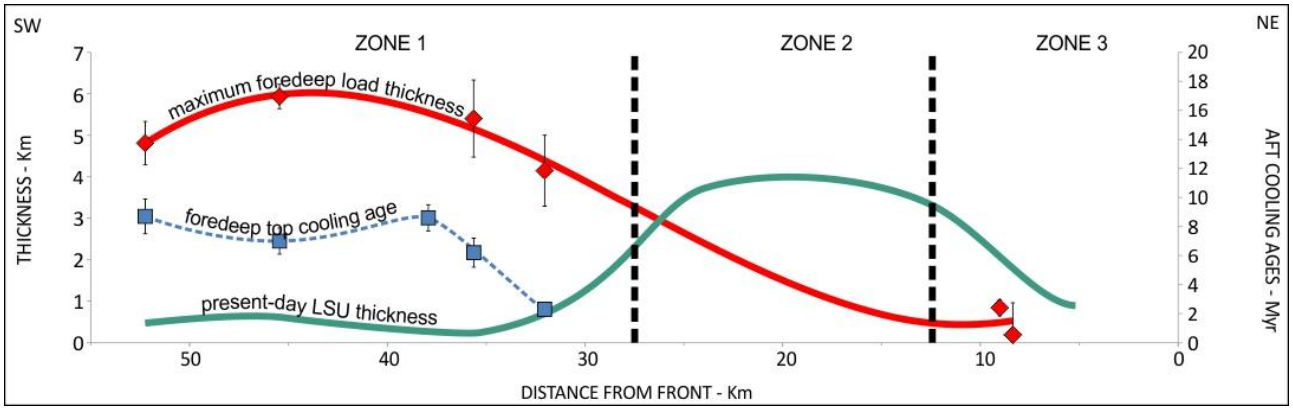

Fig. 5.5: synthesis of geological, thermal and thermochronological data related to the LSU thickness plotted along an ideal SW-NE-oriented profile, versus the distance from the NE front of the Apenninic orogen. The red diamonds and line represent the maximum burial of the foredeep units (and thus the maximum thickness of LSU and Epiligurian succession) obtained by the organic and inorganic thermal indicators; the green line represents the present-day geometry of the LSU (see fig. 5.3); the blue squares and line represent the foredeep units cooling ages.

The maximum burial of the Tuscan and Umbria-Romagna units in the study area generally decreases moving from the inner zone (SW, Zone 1) to the outer one (NE, Zone 3) (fig. 5.5). We didn't collect any sample inside Zone 2, where mostly only the upper portion of the LSU crop out, thus no signal recording the evolution at the basal contact could be found.

Thus, starting from the outermost Zone 3, the present-day thickness is lower than ~1000 m, very similar to the calculated maximum burial experienced by the cropping out foredeep deposits of the Umbria-Romagna units (green line, red diamonds and line, respectively, in fig. 5.5). These values together with the old AFT age (76.9±5.9 My) confirm that this area has never been buried under loads thicker than ~1.7 km.

Within Zone 1 the calculated maximum burial spans between > 6000 and ~4000 m (fig. 5.5, red diamonds and line) which, once plotted together with the present-day thickness of the LSU, as deduced by surface-subsurface geological data (fig. 5.5, green line; figs. 5.2, 5.3), reveals a

thickness discrepancy of at least 3000 m (i.e., the difference between > 4000 and 1000 m, which are the maximum experienced load and the present-day burial inside Zone 1, respectively). This observation implies that within Zone 1 at least 3000 m of LSU have been removed from above the Tuscan foredeep units.

Apatite fission tracks indicate that the Tuscan foredeep units underwent cooling and denudation between 10My and 2.3My, in particular between ~10 and ~6 Ma in the Oligocene Macigno foredeep units (Subzone 1a in fig. 3.1), and between ~6 and 2.3 Ma in the Aquitanian-Langhian Cervarola succession (Subzone 1b in fig. 4.10). These constraints are very important for arguing about the mechanisms responsible for this removal as it will be treated and discussed in the next chapter.

5.6 Summary and discussion: the uplift and reshaping of the LSU and implications for coeval extension and compression in the Northern Apennines orogenic wedge

The investigation of the evolution of the Northern Apennines orogenic wedge since the late Miocene revealed that the far-travelled/allochthonous LSU were deeply reshaped through thinning and thickening processes till they acquired the present-day geometry, a double tapered wedge which displays the following characteristics (fig. 5.3):

- low thickness in the innermost SW portion (~1000-2000 m) – Zone 1;
- highest thickness in the central portion (>4000 m) – Zone 2;
- low thickness in the external NE tip (<1700 m) – Zone 3;

The integration of vitrinite reflectance, clay mineral-based geothermometers and AFT data reveals that ~4000-6000 m of LSU and Epiligurian succession have been removed since ~10 Ma within Zone 1, when the underlying foredeep units began to cool down. The partial thickness removal of the LSU becomes younger towards the outer portions of Zone 1-subzone 1b (figs. 3.1, 5.4; see § 5.4). It is remarkable that the missing thickness of the LSU within Zone 1 (figs. 3.1, 5.4), is totally comparable to the LSU present-day thickness in Zone 2 (figs. 3.1, 5.4). These data suggest that, at present, the middle Miocene foredeep units buried under the LSU in Zone 2 should experience loads which older foredeep units inside Zone 1experienced between ~20 Ma (end of deposition of the Macigno succession) and ~10 Ma (inception of denudation processes of the same unit). On the contrary, in Zone 3 the LSU and underlying foredeep units (figs. 3.1, 5.4) did not experience loads greater than those

preserved at present (~1000 m) (fig. 5.4) (see § 5.4). This implies that in Zone 3, the present-day thickness of the LSU is not so different from that acquired during their final emplacement (late Messinian to Recent - see § 2, 5.1). Within this framework, the discrepancy between the present-day thickness of the LSU and the maximum burial recorded by the foredeep units within Zone 1 led us to conclude that the innermost portion of the outcropping LSU underwent thinning processes. The latter processes had to remove material/load (i.e., constituted by LSU and Epiligurian succession) successively accumulated in Zone 2 (figs. 3.1, 5.4). In addition, as already mentioned (see chapter § 5.2.1), in many areas of Zone 1 underneath the preserved Epiligurian Succession, the thickness of the LSU is ~1000-2000 m. This implies that the thinning processes had to act within the LSU themselves, leaving almost unmodified both the upper contact (with the overlying Epiligurian succession) and the lower contact (with the underlying foredeep units). The above observations, together with the low angle normal faults, cropping out between Zones 1 and 2 (§ 5.2.1), led to the conclusion that the thinning processes developed through diffuse zones of extensional shearing and/or localized low-angle normal faults, activated along weakened surfaces and already existing discontinuities inside the LSU (see § 5.2.1).The most important factor contributing to the triggering of the low-angle extension inside the LSU within Zone 1 has been interpreted to be the fold and thrusting which led to the uplift and exhumation of the Apenninic foredeep units; these processes would have caused the LSU and Epiligurian load to become gravitationally unstable and the subsequent onset of tensional stresses, responsible for the shallow extensional tectonics, localized inside the LSU.

Concerning the timing of these thinning processes, the AFT data related to the Tuscan units in Subzone 1a revealed that they started to cool down at ~10-6 Ma. This time interval corresponds to the translation of the LSU tip from the position reached in the middle Miocene (~12 km SW of the present day topographic front; see fig. 3.1) to the frontal ranges of the Northern Apennines (south of the Po Plain) (Artoni et al., 2010; Pieri and Groppi, 1981; Roveri et al., 2001) (see § 5.1). Even though there are few strong constraints on the age of the folding and thrusting of the foredeep units within Zone 1, evidences of a compressional regime and hinterland load of thickened crust have been observed north of the study area, in the outer portions of the Umbria-Romagna units. The recognized processes likely caused major shifts of the foredeep basins depocenters during late Miocene (Argnani & Ricci Lucchi, 2001 and references therein). On the basis of the above considerations and taking into

account that before ~5 Ma the Apenninic chain was still under the sea level (preventing the onset of surface erosive processes), it is envisaged that the early exhumation (between ~10 and 6 Ma) of the foredeep units along the main ridge, specifically inside Subzone 1a, was basically tectonic and driven by low-angle extensional faults inside the LSU (see § 5.2.1). This kind of low-angle extensional faults is comparable to the ones recognized in the Southern Apennines (Corrado et al., 2005; Mazzoli et al., 2008).

Progressive exhumation and denudation of the foredeep units continued after ~6 Ma until, at least, 2.3 Ma, as testified by the AFT ages (see § 5.4). However, since ~5 Ma the contribution of subaerial erosion becomes more and more relevant, because the Northern Apennine chain became progressively exposed above the sea level. As a matter of fact, the onset of significant surface erosive processes, in this portion of the Northern Apennines, is testified by: 1) the age of the first continental deposits inside the Neogene Tuscan basins (Bernini et al., 1990); 2) the late Messinian post-evaporitic fluvio-deltaic deposits cropping out at the foothills of the Apenninic chain (Martini and Zanzucchi, 2000; Artoni et al., 2010; Roveri et al., 2001); 3) the Pliocene age of the top of the proximal to shallow water Epiligurian succession, a few kilometres SE of the study area (Panini et al., 2002). Therefore, the surface erosion processes have been hypothesized to be responsible for the whole denudation of the main ridge area of the Apenninic chain since 5 Ma, but they cannot explain the removal of all of the 4000-6000 m of LSU and Epiligurian succession inside Zone 1 without implying average erosion rates higher than 1.0 mm/yr. This value is incompatible with published estimates of denudation rates in the Northern Apennines and volumetric analyses of sediment supply inside the youngest Po Plain foredeep, which assessed average erosion rates of ~0.6 mm/yr over the last 15 Ma (Balestrieri et al., 2003; Bartolini et al., 1996; Bartolini et al., 2003; Fellin et al., 2007). Furthermore, the sole action of surface erosion would neither explain the Epiligurian succession at ~1000-2000 m of distance from the foredeep units inside Zone 1.

After ~6 Ma, the coexistence of compressional and extensional tectonics has been better constrained in the most recent phases. In particular, compressional tectonics is testified by: 1) an important shift in the foredeep depocenter during the Messinian that require a thickened and uplifting crust in the hinterland (intra-Messinian pulse/tectonic phase of Ricci Lucchi et al., 1982, Fusignano Fm in Argnani and Ricci Lucchi, 2001); 2) the occurrence of a subsiding and thrust-controlled Pliocene-Pleistocene foredeep in the Po Plain (Argnani

and Ricci Lucchi, 2001); 3) deep (>45km) compressive/transpressive focal mechanisms (Eva et al., 2005; and reference therein; http://bollettinosismico.rm.ingv.it/). During the same time interval, in the hinterland portion of the Northern Apennines (S of the main ridge), the extensional tectonics is represented by systems of high-angle normal faults system (Bernini et al., 1990). Throughout the northeast slope of the western portion of the Northern Apennines, the presence of high-angle extensional tectonics is still a debated question. Possible high-angle extensional faults are highlighted by the geological cross sections (see figs. 3.1, 5.1a, 5.2a) and in the literature (Bettelli et al., 2002; Bertotti et al., 1997) but they do not overprint the NE portion of the mountain belt as deeply as the hinterland portion. The extension of the Apennine hinterland is mainly related to the opening of the Tyrrhenian Sea and/or to the exhumation of the Apuane Alps metamorphic complex (Bernini et al., 1990; Boccaletti et al., 1990; Carmignani and Kligfield, 1990). The denudation of the Apuane Alps has been interpreted to be due to tectonic processes (high angle normal faults at ~13-5 Ma) and subsequently mainly to surface erosion (~4-0 Ma) (Fellin et al., 2007). The timing of these two phases are quite coeval to the two groups of ages (~10-6My and ~5-0My) recognized inside Zone 1 of the study area.

The evidences of both exhumation and denudation processes led to invoke tectonic-erosional mechanisms responsible for the reshaping of the LSU; these mechanisms are depicted in the following evolutionary sketch represented on a cross-section SW-NE oriented, modified from fig. 5.3h (fig. 5.6):

- stage 1) (before ~10 Ma) at the boundary between the Serravallian and the Tortonian, the late Oligocene, early and middle Miocene foredeep units were already buried under the LSU-Epiligurian stack; the largest thickness of the pile (4000-6000 m) covered mainly the late Oligocene Tuscan foredeep units; the LSU wedge was likely tapering out toward north and its tip was partially reshaped by mass-transport deposits moving inside the foreland basins system (Marnoso-arenacea foredeep);
- stage 2) (~10-6 Ma) exhumation and uplift of the late Oligocene Tuscan units is interpreted to be the cause triggering the activation of the low-angle normal faults within the LSU (LSU thinning in the hinterland, Zone 1, and accumulation in the middle-slope – Zone 2); the Tuscan foredeep units consequently were tectonically

denudated/exhumed; the LSU tip is estimated to have advanced for ~12 km towards N-NE, close to its present-day position; a new foredeep depocenter was forming ahead (NE) of the outermost thrust; at the very end (Messinian?) of this phase high angle normal faults in the hinterland (SW of the study area) began to enucleate;

- stage 3) (~6-0(?) Ma) exhumation processes migrated towards NE, involving the early Miocene Cervarola foredeep deposits, and low-angle extensional faults possibly continued to act, at least in the outer portion of Zone 1 (Subzone 1b). In the hinterland area of the Apennine, high-angle extensional tectonics developed (Bernini et al., 1990) while, inside the study area, NE-dipping high angle extensional faults cross-cut the previous low-angle extensional faults. A new foredeep depocenter, mainly overlapping the one generated during the previous stage, wa forming (intra-Messinian tectonic pulse and Fusignano Fm, see above). During this stage, the subaerial erosion started to be significant, denudated the buried foredeep deposits and shaped the present-day topography of the main ridge; ongoing activity of high angle normal faults enhanced the denudation processes.

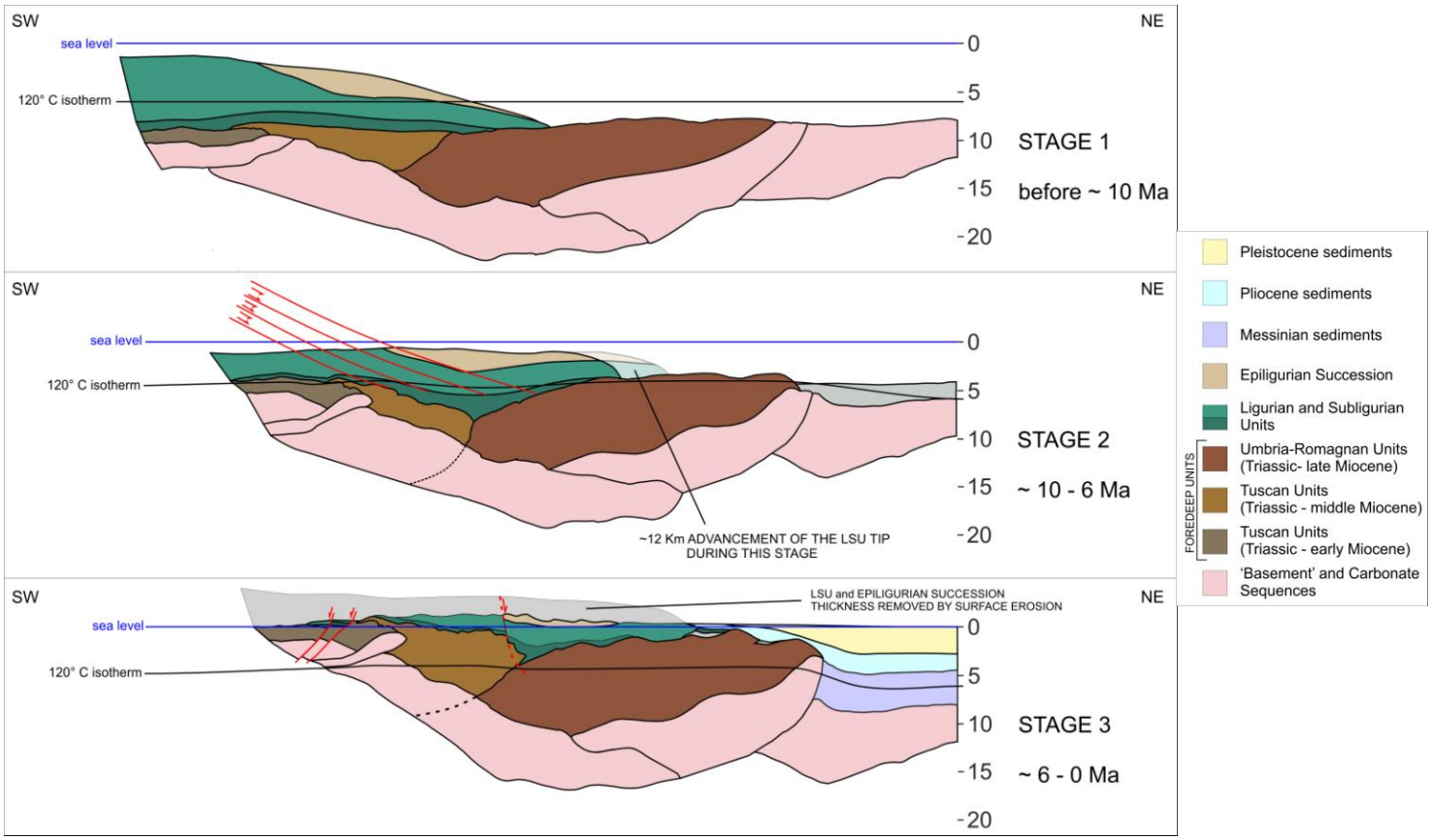

5.6.1 Implications for coeval extension and compression in orogenic wedges

The present study reveals that the far travelled/allochthonous units (LSU) of the Northern Apennines recorded two types of extensional tectonics acting during their translation and the orogenic wedge building processes. They first (10-6 Ma) were affected by low angle extensional faults whose most important triggering-factor is likely to be the exhumation and uplift of the Tuscan units, caused by folding and thrusting; the uplifted portion of the Tuscan unit would successively form the present-day chain's main ridge (Zone 1). The compressional tectonics acting during this stage thickened the Apenninic orogenic wedge within Zone 1 and increased its surface slope angle; this fact generated an excess of gravitational potential energy which would have been balanced by internal deformation of the orogenic wedge (i.e., low angle extensional tectonics) affecting its relatively shallower (i.e., ~0-6 km deep) portions. These low angle extensional faults, acting inside the LSU between ~10 and 6 Ma, lowered the critical angle of the orogenic wedge which regained a meta-stable gravitational equilibrium (Davis et al., 1983; Dahlen et al., 1984; Platt, 1986).

After 6 Ma folding and thrusting processes continued to affect the Tuscan foredeep units (see above, stage 3), propagated northeastward and locally are still active nowadays (see §2) confirming that the stress regime inside the orogenic wedge is on the whole compressive. As a consequence, the denudation and uplift of these units continued, enhanced by and favouring the increase in surface erosion that became more important because of the progressive emersion of the Apenninic chain above the sea level. During this second stage, the ongoing exhumation and uplift of the Apenninic main ridge and Apuane Alps, are, at least partially, responsible for the (Messinian?)Pliocene-Pleistocene onset of high angle extensional tectonics which affected all the Apenninic Tyrrhenian side (S of the main ridge) and possibly portions of the slope N of the main ridge. In this perspective, also during this younger phase (~6-0 Ma) the orogenic wedge continued to undergo over-thickening, increase the surface slope angle, consequent creation of excess of gravitational potential energy, and new achievement of an equilibrium state through internal wedge deformation (shallow high-angle extensional tectonics).

Fig. 5.6: Simplified geological sketch from before 10 Ma to Present, indicating a three stages evolution for the LSU. The red lines indicated inferred (dashed) and certain (solid) low- and high-angle extensional faults in the considered portion of the orogenic wedge; the blue line represents the sea level; the black line represents the evolution of the 120°C isotherm through time ("closure" temperature of the AFT system, see § 4), as a function of the heat advection caused by exhumation processes.

5.7 Conclusions

The Northern Apennines of Italy share many common features with other peri-mediterranean orogens, in particular the coexistence of compressional and extensional tectonics, coupled with the emplacement of far-travelled/allochthonous tectonic units, which, in the evolution of the last 12 My of the Apenninic chain have played a fundamental role.

The preservation of the shallow far-travelled/allochthonous units (the LSU) in the Northern Apennines, and in particular of their basal contact, resulted to be a powerful tool in the study of the timing and mechanisms of coeval compressional and extensional tectonics, which, in the westernmost portion of the Northern Apennines, are bound by tight cause/effect relationships and can be set in a unique evolutionary geodynamic frame.

The present study reveals that in the Northern Apennines the far-travelled/allochthonous units recorded extensional tectonics as related to the formation of tensional stresses in response to an over-thickened orogenic-wedge dominated by an overall compressive stress regime testified by uplift and coeval foredeep depocenter shifts. Thus the relationship existing between extensional and compressional tectonics in the study area is tightly of cause/effect type, meaning that extension is the effect of the internal deformation of an orogenic wedge undergoing overall compression and phases of gravitational destabilization. According to seismological studies, this picture is representative also of the present day tectonic framework in the Northern Apennines.

In particular the late Miocene deep folding and thrusting of the foredeep units contributed to the development of an orogenic wedge which is over-thickened and prone to be gravitationally unstable. This gravitational potential energy excess has been counterbalanced, at a first stage (10-6 Ma), by NE-dipping low-angle normal faults, thinning the LSU and reshaping them in a doubly-tapering wedge. This tectonic elision, in turn, became responsible for the tectonic denudation and enhancement of the exhumation of the underlying Tuscan units.

Subsequently (6-3(0?) Ma), the ongoing uplift and exhumation of the foredeep units (accompanied and intensified by surface erosive processes) likely led to a new state of gravitational instability and to the development of high-angle normal faults, which cross-cut the previous low angle fault contacts. The high-angle extensional faulting acquired much

more importance on the Tyrrhenian slope of the Northern Apennines, where it caused the opening of late Miocene-Pleistocene intramontane basins.

This study revealed that the coexistence of compressional and extensional tectonics, since the late Miocene, developed inside a sort of feedback mechanism in which the deep-seated compressional tectonics, characterizing the whole growing Apenninic orogenic wedge, favoured the onset of instability states and the consequent development of shallow (0-10km) extensional features. Even if these extensional features differ in time and space, they represent, however, expressions of the orogenic wedge internal deformation, which, on the verge of failure, is continuously achieving new critically stable states.

6. Late Miocene to Recent activity of late orogenic thrust-related antiforms constrained by structural, thermochronological and geomorphologic data

The content of this chapter constitutes the core of an extended abstract published in 2012 (Carlini et al., 2012).

Because of the young cooling ages obtained by the AFT analysis (i.e. younger than ~5 Myr) and their possible relationship with the activity of deep Apenninic compressional structures (see § 5) led us to investigate the most recent evolutive phases of these processes through the integration of geomorphological data (Provincia di Parma, 2007; Chelli et al., in press; Tellini and Chelli, 2003), geological surface data, thermochronologic data and a new interpretation of seismic lines crossing the study area (see § 3), described in a published extended abstract (Carlini et al., 2012, attachment A1), constituting the content of chapter 6.

6.1 Subsurface analysis

The regional scale architecture of the chain has been investigated through the interpretation of commercial seismic reflection profiles and drill holes dataset in collaboration with ENI E&P which made available the dataset at their offices in Milan (Italy) (see § 3). The available dataset includes both longitudinal and transversal 2D reflection profiles, providing a good coverage of the area of interest, down to a depth of 4-6 s TWT, and four wells. 2D Move software (Midland Valley ®) has been used to validate the seismic interpretation and to perform a time-to-depth conversion of the interpreted seismic lines (Fig. 6.1b).

The preliminary results show a deep subsurface structure characterized by five embricated main blind thrusts, SW-dipping, which overprint and cut the contacts between the main tectonic units of the chain. The thrusts are labeled with letters from A to E, from the most internal to the most external, in text and figures (Figs. 6.1, 6.2).

The vertical offset of the interpreted thrusts ranges from few hundred of meters up to more than 1500 m, while their lateral extension is sometimes difficult to estimate because the available seismic data related to the north-westernmost part of the study area are scattered and of poor quality. Thrust A, involving the Macigno Fm., is the less extended and shows a termination to the NW with a lateral ramp in correspondence of the Pracchiola tectonic window and the “Taro line”, a long recognized regional-scale transverse lineament (Argnani et al., 2003 and reference therein) (Fig. 6.1). On the contrary, thrust E seems to extend through the whole investigated area,

from the Secchia River (to the SE) to the Ceno Torrent (to the NW). There are some uncertainties in the interpretation of the lateral extension of the thrusts labeled B, C and D, mainly due to the low quality of the seismic data.

The thrust faults show an average dipping angle between 25° and 40°; their tip can be observed at shallow depths (~ 500 – 1500 m), in correspondence of the lower contact of the Ligurian or Subligurian Units; the deep seating of these thrusts (i.e. their breaching point from an eventual main detachment) is deeper than the available seismic data. Based on the geometries of the visible structures, it is however possible to estimate that the main thrust faults extend down to a depth of 25 - 30 km in correspondence of the frontal margin of the Apennines and 30 - 35 km in correspondence of the principal divide of the chain.

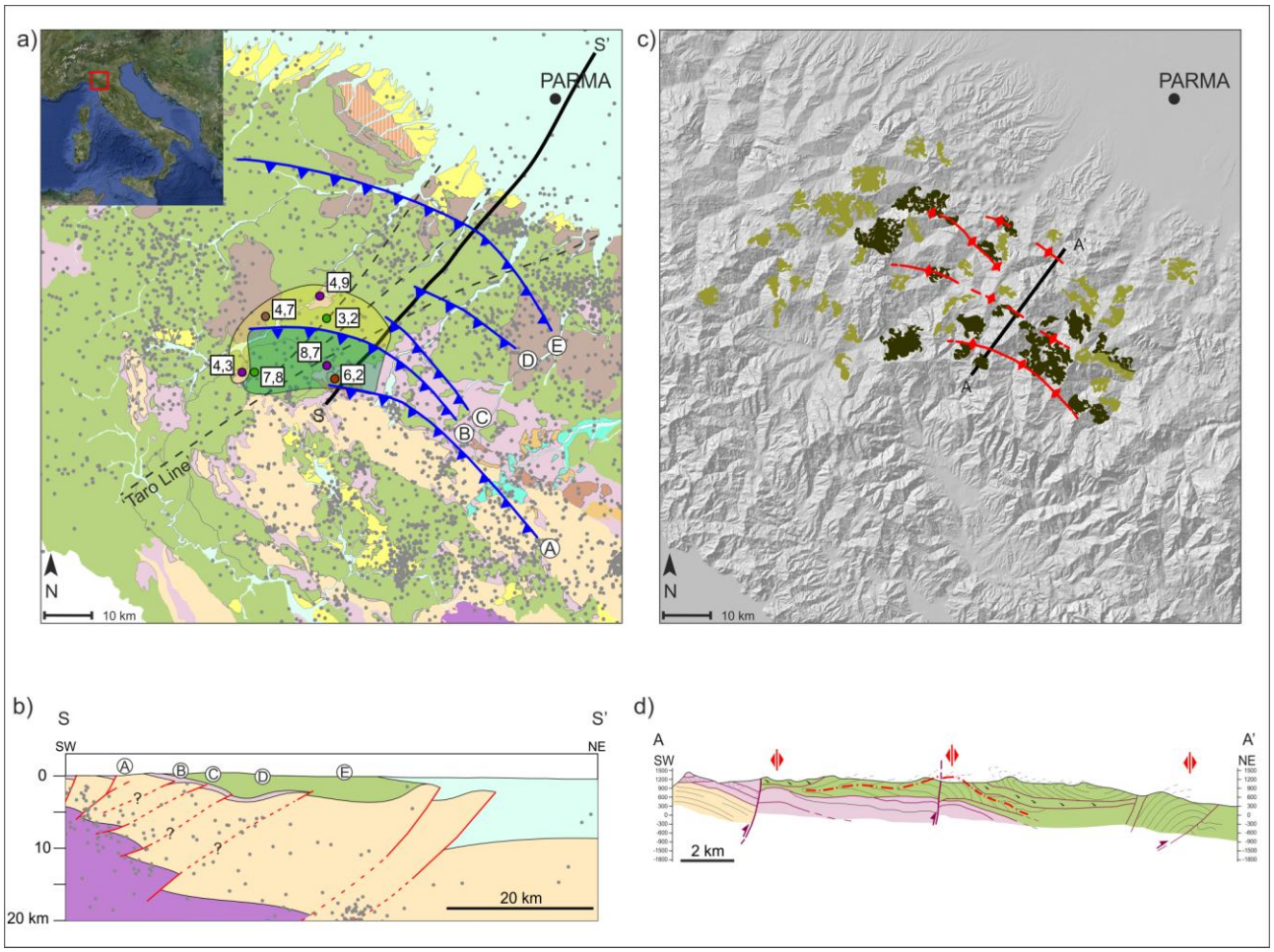

Fig. 6.1 – a) geological map, apatite fission-tracks cooling ages, trace of the main thrusts tips (A, B, C, D, E) resulted from the subsurface stuctural analysis and trace of the preliminary geologic cross-section S-S'; b) preliminary geological cross-section derived from depth –converted seismic reflection profiles; c) DTM of the study area with location of the main antiforms hinges (in red), the large landslides and DSGSDs (light green: unrelated to the antiforms; dark green: presumably related to the antiforms), and the trace of the geologic cross-section A-A' shown in Fig. 6.1d; d) geologic cross-section through the study area. (TUM: Tuscan-Umbrian Units; SLU: Subligurian Units; LIG: Ligurian Units; EPIL: Epiligurian Succession; qr: Quaternary to Recent deposits).

Cross-cutting relationships permit to constrain the relative timing of the thrust activity, which seems to be younger than the emplacement of Ligurian and Subligurian Units onto the foredeep units, as already shown in Camurri et al. (2001).

6.2 Thermochronological data analysis

In order to give a better time constraining, a suite of 11 new apatite fission-track (AFT) data have been produced (see § 4.5.1, 5.4). Samples have been collected from all the main tectonic units of the Northern Apennines, from the deepest to the shallowest ones, in order to investigate the exhumation pattern of the whole structure.

All the samples have undergone complete fission-track reset, meaning that the rocks have all cooled down from a temperature > 120°C. The distribution of the cooling ages indicates a general trend which permits to individuate two slightly different zones (Fig. 6.1a): one covering the innermost portions (SW) of the chain, characterized by cooling ages of ~ 8.7- 6.2 Myr, and the other one placed in a more external position (NE), characterized by ages of ~ 4.9 - 3.2 Myr. This trend well correlates with a long-recognized and regional-scale pattern in the Northern Apennines, where the progressive NE-ward migration of the Apenninic orogenic and lithospheric processes is responsible for the thermochronological ages to become younger from the Tyrrhenian (SW) to the Adriatic side (NE) of the chain (Abbate et al., 1999, Corrado et al., 2010, Thomson et al., 2010 and references therein).

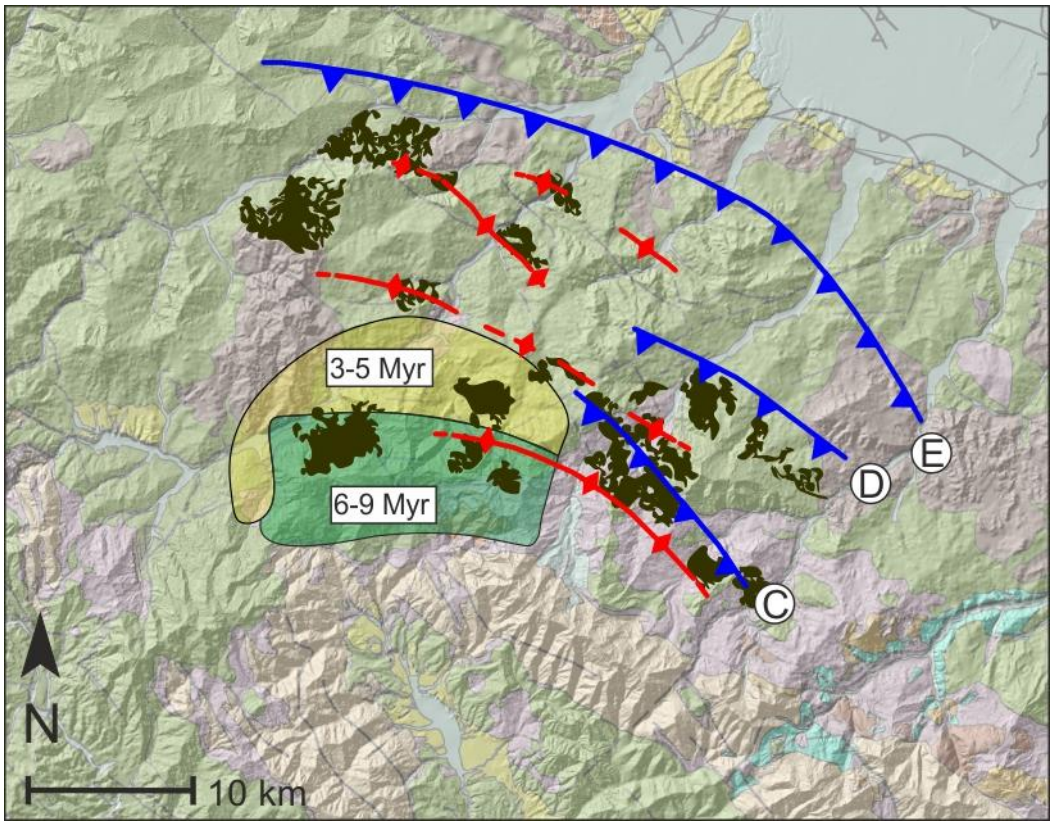

6.3 Surface structural analysis and geomorphologic data

In the investigated area, large landslides and DSGSDs characterized by a surface larger than 1x106 m2 were extracted from the Landslide Inventory Map of the Parma Province (Provincia di Parma, 2007) and a structural-tectonic map, compiled from existing and new data, was created (Chelli et al., in press). Several geologic cross-sections, perpendicular to the main Apennines structures have highlighted the existence of uplifted antiforms related to the neotectonic evolution of the chain.

The overlapping of these two maps (Fig. 6.1c) allowed to analyze the spatial relationships between large landslides and geological features, highlighting some coincidence between late antiformal structures and the slope processes (Chelli et al., in press). In fact, mostly in the central-southern portion of the study area, large landslides seem to arrange themselves along the hinge axes of the antiforms or in the area immediately close to them.

In particular the investigated landslides and DSGSDs constitute several clusters: part of them is located in correspondence of structural features promoting the landsliding, whereas other clusters are aligned along the strike of the uplifted antiforms. A spatial relationship between landslides and antiforms, thus, seems to exist, and this relationship may be the effect of a causal factor of landsliding processes themselves. The landslides, in fact, could be the slope response to the disequilibrium induced by the topographic growth and the increase of energy relief due to tectonic uplift and folding. As it's been already observed (Chelli et al., in press), in the whole area the large landslides related to the late antiforms are chiefly rock slides and complex landslides, while the earth flows seem to be more related to the lithologic condition of the slopes.

Fig. 6.2 – Synthetic map integrating surface and subsurface structural data, mean apatite fission-track ages and geomorphologic data in the study area. See text for explanation. The cooling age distribution shows an almost complete independence of the ages from the sampled tectonic units and from other important regional-scale features. Inside the two zones in which the ages have been grouped, all the tectonic units seem to have cooled down in a relatively short time span; this observation might be indicative of a quite rapid denudation event and of the fact that the main contacts between the Apenninic tectonic units have not suffered an extensive reactivation at least in the last ~5 My. The two areas in which the AFT ages have been grouped fairly coincide with two of the thrust slices intepreted in the seismic lines and confined by thrusts A, B and C (Fig. 6.1a). Thus the cooling ages can also be interpreted as diagnostic of a period in which the thrust faults were probably active.

6.4 Results and conclusions

Integrating subsurface and surface structural analysis results in a striking relationship between the orientation of the surficial antiform hinges and the surface projection of the tips of the three most external thrust faults; thus these antiformal structures can be regarded as the surficial expression of the blind deep-seated thrusts.

Thrust activity seems to have influenced the recent exhumation of certain portions of the chain, and their inception age can therefore be constrained by thermochronological data to around 10 – 9 Ma in the internal sector and 5 – 4 Ma in the external sector of the study area. Since the onset of large slope processes in the last 0.020-0.025 Myr (Tellini and Chelli, 2003) can be related (at least in part) to the effect of the most recent activity of the same antiforms (Chelli et al., in press), it is reasonable to infer that this sector of the Appenninic mountain chain has been characterized by a reactivation of the deep compressive structures during Recent (Holocene) time.

It can be concluded that the tectonic evolution of the examined portion of the Northern Apennines, occurred in the last 10 Myr, seems to be related to the activity of five embricated thrust faults and related antiforms; these antiforms are late orogenic structures which may be considered a causal factor promoting Holocene denudation processes and, in details, large landslides and DSGSDs.

These results are a promising base for future studies addressed to investigate exhumation and denudation rates during late orogenic stages of the Apenninic mountain chain. A first attempt in calculating erosion rates has been done using a numerical modeling of the collected AFT data collected in the present study (see the following chapter § 7)

7. Exhumation/denudation rates derived from low-T thermochronology

The processes described in the previous chapters are strictly connected to the rates at which uplift and denudation occurred in the Northern Apennines since ~10 Ma. A good knowledge of these rates and their evolution through time, then, can be very useful in better constraining the late tectonic events affecting the study area (see § 5, 6) and reveals also important information about the eventual steadiness of orogenic processes throughout the mountain belt.

Uplift and erosion rates have been determined in different portions of the Northern Apennines using techniques which analyze processes responding to changes in the orogen activity at different timescales, being characterized, therefore, by different temporal resolutions. In particular the adopted techniques are mainly short- and long-term sediment yield estimates (Bartolini et al., 1996; De Vente et al., 2006), fluvial incision rates (Simoni et al., 2003), short-term uplift rates (geodetic re-levelling, D'Anastasio et al., 2006; coastal uplift, Vannoli et al., 2004), low-T thermochronology (AFT dating, Balestrieri et al., 2003; Zattin et al., 2002), and cosmogenic nuclides data (Cyr & Granger, 2008), which indicate average uplift and erosion rates spanning between ~0.3 km/Myr (mainly short-term analyses) up to > 1.5 km/Myr (mainly long-term analyses). This large erosion and uplift rates difference depends mainly on the fact that processes such as hillslope erosion or coastal uplift respond to changes in the orogen activity much more fast (and thus reach more easily a dynamic equilibrium) than processes like river profile adjustment or orogenic wedge gravitational re-equilibration, implying, thus, that in the eastern Northern Apennines only over relatively short time scales it is possible to infer the existence of flux steady states (sensu Willett and Brandon, 2002), while on longer timescales it is necessary to take into account high relief change (Cyr and Granger, 2008 and references therein).

Analyses which allow to investigate uplift and erosion rates at proper timescales for the processes treated in this work (i.e. on the order of Myrs) are mainly long-term sediment yield estimates and low-T thermochronology; this kind of studies are lacking inside our study area, where, therefore, it becomes relevant to more deeply investigate uplift and erosion rates, which, otherwise, can only be interpolated by published data related to nearby areas of the Northern Apennines, which resulted in average rates of 0.7-1.7 km/Myr over the last ~12 Myr (Balestrieri et al., 2003; Bartolini et al., 1996; Zattin et al., 2002).

The terms exhumation, denudation/erosion and uplift rates have been used in literature in relation to a variety of different meanings, creating in some cases confusion and

misunderstandings; this situation led to the necessity of clarifying what these terms specifically mean and how they are related one to each other.

Following England and Molnar (1990) the first important distinction has to be done between the meaning of the terms surface uplift, rock uplift and exhumation. Surface uplift refers to the Earth's surface displacement with respect to the geoid, rock uplift to the displacement of rocks with respect to the geoid and exhumation means displacement of rocks with respect to the surrounding rocks; these definitions lead to the following relationship among the three terms:

surface uplift = rock uplift – exhumation;

this relationship implies that the three values can never be equal (except if they all are zero), and that rarely surface uplift is equal to rock uplift, because it would mean that exhumation is equal to zero (often difficult to justify).

The exhumation process, therefore, implies that a certain area is characterized by the presence at surface of rocks which derive from greater depths and which, consequently, have been denudated at higher rates with respect to the surrounding host rocks. The denudation of these rocks can be mainly operated by surface erosive and/or extensional tectonic processes; if the denudation rate can be considered, at a good approximation, directly comparable to the exhumation rate, thus, erosion rate can be considered equivalent to the exhumation rate only in cases we know for sure that extensional tectonics didn't play any role in the exhumation of the studied rocks.

Because of the strong dependence and feedbacks existing among exhumation, erosion rates and geothermal gradients, in order to quantitatively investigate these processes in contexts which are transient over time it is necessary to use numerical methods. In particular we used Pecube and G.L.I.D.E. (Braun, 2003; Fox et al., in press, respectively) two finite element codes which calculate exhumation/erosion rates basing on low-T thermochronologic data. The modelling per formed with G.L.I.D.E. is still at a preliminary stage and its results won't be integrated in the conclusive chapter of this work, but only attached as Supplementary Material 2.

7.1 Pecube

Pecube is a finite element code which solves the 3D heat transport equation in a specified crustal block undergoing uplift and surface erosion, and characterized by an evolving surface topography (Braun, 2003).

In order to understand the temporal evolution of denudational processes basing on low-T thermochronology, thus, it is important to take into account the effect of an evolving topography on the shape of the isotherms (Turcotte and Schubert, 1982; Stüwe et al., 1994; Mancktelow and Grasemann, 1997, Stüwe and Hintermüller, 2000; Braun, 2002).

Previous studies, however, approached these analyses considering only "static" surface topographies cases, where the steady-state case was solved by analytical solutions, while in tectonically active regions and for relatively low-T thermochronologic systems it is important to consider the effect of an evolving topography and the consequent transient solution requires the use of numerical methods.

Pecube calculates the temperature field in the investigated crustal block by solving the transient, three-dimensional heat transfer equation taking into account both heat conduction and advection, and written as (Carslaw and Jaeger, 1959):

$$\rho c\left(\frac{\partial T}{\partial t}+v\frac{\partial T}{\partial z}\right)=\frac{\partial}{\partial x}k\frac{\partial T}{\partial x}+\frac{\partial}{\partial y}k\frac{\partial T}{\partial y}+\frac{\partial}{\partial z}k\frac{\partial T}{\partial z}+\rho A,$$

where, T is the temperature as a function of space and time (x, y, z, t), ρ is rock density, c is heat capacity, v is the vertical velocity of rocks with respect to the base of the crustal block, k is thermal conductivity and A is radiogenic heat production.

In tectonically active contexts it is very important to take into account the contribution of heat advection to the total heat transfer towards the surface, which can be much more influent than the contribution of heat conduction. Heat conduction, in fact, represents the flow of heat through rocks exposed to a temperature gradient, while heat advection indicate the material transport of hot rock particles through colder host rocks, which is operated in many cases by the tectonic activity that leads to the exhumation of deep rocks. The relatively low thermal conductivity and high heat capacity of rocks leads to the fact that physically moving a hot rock through cold rocks rather than letting the heat flow through them is a much more effective way to

transport heat inside the earth's crust; heat advection, therefore, has to be strongly taken into account in regions characterized by active tectonics.

The software at this point is able to predict T-t paths for rock particles since the time at which the model starts until the position these particles presently occupy at surface, whose elevation is introduced in the calculations by the use of a DTM. The integration of subroutines which calculate annealing processes characterized by different closure temperatures allows, then, to produce synthetic cooling ages for several low-T thermochronologic systems (U-Th/He in apatite and zircon, apatite and zircon fission tracks, K-Ar in feldspar, biotite, muscovite, horneblende and fission tracks length distribution).

The input information for Pecube is constituted by parameters related to time, topography, thermal and tectonic properties of the modelled crustal block, in particular the basics one are:

- DTM of the study area;
- Number of time steps run by the model (including, for each step, starting time and eventual amplification of the present topography);
- Crustal block properties (block thickness, resolution in the depth direction, thermal diffusivity, temperature at the base of the model, temperature at the top of the model, radiogenic heat production, lapse rate);
- Observed thermochronologic ages (eventual natural cooling ages sampled in the investigated area);
- Age of the previous resetting event (i.e. the age characterizing the rocks which have not been reset in the event which is going to be modelled);
- Erosional timescale (used when the rate of change in topography between two time steps is not linear);
- Parameters for eventual flexural isostasy calculations (mantle and crustal densities, Young modulus, Poisson's ratio, elastic thickness and desired resolution for this calculation);
- Vertical velocity at the four corners of the block;
- Eventual geometry, activity age and velocity of rock particles along faults.

The software forward modelling results are a series of three-dimensional pictures which describe, through each imposed time step, the distribution of temperature with depth, the vertical

velocity vectors (or along fault planes if these latter have been included), the present day topography, the location of eventual observation data, exhumation rates and cooling ages for the chosen thermochronologic systems.

The chance to acquire as many information as possible from sources and studies based on data independent from thermochronology makes the resulting models much better constrained and allows to tune the remaining unconstrained parameters in order to get a model which better fit the natural data present in the study area. Pecube, however, in order to more precisely investigate all of the unknown parameters (and the inferred too), provides a subroutine which allows to run the software in inverse mode, through classic Monte Carlo random search methods or through the Neighbourhood Algorithm proposed by Sambridge , 1999 and Sambridge, 1999b. In this way it is possible to search through one (or multiple) parameter range and find the solution which minimizes the misfit function defined by the difference between observed and predicted cooling ages.

Inside the study area Pecube has been used to model AFT ages and to obtain exhumation rates in three different cases, two related to local geological contexts (the Macigno foredeep unit along the Val Gordana and the Gova tectonic windows, made of Cervarola foredeep sediments), and one related to a wider area comprising inner and outer portions of the Northern Apennines chain inside the study area, approximately following the course of the Taro river. In all the three cases the models have been run with the same crustal parameters:

- thickness of the model: 30km;
- temperature at the base of the crust: 540 °C;
- temperature at surface: 10 °C;
- thermal diffusivity: 27.4 km^2/Myr;
- radiogenic heat production: 4.5 °C/Myr;

basing on data of present-day heat flow and previous thermochronologic studies performed in the Northern Apennines (Zattin et al., 2002; Fellin et al., 2007; Thomson et al., 2010).

7.2 Case 1 – Val Gordana

7.2.1 General framework

Along the Val Gordana, located about 5 km W o Pontremoli, along the road all the Macigno succession crops out, from the base, overlying the Scaglia formation, until the top, underlying the Subligurian Units. The foredeep sequence is quite undeformed and, excluding the late (i.e. after Pliocene) brittle high angle normal faulting (Bernini et al., 1991), only a gentle (~W30°) tilting can be observed, which allow to follow the ~2000 m succession thickness, with basal and upper main contacts lying almost at the same elevation (Valloni, 1978; Ghibaudo, 1980).

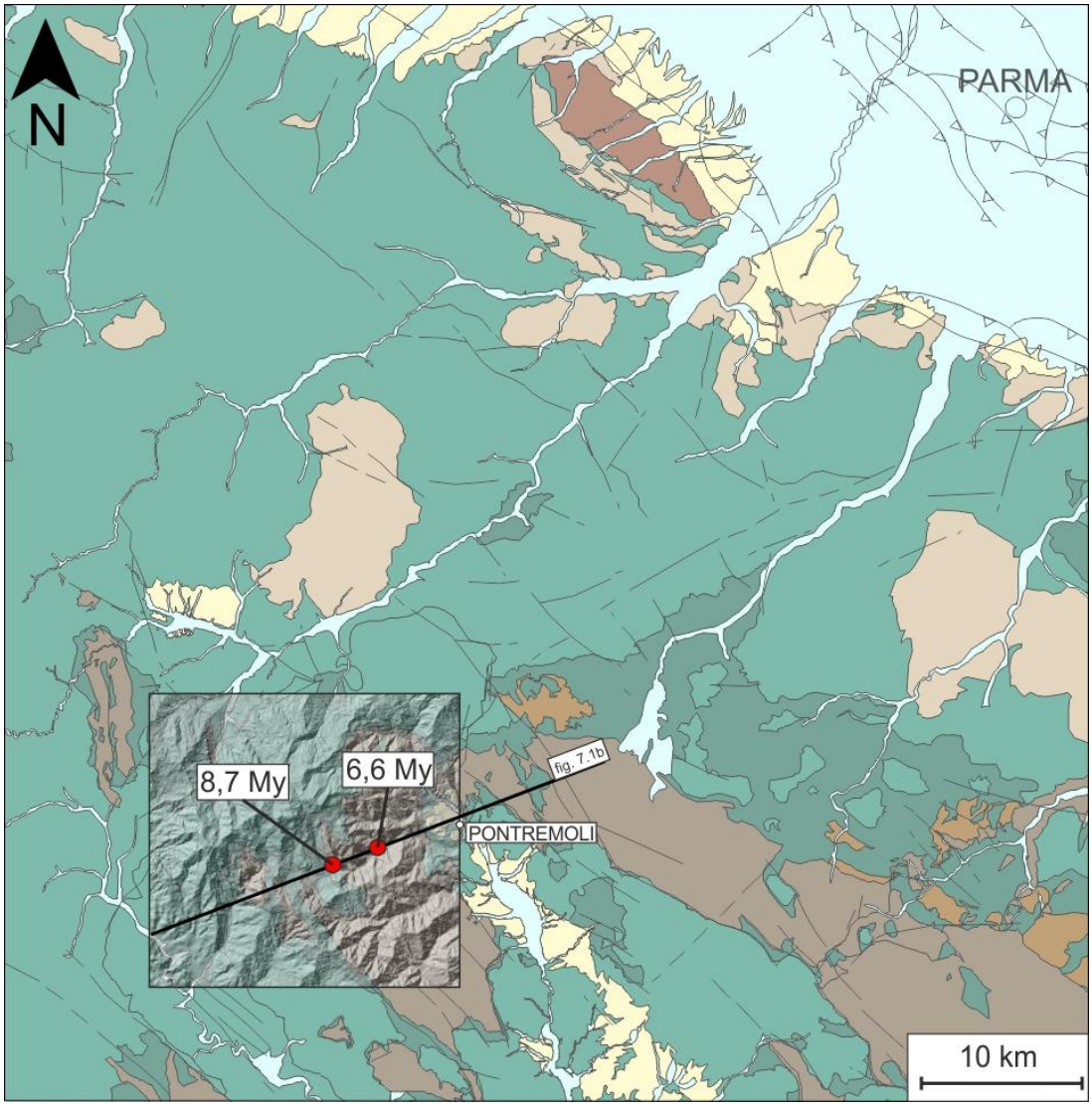

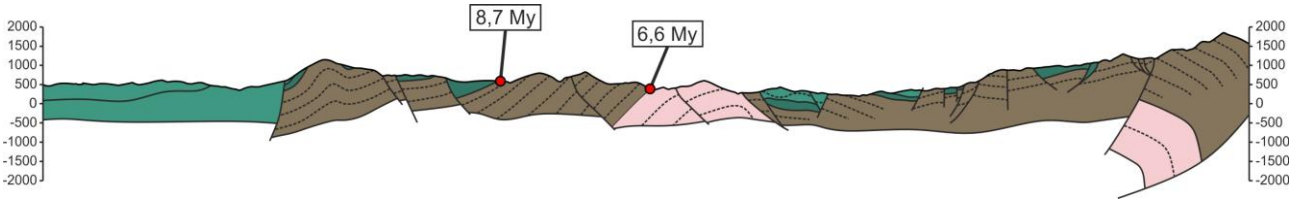

Fig. 7.1 – Geological framework for the Case 1; a) 1:250.000 geological map, for the key to the units see fig. 5.2, with a 90m resolution DTM of the modelled area, location of the AFT natural samples, and trace of the cross-section represented in fig. 7.1b; b) geological cross-section across the modelled area in Case 1, with location of the collected AFT samples, modified after Bernini et al., 1990.

The similar present day elevation of the two AFT samples we collected (PR 12 FT, top, 764 m a.s.l.,; PR 13 FT, base, 631 m a.s.l., see § 4) is related to the fact that this portion of the succession constitutes the tilted back limb of the km-scale Macigno fold representing the same regional-scale structure constituting the M.te Orsaro and most of the Western Northern Apennines main ridge (figs. 7.1a, 7.1b).

7.2.2 Presented model

The two samples we collected at the base and top of the succession are characterized by AFT cooling ages of 8.7 Myr (top) and 6.6 Myr (base), and since the difference in elevation of the base and the top of the succession decreased from ~2000 m (thickness of the undisturbed succession at the time of the deposition) down to ~133 m (present day elevation difference), we modelled the area indicated by the DTM in fig. 7.1a imposing in the E side a vertical velocity 50% higher with respect to the W side (fig 7.2). Therefore the uplift and cooling of the afore mentioned area has been modelled in the last 10 Myr through a pure vertical motion of a 30 km thick crustal block whose E and W sides underwent differential uplift.

With the names PR 12s and PR 13s we will indicate the two modelled ages which have the same coordinates and represent the synthetic equivalents of the two natural samples collected in the area (PR 12 FT and PR 13 FT, respectively).

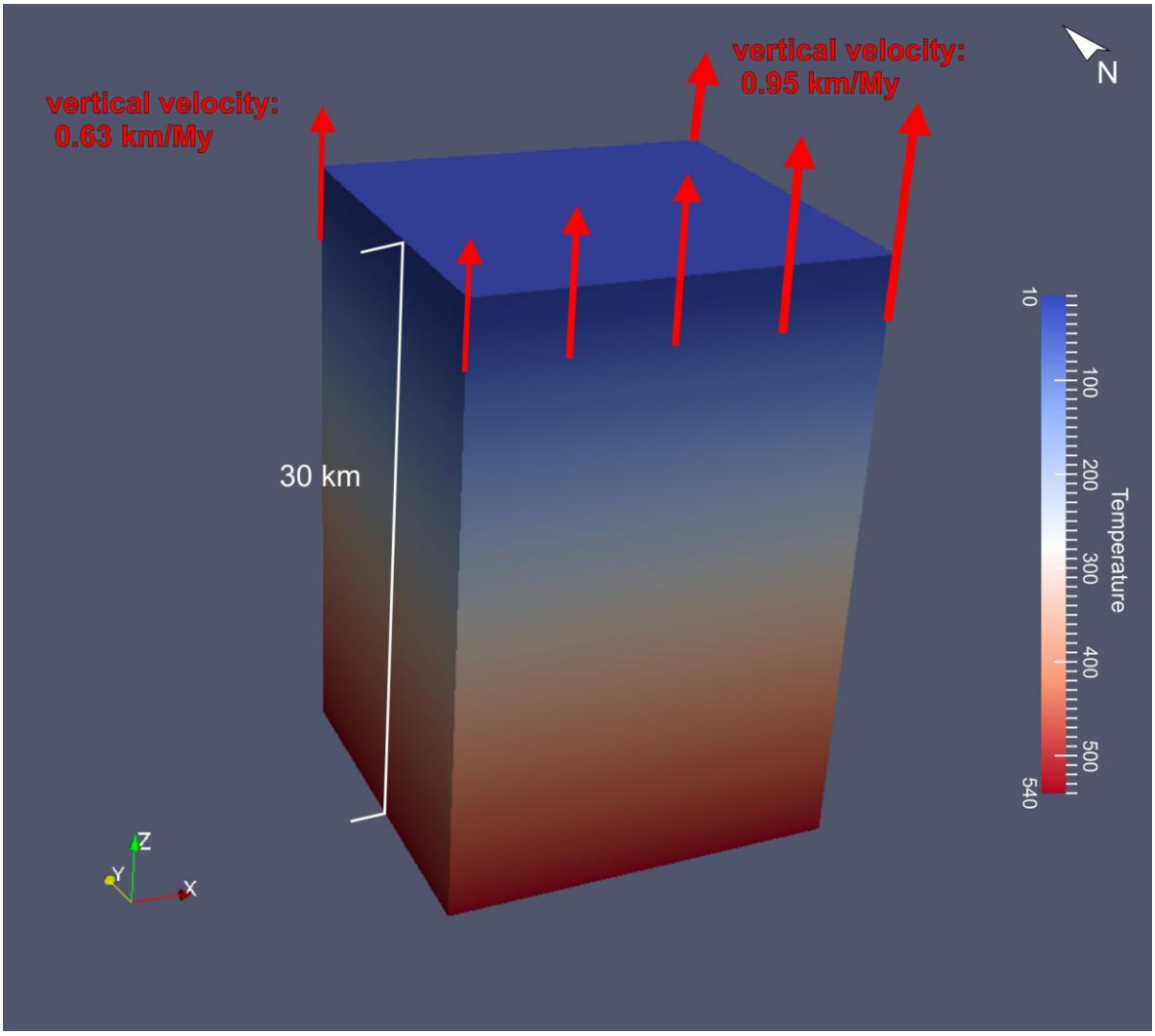

Fig. 7.2 – 3D picture of the crustal block underneath the modelled area. The colours indicate the distribution of the temperature with depth, indicated in the scale on the right. The red arrows are proportional to the vertical velocity imposed to the model, and indicate that the E side of the block is subject to a faster vertical velocity, in order to reproduce the tilting of the area.

The preliminary forward modelling have been performed setting unconstrained parameters to values which are thought to be reasonable for the study area, in particular the onset age of an eroding topography has been set to 5 Ma, the age at which the exhumation and uplift of the Macigno foredeep begun to 9 Ma, and the entity of the exhumation rate to 0.7 km/Myr. Then 224 iterations have been run in inverse modelling through the Neighbourhood Algorithm in order to better constrain the three afore mentioned parameters, and the obtained values for these latter, with a least misfit of 0.1914, were introduced in the model which best fit the natural samples data (fig. 7.3).

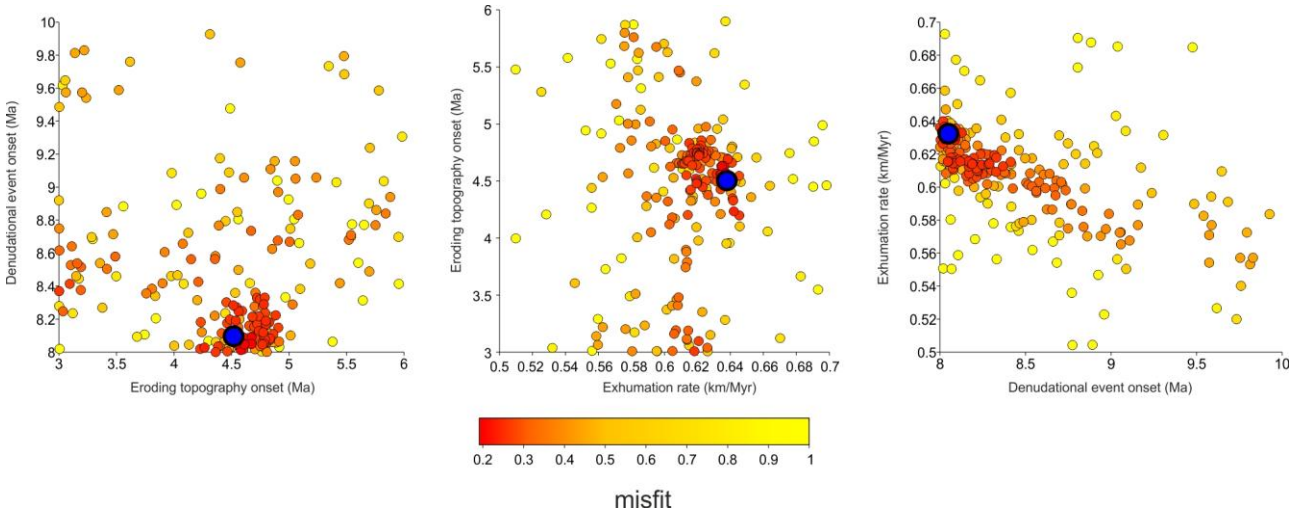

Fig. 7.3 – Results of the Neighbourhood Algorithm inversion for the three unconstrained parameters. In each diagram two of the three parameters and plotted one versus the other and each dot represents one of the 224 forward modelling run to find the best fitting model (indicated by the blue dot), which minimizes the misfit function, i.e. the difference between modelled and natural AFT ages.

The main parameters used in the presented model, therefore, are the following:

Number of time steps: 3 (10, 4.5 and 0 Ma);

Starting time: 10 Ma;

Onset of eroding topography: 4.5 Ma;

Vertical uplift starting time: 8.1 Ma;

Vertical uplift velocity: 0.63 km/Myr (resulting in 0.63 km/Myr on the W side and 0.95 km/Myr on the E side, see text for explanation);

Step 0 shows the situation 10 Ma, before the vertical movement of the foredeep units started (i.e. 8.1 Ma), with an undisturbed thermal field characterizing all the crustal block (fig. X5a). Samples PR 12s and PR 13s in this step are both below the AFT closure temperature (120°C isotherm indicated in red in fig. 7.4a) and the sample located at the base of the succession (PR 13s) lay ~2 km under the sample at the top (PR 12s).

Step 1 shows the situation at 4.5 Ma, just before the onset of an eroding topography, as constrained by the inverse modelling. At this time the vertical uplift and consequent denudation of the Macigno succession has already started since 3.6 Myr before, both samples have already cooled down under 120°C and they are located at ~2 km of depth under the surface (fig. 7.4b). The thermal field is deformed with respect to the previous step, and the isotherms are pushed towards the surface, because of heat diffusion and above all heat advection, which can be much more relevant in tectonically active regions, as stated in § 7.1.

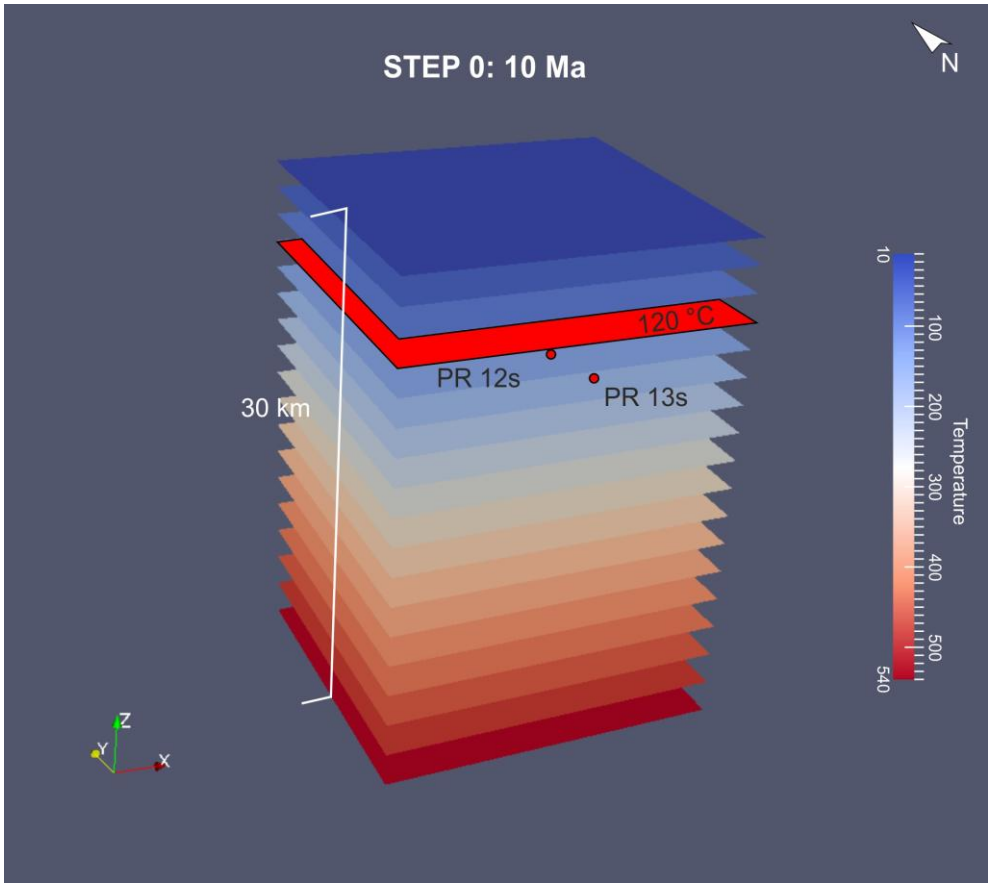
STEP 0: 10 Ma
N
120 °C
PR 12s
PR 13s
30 km
10
100
200
300
400
500
540
Temperature
Z
Y
X

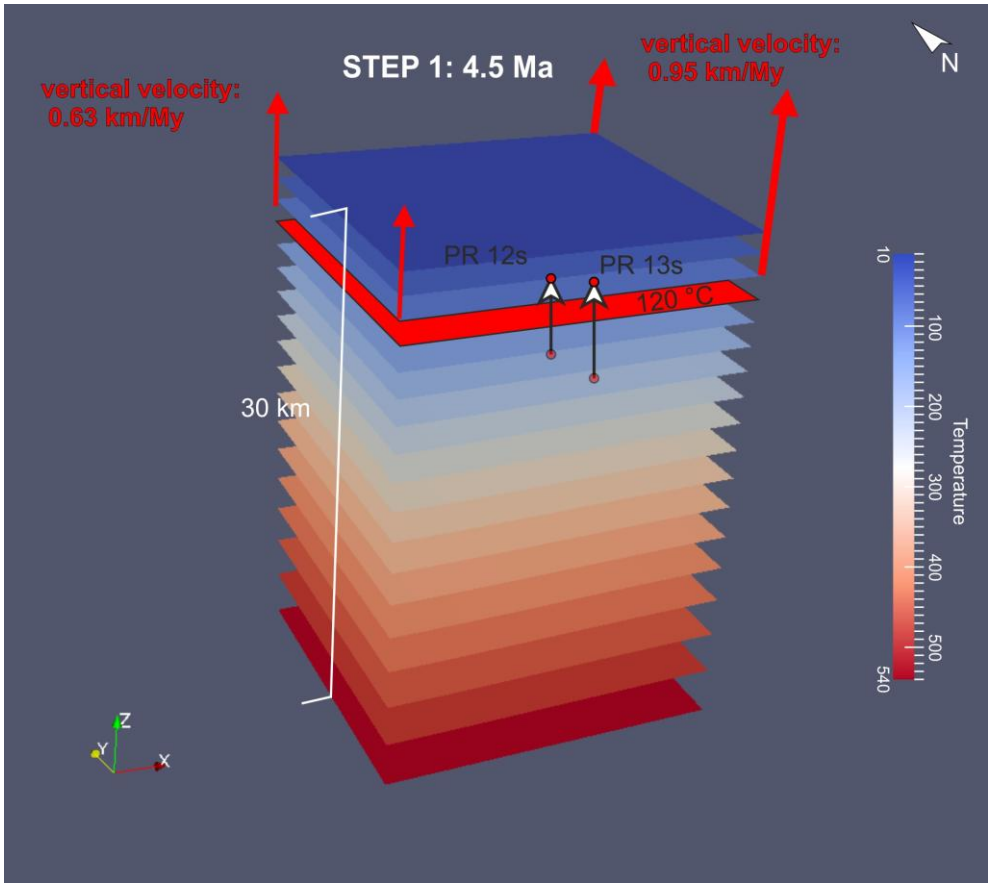
STEP 1: 4.5 Ma
vertical velocity:
0.63 km/My
vertical velocity:
0.95 km/My
N
PR 12s
PR 13s
120 °C
30 km
10
100
200
300
400
500
540
Temperature
Z
Y
X

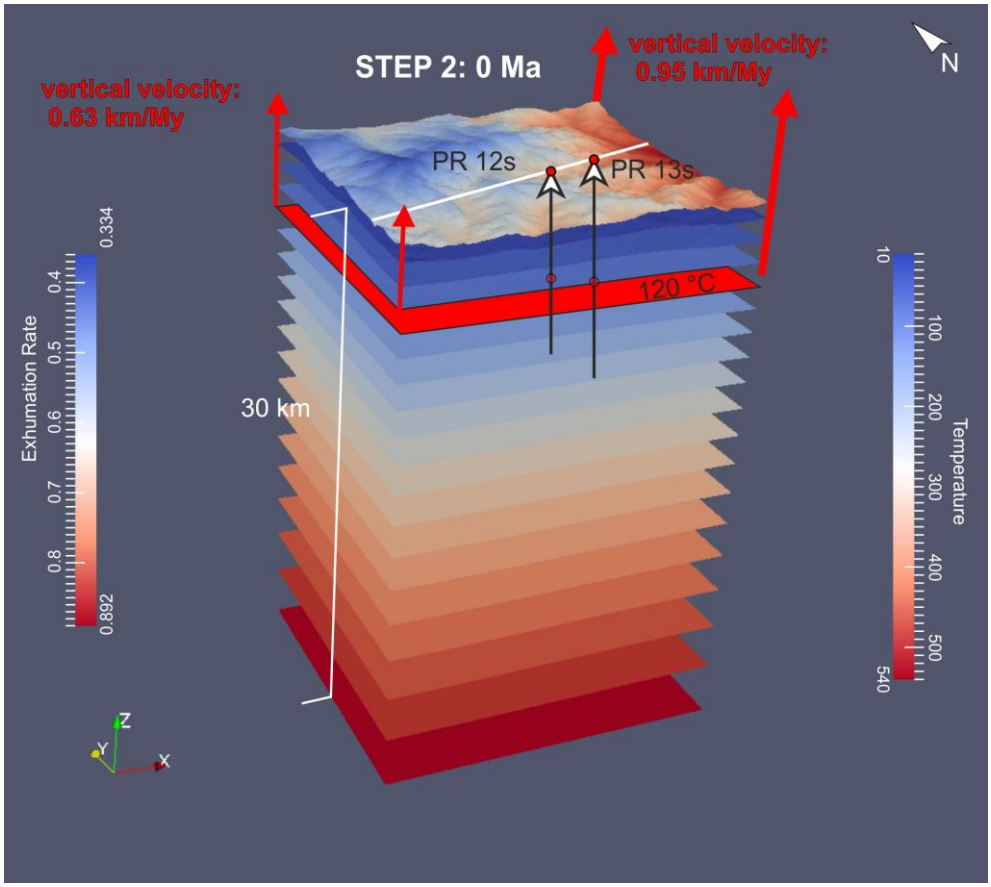

Fig. 7.4 – 3D pictures representing the three steps of the best fitting model (see text for description); the coloured planes represent isotherms every 30°C form surface to the bottom of the model, and the reference temperature is indicated in the right bar. a) Step 0, at 10 Ma; b) Step 1, at 4.5 Ma; c) Step 2, at 0 Ma; the left bar represent the exhumation rates depicted on the topography.

Since the crustal block is being uplifted differentially, because of the SW tilting of the foredeep succession related to the regional-scale deformation (fig. X1), the E side uplifts faster than the W side, and after 3.6 Myr from the beginning of the tectonic activity the difference in elevation in the two samples is much lower with respect to the previous step, being the sample at the base of the Macigno succession (PR 13s) at this time located closer to the faster edge of the model (i.e. the E side).

Step 2 represents the situation at 0 Ma, when both samples have reached the surface and they occupy their present-day location, with a difference of ~117 m in elevation, slightly lower than the elevation difference in the two natural samples (~ 133 m) (fig.7.4c).

The presented model resulted in AFT cooling ages for the two synthetic samples of 8.08 Myr (PR 12s) and 6.79 (PR13s), abundantly inside the analytic error of the two natural samples, as shown in fig. 7.5.

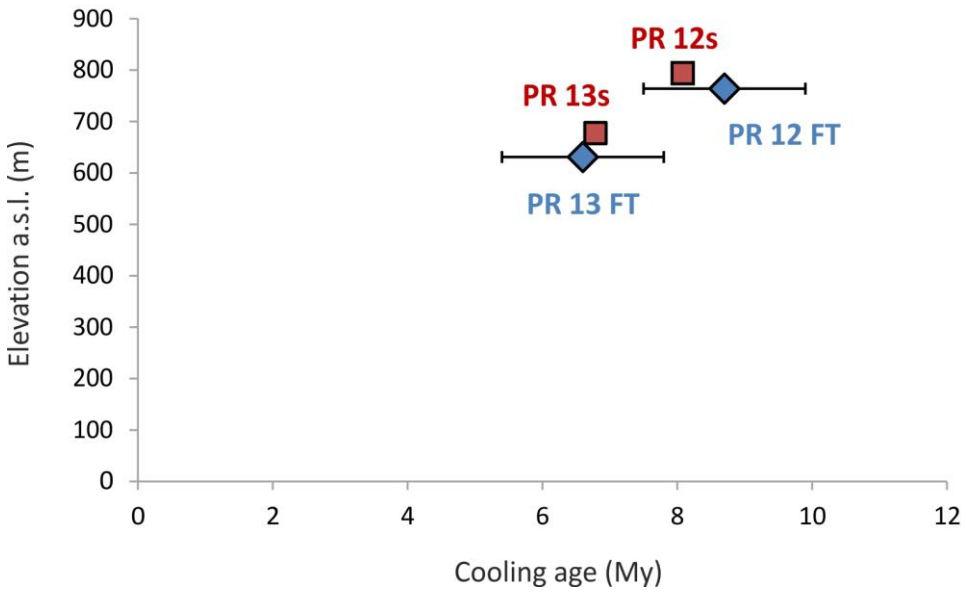

Fig. 7.5 – Plot of the age vs elevation of the natural (blue) and synthetic (red) samples in the study area. The two produced synthetic samples fall abundantly inside the error range of the natural samples, as highlighted by the black error bars.

The exhumation rate inside the modelled area is a function of the imposed differential vertical velocity, and varies between 0.63 and 0.95 km/Myr between 8.1 and 4.5 Ma and decreases between 0.33 and 0.89 km/Myr between 4.5 and 0 Ma. The mean exhumation rate for the area can be estimated in ~0.7 km/Myr, more specifically varying between 0.79 and 0.61 km/Myr respectively bef

ore and after the onset of an eroding topography.

7.3 Case 2 – Gova tectonic window

7.3.1 General framework

The Gova tectonic window, confined between the Secchia river and one of its right tributaries (Dragone torrent), constitutes the NE-most exposure of middle Miocene foredeep units (Cervarola foredeep), lying immediately under the LSU, whose lower portion in this area can be considered a lateral equivalent of the Subligurian Units, called Sestola-Vidiciatico tectonic Unit (SVU, Remitti et al., 2011) (fig. 7.6). The foredeep units, pretty undeformed, lie almost horizontal at the outcrop scale and constitute a gentle NE-verging thrust-related anticline, in strong contrast with the highly deformed lower portion of the LSU (Remitti et al., 2012 and references therein).

The three AFT samples collected inside the area gave cooling ages of 2.3 Ma (PR 20 FT, foredeep units), 2.5 Ma (PR 22 FT, SVU – lower portion of the LSU) and 4.7 Myr (PR 23.1 FT, Ligurian Units – upper portion of the LSU), and record the most recent and fast exhumation of Cervarola foredeep units throughout the NE side of the Northern Apennines (see § 5).

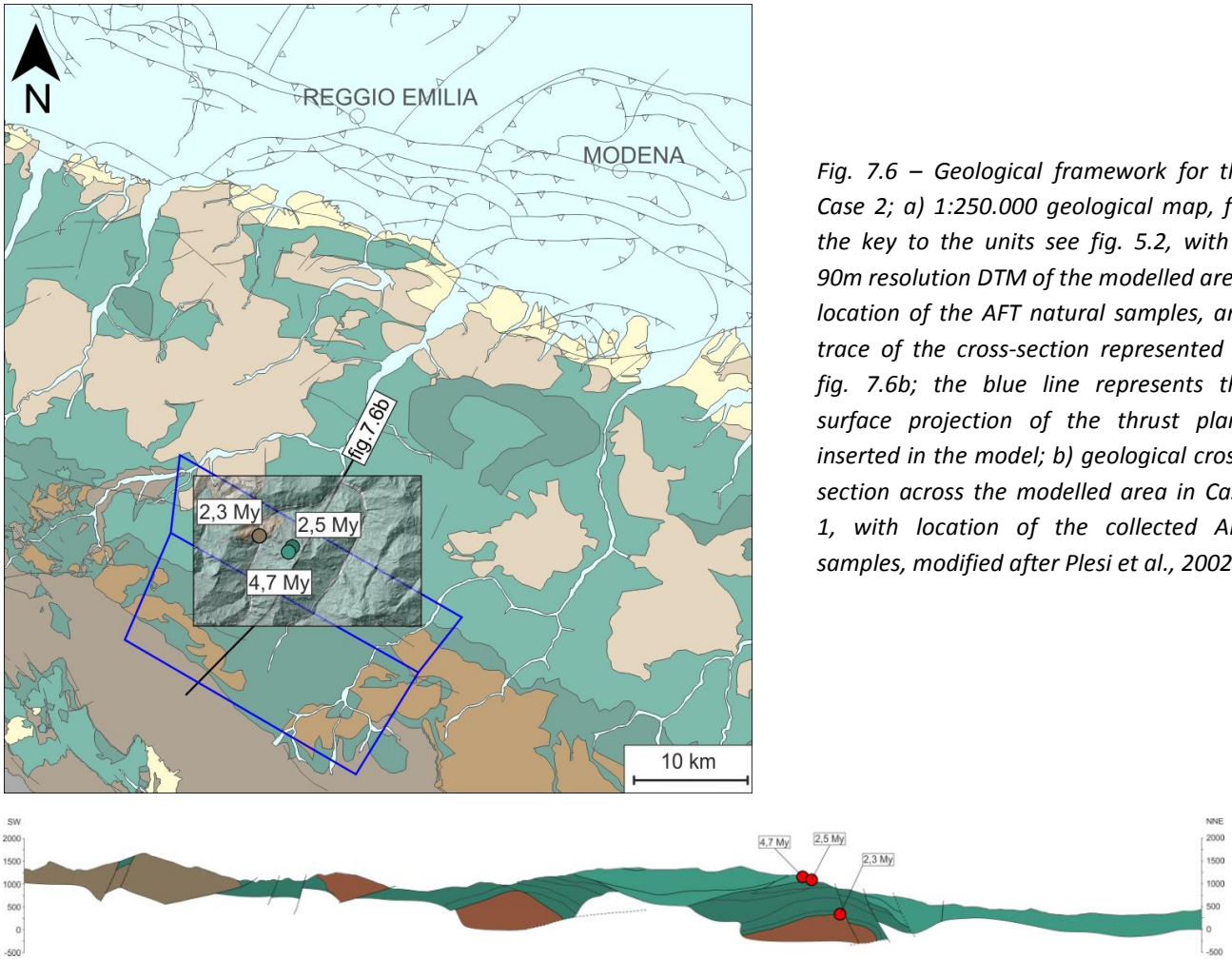

Fig. 7.6 – Geological framework for the Case 2; a) 1:250.000 geological map, for the key to the units see fig. 5.2, with a 90m resolution DTM of the modelled area, location of the AFT natural samples, and trace of the cross-section represented in fig. 7.6b; the blue line represents the surface projection of the thrust plane inserted in the model; b) geological cross-section across the modelled area in Case 1, with location of the collected AFT samples, modified after Plesi et al., 2002.

7.3.2 Presented model

In this case, in order to reproduce the natural samples, a thrust fault has been introduced in the model, whose geometry, constrained integrating data from the new seismic lines interpretation presented in chapter 4, allowed to build a velocity field along the fault plane which represent the rock particles' paths and fairly reproduces the growth of the Gova anticline. The synthetic ages corresponding to the natural samples have been named as follows: PR 20s and PR 22s, corresponding to natural samples PR 20 FT and PR 22 FT, respectively. Also in this case the unconstrained parameters were the onset of an eroding topography, the beginning of the activity along the main fault plane and the velocity of the movement along the fault. The NA inversions returned, after 608 runs, results for these three parameters with a misfit of 0.0561 (fig. 7.7), only

taking into account the natural samples PR 20 FT and PR 22 FT, because of the large 1σ error (~0.8 My) between samples PR 23.1 FT and PR 22 FT.

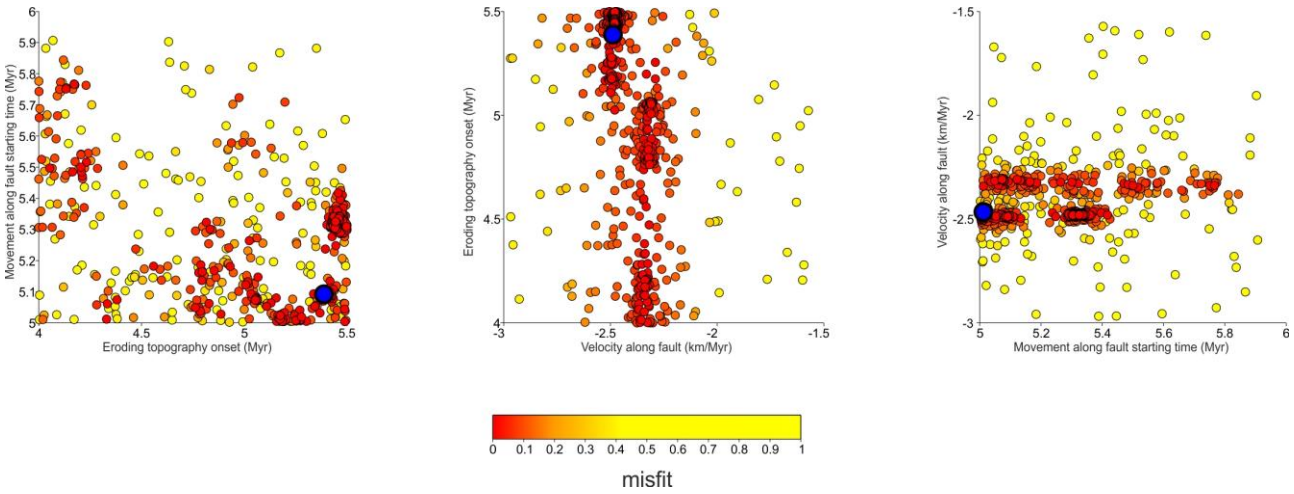

Fig. 7.7 - Results of the Neighbourhood Algorithm inversion for the three unconstrained parameters. In each diagram two of the three parameters and plotted one versus the other and each dot represents one of the 608 forward modelling run to find the best fitting model (indicated by the blue dot), which minimizes the misfit function, i.e. the difference between modelled and natural AFT ages.

The parameters introduced in the presented model input, therefore, are:

Number of time steps: 2 (5.34 and 0 Ma);

Starting time: 5.34 Ma;

Onset of eroding topography: 5.34 Ma;

Activity along the thrust fault starting time: 5.08 Ma;

Velocity along the thrust fault plane: 2.49 km/Myr;

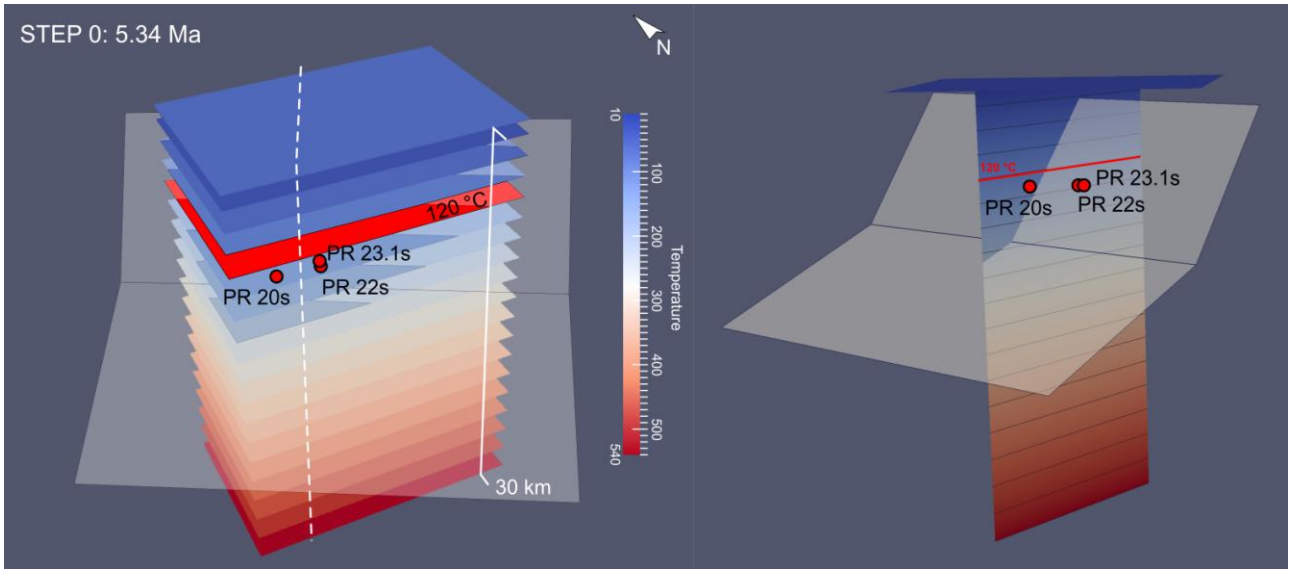

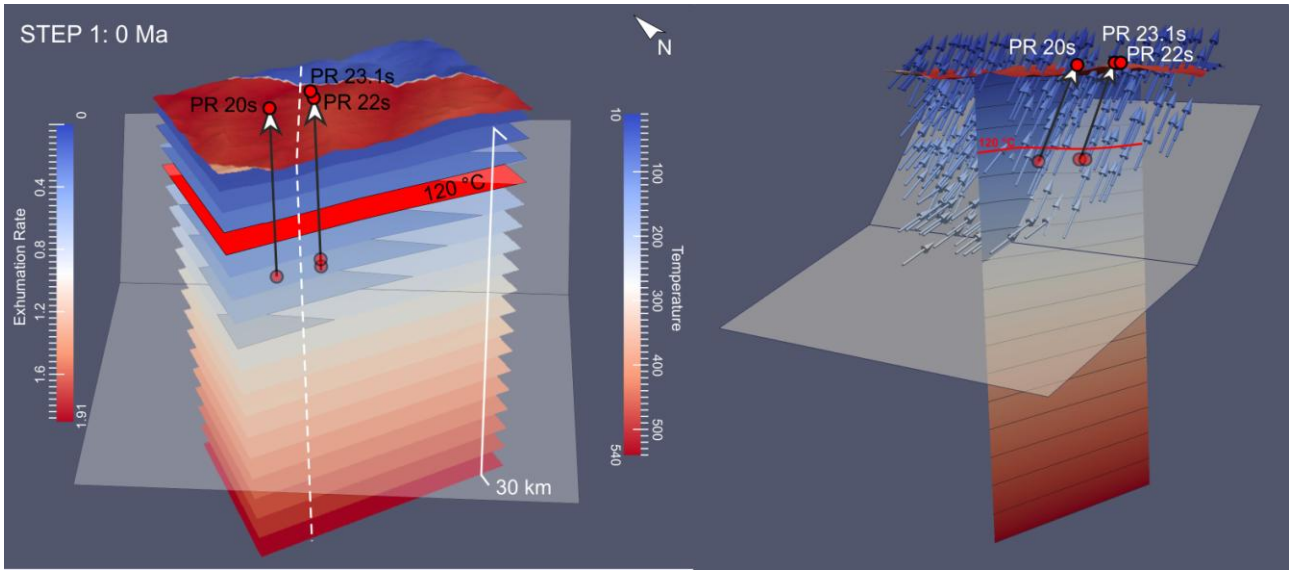

Fig. 7.8 – 3D pictures representing the two steps of the best fitting model (see text for description); the coloured planes represent isotherms every 30°C form surface to the bottom of the model, and the reference temperature is indicated in the right bar. The right panels represent a cross-section through the crustal block (traced by the white dashed line in the left panels) which clarifies the ongoing of the thrust fault plane and the distribution of the velocity vector (coloured arrows) along the same fault plane; a) Step 0, at 5.34 Ma; b) Step 1, at 0 Ma; the left bar represent the exhumation rates depicted on the topography.

Step 0 shows the situation 5.34 Ma, just before the onset of the eroding topography and few hundreds of years before the initiation of the movement along the thrust fault (fig. 7.8a). At this time the thermal field is still undisturbed and the synthetic samples are located at temperatures >120 °C.

Step 1 shows the present day situation, in which the topography has fully formed and, starting from 5.08 Ma, the activation of the thrust fault under the foredeep unit brings the samples to their present position at surface (fig. 7.8b). The T-t path followed by the rock particles, and thus by the synthetic samples, in this case is not purely vertical, but it has also a horizontal component related to the inclination of the fault plane. At temperatures lower than ~180°C it is possible to appreciate a discrete perturbation of the isotherms due to the heat advection caused by the motion of hot rocks along the fault, while below ~50°C the isotherms are even more perturbed, because of both heat advection and topographic effect (fig. 7.8c).

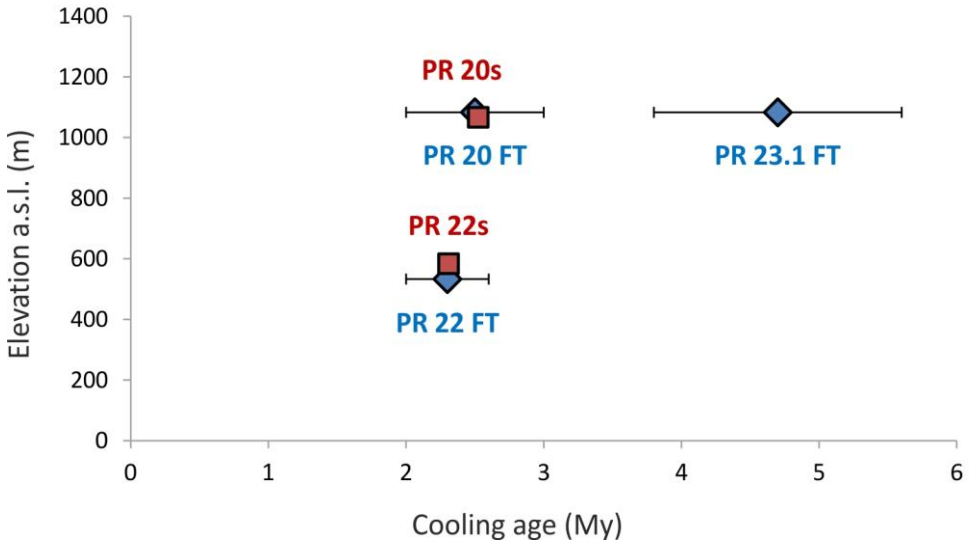

Fig. 7.9 – Plot of the age vs elevation of the natural (blue) and synthetic (red) samples in the study area. The two produced synthetic samples fall abundantly inside the error range of the natural samples, as highlighted by the black error bars .

The exhumation rates resulting from this model range between 0 (on the footwall of the thrust fault) and 1.91 km/Myr (on the hanging wall of the fault), with a mean value, inside the exhumed area, of 1.82 km/Myr.

The AFT cooling ages for the synthetic samples PR 20s and PR 22s are respectively 2.31 and 2.52 Myr, fairly coincident with the natural samples cooling ages (fig. 7.9).

7.4 Case 3 – Area comprised among Magra river, main ridge and Taro river

7.4.1 General framework

The area considered in this third model extends from the Lunigiana graben, W of the Apennines main ridge, to the middle-lower slope of the NE side of the Apenninic chain, towards the NE external margin of the chain, and comprises all the main tectonic units constituting the Western Northern Apennines (Tuscan foredeep units, Subligurian and Ligurian Units and Epiligurian Succession) (fig. 7.10a, § 2).

The AFT samples have been collected in all the main units and then integrated with previously published AFT data, mainly related to the Macigno foredeep units (Thomson et al., 2010, see § 5 for discussion).

As discussed in § 5 the two main zones individuated by the AFT ages (subzones 1a and 1b, 10-6 Ma and 5-0 Ma, respectively), which highlight a SW-NE younging trend, can be interpreted as

diagnostic of NE-ward migrating orogenic processes, among which the deep thrusting and folding and consequent increased erosion rates and exhumation of deep tectonic units play a lead role (see § 5); in particular the two subzones seem to be affected by the diachronous activity of the Macigno subsequently and Cervarola foredeeps frontal thrusts.

The geometry of the thrusts has been constrained thanks to the new interpretation of seismic lines inside the study area which allowed to recognize the presence of five main imbricate thrust faults which seem to play a major role also in the most recent tectonic evolution of the chain (see § 5, § 6).

7.4.2 Presented model

In order to reproduce the natural samples in this area, therefore, two blind thrusts which approximately represent the frontal thrusts of the Macigno and Cervarola foredeeps have been introduced.

The activity inception along the faults has been constrained through 608 runs in inversion mode with the Neighbourhood Algorithm to 12 Ma for the innermost Macigno thrust (indicated in blue in figs. 7.10a, 7.11), with a mean velocity along the fault plane of 0.94 km/Myr, and to 6.00 Ma with a velocity 0.95 km/Myr for the outermost Cervarola thrust (indicated in red in figs. 7.10a, 7.11). The lowest resulting misfit from the inversion is 0.5703, value which is much higher with respect to the misfits obtained in the two previous modelled areas (0.1914 and 0.0561). The higher obtained misfit value is mainly related to the fact that the considered area is more than five times larger than the areas modelled in § 7.1.1 and 7.1.2; the larger dimensions of the modelled area don’t permit to take into account all the late geological processes and features affecting local contexts.

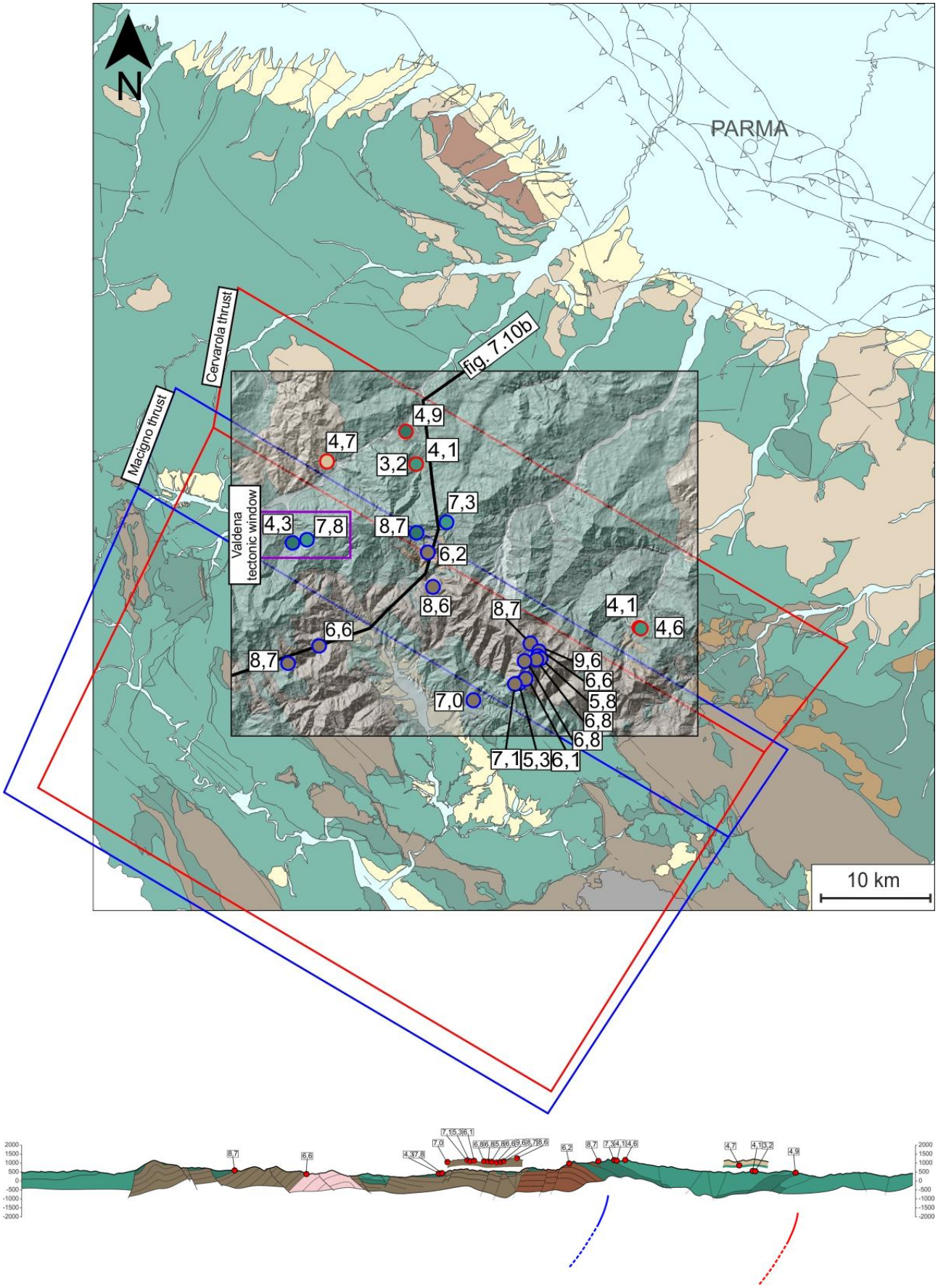

Fig. 7.10 – Geological framework for the Case 2; a) 1:250.000 geological map, for the key to the units see fig. 5.2, with a 90m resolution DTM of the modelled area, location of the AFT natural samples (blue-bounded: cooled during the older activity of the Macigno thrust, red-bounded: cooled during the later activity of the Cervarola thrust, see text), and trace of the cross-section represented in fig. 7.10b; the blue and red lines represent the surface projections of the thrust plane inserted in the model; b) geological cross-section across the modelled area in Case 1, with location of the collected AFT samples, modified after Bernini et al., 1990, Vescovi et al., 2002.

In particular one of the main process contributing to major AFT cooling ages variations in samples located close to each other is the tectonic elision described in § 5, which, reactivating older contacts such as the Eocene thrusting of the Ligurian over the Subligurian Units as low angle normal faults, brings shallower units (characterized by older AFT ages) in direct contact with deeper units (characterized by younger cooling ages), as in the case of the Valdena tectonic window (see § 5.3.1 in chapter article).

The other parameter constrained with the model inversion was once again the onset of the eroding topography, thus the input parameters for the presented model were:

Number of time steps: 3 (12, 5.35 and 0 Ma);
Starting time: 12 Ma;
Onset of eroding topography: 5.35 Ma;
Activity inception along the innermost (blue) thrust fault: 12 Ma;
Velocity along the innermost thrust fault: 0.94 km/Myr;
Activity inception along the outermost (red) thrust fault: 6.00 Ma;
Velocity along the outermost thrust fault: 0.95 km/Myr;

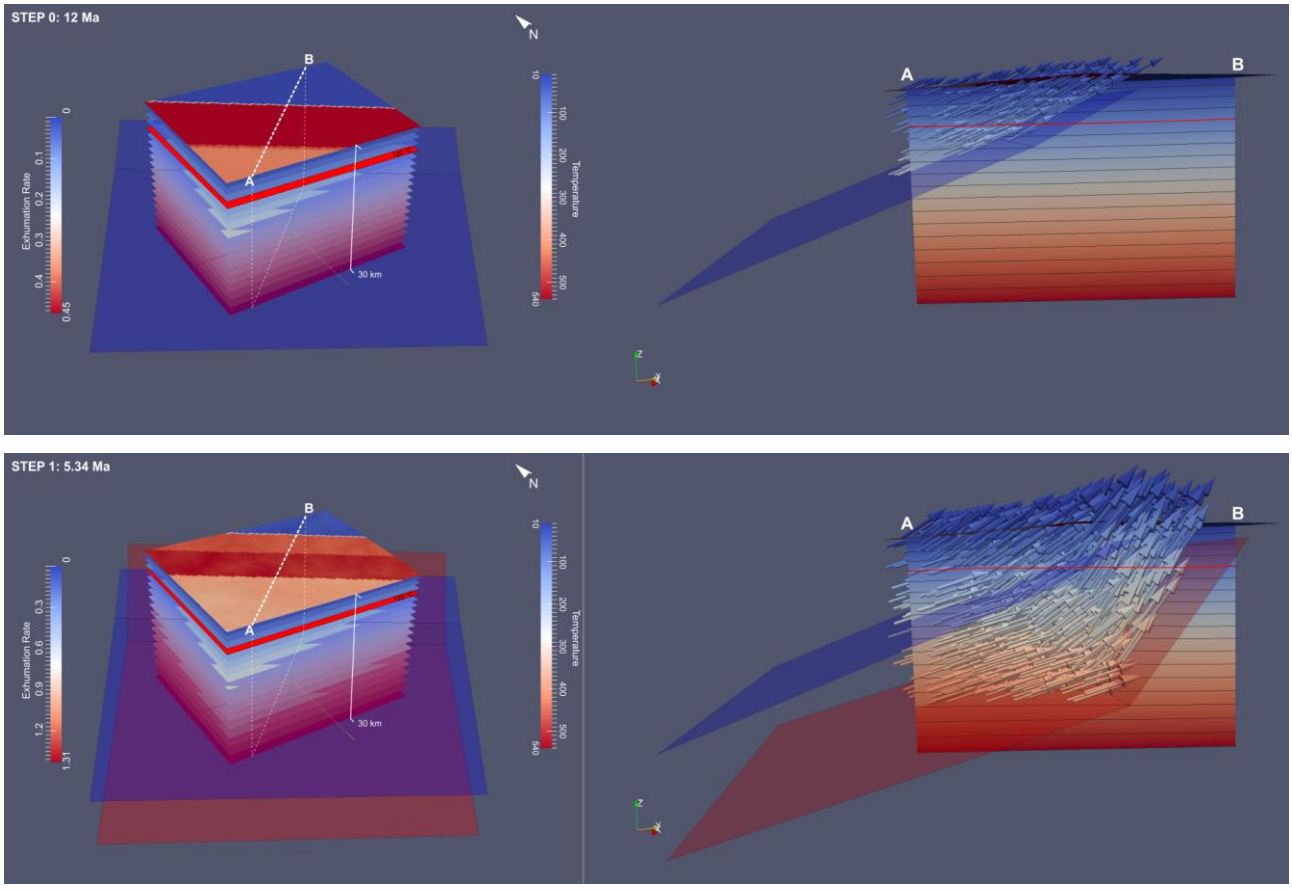

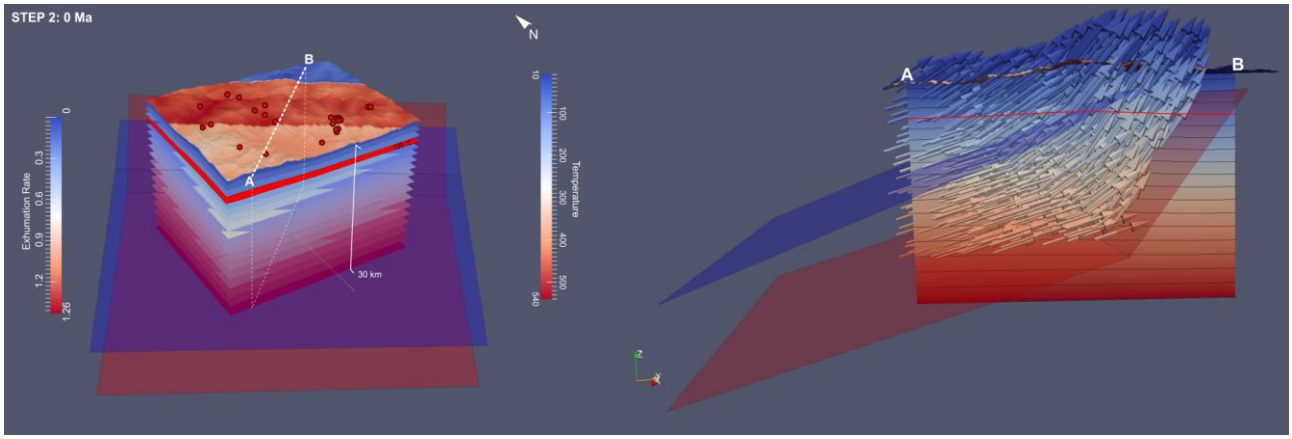

Fig. 7.11 – 3D pictures representing the three steps of the best fitting model (see text for description); the coloured planes represent isotherms every 30°C from surface to the bottom of the model, and the reference temperature is indicated in the right bar. The right panels represent a cross-section (A-B) through the crustal block (traced by the white dashed line in the left panels) which clarifies the ongoing of the thrust fault planes and the distribution of the velocity vector (coloured arrows) along the same fault planes; a) Step 0, at 12.0 Ma; b) Step 1, at 5.35 Ma; c) Step 2, at 0 Ma; the left bar represent the exhumation rates depicted on the topography.

Step 0 represents the situation 12 Ma, when the tectonic activity along the Macigno thrust (innermost one, blue-coloured) begins. At this time the thermal field is only minimally perturbed and the samples are buried at temperatures higher than 120 °C (fig. 7.11a). The red area in left panel of fig. 7.11a, located on the hanging wall of the Macigno thrust fault is the only interested by exhumation acting at rates between 0.32 and 0.45 km/Myr.

At 5.35 Ma, step 1, the activity on the Cervarola thrust (outermost one, red coloured) is just started (6 Ma) and an eroding topography is starting to form, principally in the presently most elevated areas (i.e. Apennines main ridge area) (fig. 7.11b). The exhumed area widens towards NE, where also the Cervarola thrust hanging wall is active, and the exhumation rates range from 0.76, in the SW-most portion of the area, to 1.31 km/Myr, at the tip of the Macigno inner thrust. This last area, in fact, corresponds to where the chain main ridge will form in the next time step, and hosts the most deeply exhumed and uplifted rocks. Only the samples affected by the innermost foredeep thrusting have cooled down under 120°C at this time.

Step 2 shows the present-day situation, in which all the samples have cooled down under the AFT closure temperature and reached their present-day location (fig. 7.11c). The topography has completely formed and the exhumation rates range from 0.56 (SW portion of the block) to 1.26 km/Myr (main ridge area).

7.5 Exhumation and denudation rates in the study area

The first two presented model (Valgordana and Gova cases) are related to small areas whose exhumation and denudation are primarily affected by the growth of localized km-scale structures, therefore the obtained exhumation rates are only partially representative of a regional trend. In any case, the growth of these structures is related to the same orogenic-scale processes causing regional uplift and denudation, and the obtained exhumation rates (~0.7 km/Myr, Val Gordana case; ~1.8 km/Myr, Gova case) fairly agree with the afore-mentioned published estimates related to areas located in proximity of the case study (~0.7 – 1.7 km/Myr).

The third model (Taro case), on the other hand, is able to give more precise constraints on the evolution through time of exhum1ation/denudation rates at a regional scale. Fig. 7.12 shows, along section A-B traced in fig. 11, the evolution of the exhumation rate through the tree time steps of the model. The mean exhumation rate, represented by the black dashed line, changes from 0.15 to 0.72 and 0.63 km/Myr, with positive peaks in steps 1 and 2 (5.35 and 0 Ma, respectively) of 1.18 and 1.04 km/Myr. Therefore it is possible to infer that inside the study area the average exhumation rates in the last ~12 Myr well agree with previously recognized estimates in other areas of the Northern Apennines (e.g. in the Apuane Alps). ~6 Ma an important increase in the denudation rates seems to occur, mainly in relation to the beginning of the activity along the Cervarola (outermost) main thrust, and to remain almost stable until present. A similar increase in exhumation rates (from 0.4-0.6 km/Myr to 1.3-1.8 km/Myr) has been testified in the Apuane Alps between ~6 and 4 Ma (Balestrieri et al., 2003). It is remarkable that the tectonic/exhumational/denudational histories of both the study area and the Apuane Alps share many features in common, such as exhumation rates, changes in exhumation rates through time and how exhumation processes evolved through time (see § 5).

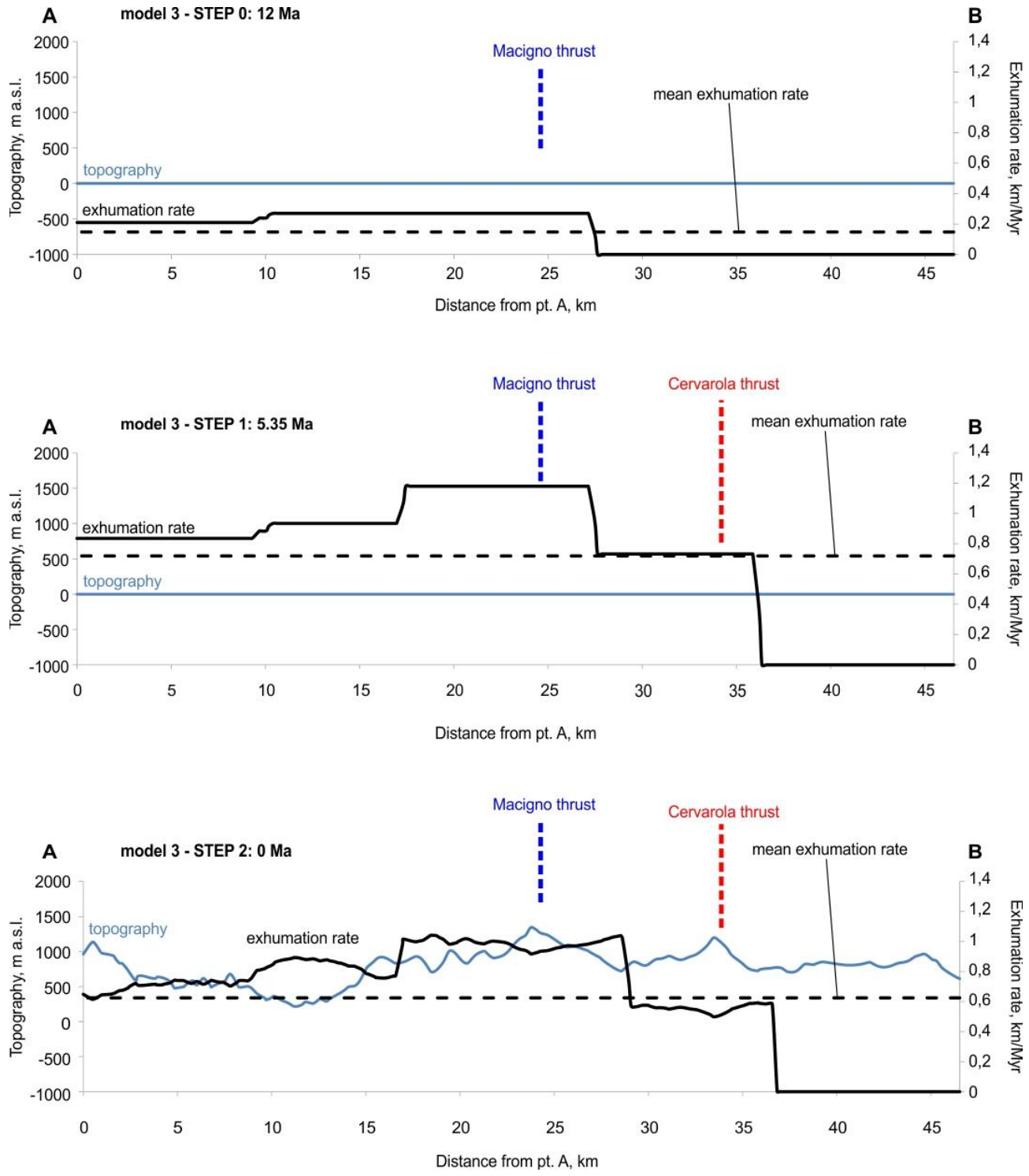

Fig. 7.12 – Evolution of exhumation rate and topography in the third model (Case 3), along section A-B, traced in fig. 7.1. The blue line represent the topography, the solid black line the exhumation rate, the dashed black line the mean exhumation rate, the blue and red dashed lines represent the surface projection of the buried thrust tips, compare with fig. 7.11; see paragraph 7.4.2 for description of the single model steps; a) step 0, 12 Ma; b) step 1, 5.35 Ma; c) step 2, 0 Ma.

8. Discussion and conclusive remarks

The investigation of the middle Miocene to Recent tectonic evolution of the western Northern Apennines revealed the existence of two main evolutionary stages (~10-6 and ~6-0 Ma) characterized by relatively shallow extensional tectonics related to deep compressional tectonics affecting the whole Apennine orogenic wedge; these two stages have been revealed by investigating the Apennines far travelled/allochthonous LSU and the underlying foredeep deposits through an integrated study which took into account surface and subsurface geological data, paleothermal and thermochronological analyses (§ 3-5).

The first stage (~10-6 Ma) was characterized by folding and thrusting and subsequent uplift and denudation of the upper Oligocene Tuscan units (Macigno foredeep unit). These processes contributed to the formation of gravitational instabilities inside the orogenic wedge and consequent activation of shallow low angle extensional tectonics, responsible for the tectonic elision and deep reshaping of the LSU. Further field studies might be needed to better characterize and define the entity and relevance of the evidenced low angle normal faults at a regional scale (fig. 3.1).

During the younger stage (~6-0 Ma) the continuous compressional tectonic regime produced further uplift and denudation of the foredeep units at the main ridge of the chain. These events, responsible for the onset of new gravitational instabilities, were accommodated mainly by high angle extensional tectonics and possibly also ongoing of the low angle one. During this second stage, the contribution of tectonic versus erosional denudation is difficult to unravel; in fact, surface erosion processes, which more and more intensively shaped the emerging Apennine chain since ~5 Ma, are poorly constrained. In the present study, the contribution of surface erosion has been quantitatively estimated through the numerical modelling of the AFT data and the results (average 0.64 km/My over the last 5.35 My, § 7), fully consistent with previously published erosion rates estimates, allowed to infer a total amount of ~3.2 km thickness removed exclusively by surface erosion. This result confirms that: a) surface erosion processes alone were not enough to remove the whole thickness of the far travelled/allochthonous LSU, constituting the burial of foredeep units at the main ridge of the Northern Apennines (4-6 km, see § 5); b) the tectonic elision of the LSU had to play an important role in exhumation/denudation of the Tuscan foredeep units.

The AFT data modelling, however, is not strongly constrained in the most recent phases (i.e. younger than ~4 Ma, §7), but the present study revealed data suggesting that the Apennine deep compressional structures might have been activated or reactivated in Recent times, in particular:

- scattered AFT ages younger than 3.0 Ma (e.g., Gova tectonic window, fig. 5.6c, § 5);
- strong spatial and possible genetic relationships between some of the deep-seated Apennine thrust faults, late orogenic antiforms (i.e., related to the neotectonic evolution of the chain) and Holocene surface gravitational processes and DSGSDs (§ 6).

Previously published works had already highlighted the Pliocene to Recent activity of the Macigno main thrust (marked as thrust "A" in § 6), the Apennine-Po Plain frontal thrust and the Emilia-Ferrara arcuate thrust systems buried under the Po Plain (Boccaletti et al., 2011 and references therein; Picotti and Pazzaglia, 2008; Toscani et al., 2009; Wilson et al., 2009). Even though in a preliminary way, the new data and results not only reinforce these latter observations, but also suggest that many other deep-seated compressive structures of the western Northern Apennines might have been locally reactivated during finite amounts of time during the latest and most recent collisional phases of the Apennines.

In a more regional perspective the new AFT data extended towards west the previously published thermochronological dataset (cfr. figs. 4.9 and 4.10), and allowed to shed new lights and raise new questions about the complex and laterally varying geodynamic evolution of the Northern Apennines orogenic wedge. As already highlighted by previous authors, a single model for the geodynamic evolution of the Apenninic chain is inappropriate and inconsistent with the along-strike variations observed in surface and subsurface geological data, thermochronological and GPS data (Bennet et al. 2012; Thomson et al., 2010). While subsurface and field geological data heterogeneity across the Northern Apennines have already been discussed in previous chapters (see § 5), recent published thermochronological and GPS data highlighted the presence of two clearly distinguished sectors within the chain, separated by a long recognized regional scale transverse feature (the "Livorno-Sillaro Line", Ghelardoni, 1965; Bortolotti, 1966; Nirta et al., 2007, fig. 2.1): a) an eastern sector, characterized by SW-directed horizontal motion of material through the orogenic wedge; b) a western sector (constituting part of our investigated area) dominated by overall vertical motion. Even if the interpretation of all these data is not yet completely clear, the changes across the Apennine chain have to be related to lithospheric-scale processes, since they

have been highlighted also by seismic tomographic data (Piromallo and Morelli, 2003 and references therein; Vignaroli et al., 2008) and gravity anomaly maps (APAT, 2005). The cited GPS and thermochronological data patterns have been used, therefore, to produce dynamic models in which basically a general compressive context created an eastern Apenninic sector dominated, since post-late Miocene times, by slab retreat and consequent NE-younging frontal accretion, and a western sector dominated by underplating and/or slab retreating slowdown and cessation.

Inside this framework, the new data and results of this study have been helpful in further constraining the timing and mechanisms affecting the western Northern Apennines. Specifically, since at least the middle Miocene, the investigated area was characterized by two major episodes of vertical material motion and both episodes are underlined by the recognition of important uplift processes, orogenic wedge overthickening and subsequent reequilibration to a stable orogenic wedge conditions through shallow extensional tectonics (first stage) and surface erosional processes (probably predominant in the second stage) (see § 5, 6). Nonetheless, the new thermochronological ages also highlight a NE-directed younging trend which reflects the evolution and migration through time in the orogenic processes; these processes would have been active, thus, also to the west of the Sillaro Line, implying that not precisely constrained episodes of orogenic frontal accretion, horizontal material motion and, possible slab retreat (as interpreted in the Eastern Northern Apennine) had to occur in the last ~10 My also in the Wetsern portion of the Northern Apennines. These observations shed a new light on the middle Miocene to Recent evolution of the western Northern Apennines, depicting this sector of the chain as affected by a complex sequence of deep underplating (vertical motion) and frontal accretion (horizontal motion) events, acting inside an overall compressional regime which enhanced episodes of shallow (<10 kilometres) extensional tectonics.

9. References

AGIP, 1977. Temperature Sotterranee.

Amorosi, A., Colalongo, M.L., Vaiani, S.C., 1993. Le unità epiliguri mioceniche nel settore emiliano dell'Appennino settentrionale. Biostratigrafia, stratigrafia sequenziale e implicazioni litostratigrafiche. Palaeopelagos 3, 209–240.

Argnani, A., Barbacini, G., Bernini, M., Camurri, F., Ghielmi, M., Papani, G., Rizzini, F., Rogledi, S., Torelli, L., 2003. Gravity tectonics driven by Quaternary uplift in the Northern Apennines: insights from the La Spezia-Reggio Emilia geo-transect. Quaternary International 101-102, 13–26.

Argnani, A., Ricci Lucchi, F., 2001. Tertiary siliciclastic turbidite systems of the Northern Apennines. In: VAI G.B. & MARTINI I.P. (Eds.), Anatomy of an orogen: the Apennines and adjacent Mediterranean basins. Kluwer Academic, London 327–350.

Artoni, A., Bernini, M., Papani, G., Rizzini, F., Barbacini, G., Rossi, M., Rogledi, S., Ghielmi, M., 2010. Mass-transport deposits in confined wedge-top basins : surficial processes shaping the messinian orogenic wedge of Northern Apennine of Italy. Italian Journal of Geoscience 129, 101–118.

Artoni, A., Bernini, M., Vescovi, P., Lorenzi, U., Missorini, E., 2006. Estensione alla sommità del cuneo orogenico appenninico : contatti tettonici elisionali nella Successione epiligure di M . Barigazzo (Appennino settentrionale , prov . di Parma). Rendiconti della Società Italiana 2, 69–72.

Artoni, A., Rizzini, F., Roveri, M., Gennari, R., Manzi, V., Papani, G., Bernini, M., Rossi, M., 2007. Tectonic and Climatic Controls on Sedimentation in late Miocene Cortemaggiore Wedge-Top Basin (Northwestern Apennines, Italy). In: LACOMBE O., LAVÉ J., ROURE F. & VERGÉS J. (Eds.), Thrust Belts and Foreland Basins. From Fold Kinematics to Hydrocarbon Systems. Frontiers in Earth Sciences Series, Springer, Heidelberg 431–456.

Balestrieri, M.L., Bernet, M., Brandon, M.T., Picotti, V., Reiners, P., Zattin, M., 2003. Pliocene and Pleistocene exhumation and uplift of two key areas of the Northern Apennines. Quaternary International 101-102, 67–73.

Barbarand, J., Carter, A., Wood, I., Hurford, T., 2003. Compositional and structural control of fission-track annealing in apatite. Chemical Geology 198, 107–137.

Barchi, M., Landuzzi, A., Minelli, G., Pialli, G., 2001. Outer Northern Apennines, in: Vai, G.B., Martini, I.P. (Eds.), Anatomy of an Orogen: The Apennines and Adjacent Mediterranean Basins. Kluwer Academic Publishers, pp. 215–255.

Barchi, M.R., Minelli, G., Pialli, G., 1998. The crop 03 profile: a synthesis of results on deep structures of the Northern Apennines. Memorie della Società Geologica Italiana 52, 383–400.

Barker, C.E., Pawlewicz, M.J., 1994. Calculation of vitrinite reflectance from thermal histories and peak temperatures: a comparison of methods. n Mukhopadhyay P.K. & Dow W.G. (Eds.) (1994) - Vitrinite Reflectance as a Maturity Parameter. Applications and Limitations - ACS Symp. Ser., 570 216–229.

Bartolini, C., 2003. When did the Northern Apennine become a mountain chain? Quaternary International 101-102, 75–80.

Bartolini, C., Caputo, R., Pieri, M., 1996. Pliocene–Quaternary sedimentation in the Northern Apennine Foredeep and related denudation. Geological Magazine 133, 255–273.

Bartolini, C., D'Agostino, N., Dramis, F., 2003. Topography, exhumation, and drainage network evolution of the Apennines. Episodes-Newsmagazine of the … 26, 212–216.

Bennett, R.A., Serpelloni, E., Hreinsdóttir, S., Brandon, M.T., Buble, G., Basic, T., Casale, G., Cavaliere, A., Anzidei, M., Marjonovic, M., Minelli, G., Molli, G., Montanari, A., 2012. Syn-convergent extension observed using the RETREAT GPS network, northern Apennines, Italy. Journal of Geophysical Research 117.

Bernini, M., Boccaletti, M., Moratti, G., Papani, G., Sani, F., Torelli, L., 1990. Episodi compressivi neogenico-quaternari nell'area estensionale tirrenica nors-orientale. Dati in mare e a terra. Memorie della Società Geologica Italiana 45, 577–589.

Bernini, M., Papani, G., Dall'Asta, M., Lasagna, S., Heida, P., 1991. The upper Magra valley extensional basin: a cross section between Orsaro Mt. and Zeri (Massa province). Bollettino della Società Geologica Italiana 110, 451–458.

Bernini, M., Vescovi, P., 2002. La deformazione neogenica delle Unità di avanfossa registrata nelle sovrastanti Liguridi della media Val Taro (con Carta strutturale alla scala 1:100.000), in: Atti Del Terzo Seminario Sullla Cartografia Geologica.

Bernini, M., Vescovi, P., 2008. Carta geologica della Lunigiana, in: Di Battistini, G., Rapetti, C. (Eds.), Arenaria. Pietra Ornamentale e Da Costruzione Nella Lunigiana.

Bernini, M., Vescovi, P., Artoni, A., unpublished, Synthetic geological map of the Northern Apennines, scale 1:250.000. Department of Physics and Earth Sciences - University of Parma.

Bernini, M., Vescovi, P., Zanzucchi, G., 1997. Schema strutturale dell'Appennino Nord-Occidentale. Acta Naturalia de l'Ateneo Parmense 33, 43–54.

Bertotti, G., Capozzi, R., Picotti, V., 1997. Extension controls Quaternary tectonics, geomorphology and sedimentation of the N-Appennies foothills and adjacent Po Plain (Italy). Tectonophysics 282, 291–301.

Bettelli, G., Bonazzi, U., Fazzini, P., Panini, F., 1987. Schema introduttivo alla geologia delle Epiliguridi dell'Appennino Modenese e delle aree limitrofe. Memorie della Società Geologica Italiana 39, 215–244.

Bettelli, G., Panini, F., Pizziolo, M., 2002. Note Illustrative della Carta Geologica d'Italia alla scala 1:50.000, foglio 236 "Pavullo nel Frignano". Servizio Geologico d'Italia-Regione Emilia Romagna 168.

Bettelli, G., Vannucchi, P., 2003. Structural style of the offscraped Ligurian oceanic sequences of the Northern Apennines: new hypothesis concerning the development of mélange block-in-matrix. Journal of Structural Geology 25, 371–388.

Bevins, R.E., White, S.C., Robinson, D., 1996. The South Wales Coalfield: low grade metamorphism in a foreland basin setting? Geological Magazine 133, 739–749.

Boccaletti, M., Cerrina Feroni, A., Martinelli, P., Moratti, G., Plesi, G., Sani, F., 1990. Compressive events in the Tyrrhenian side of the Northern Appenines. Annales Tectonicae.

Boccaletti, M., Coli, M., 1982. Carta Strutturale dell'Appennino Settentrionale. C.N.R. pubbl. 429.

Boccaletti, M., Corti, G., Martelli, L., 2011. Recent and active tectonics of the external zone of the Northern Apennines (Italy). International Journal of Earth Sciences 100, 1331–1348.

Boccaletti, M., Elter, P., Guazzone, G., 1971. Plate Tectonic Models for the Development of the Western Alps and Northern Apennines. Nature 234, 108–111.

Bonazzi, A., Chierici, R., Salvioli Mariani, E., Vernia, L., 1982. Metamorfismo e diagenesi in formazioni dell'Appennino Settentrionale (Val Dolo, province di Modena - Reggio Emilia). Dati di cristallinità dell'illite. Mineralogica et petrographica acta 26, 121–141.

Bonazzi, A., Cobianchi, M., Galbiati, B., 1987. Primi dati sulla cristallinità dell'illite nelle unità tettoniche più esterne e strutturalmente più elevate delle Alpi Liguri. Atti Ticinensi di Scienze della Terra 31, 63–77.

Bonazzi, A., Costa, E., 1989. Rapporto tra deformazione tettonica e cristallinità dell'illite nell'Appennino Settentrionale. Atti Ticinensi di Scienze della Terra 32, 57–70.

Bonazzi, A., Salvioli Mariani, E., Vernia, L., 1984. Diagenesi e metamorfismo dedotti dalla cristallinità dell'illite in formazioni sedimentarie affioranti tra Pontremoli e Salsomaggiore (Appennino Tosco-Emiliano). Mineralogica et petrographica acta 28, 123–138.

Bordenave, M.L., 1993. Applied Petroleum Geochemistry.

Bortolotti, V., Principi, G., Abbate, E., in press, Note Illustrative della Carta Geologica d'Italia alla scala 1:50.000, foglio 232 "Sestri Levante". Servizio Geologico d'Italia-Regione Liguria.

Botti, F., Aldega, L., Corrado, S., 2003. Tectono-sedimentary burial evolution of the Modena-Bologna Apennines : constraints from combined organic matter, clay mineral and stratigraphic-structural data of thrust-top basins. Atti Ticinensi di Scienze della Terra - Serie Speciale 9, 116–119.

Botti, F., Aldega, L., Corrado, S., 2004. Sedimentary and tectonic burial evolution of the Northern Apennines in the Modena-Bologna area: constraints from combined stratigraphic, structural,

organic matter and clay mineral data of Neogene thrust-top basins. Geodinamica Acta 3, 185–203.

Bousquet, R., Schmid, S.M., Zeilinger, G., Oberhänsli, R., Rosenberg, C., Molli, G., Robert, C., Wiederkehr, M., Rossi, P., 2012. Tectonic Framework of the Alps.

Braun, J., 2002. Quantifying the effect of recent relief changes on age–elevation relationships. Earth and Planetary Science Letters 200, 331–343.

Braun, J., 2003. Pecube: a new finite-element code to solve the 3D heat transport equation including the effects of a time-varying, finite amplitude surface topography. Computers & Geosciences 29, 787–794.

Braun, J., Van der Beek, P., Batt, G., 2006. Quantitative thermochronology. Cambridge University Press.

Bray, R.J., Green, P.F., Duddy, I.R., 1992. Thermal history reconstruction using apatite fission track analysis and vitrinite reflectance: a case study from the UK East Midlands and Southern North Sea. Geological Society, London, Special Publications 67, 3–25.

Brovarone, A.V., Malavieille, J., Beltrando, M., Molli, G., Compagnoni, R., 2011. Field Trip 1 - Geology and petrology of Ocean Continent Transition (OCT) zones metamorphosed under eclogite facies conditions, in: Malavieille, J., Molli, G., Brovarone, A.V., Beyssac, O. (Eds.), CorseAlp 2011 - Field Trip Guidebook. pp. 1–18.

Burchfiel, B., Royden, L., 1985. North-south extension within the convergent Himalayan region. Geology 13, 679–682.

Bustin, R.M., Barnes, M.A., Barnes, W.C., 1990. Determining levels of organic diagenesis in sediments and fossil fuels, in: McIlreath, I.A., Morrow, D.W. (Eds.), Diagenesis. St. John's, Canada, pp. 205–226.

C.N.R., 1980. Sezioni Geologico-Strutturali in scala 1:200.000 attraverso l'Appennino Settentrionale. Progetto Finalizzato Geodinamica - Modello Strutturale - Gruppo Appennino Settentrionale.

Camerlenghi, A., Pini, G.A., 2009. Mud volcanoes, olistostromes and Argille scagliose in the Mediterranean region. Sedimentology 56, 319–365.

Camurri, F., 2000. Assetto stratigrafico strutturale delle unit"a profonde di "'basamento s.l.'"nell'Appennino settentrionle:dalla Val Ceno alla Valle del Reno.

Camurri, F., Argnani, A., Bernini, M., Papani, G., Rogledi, S., Torelli, L., 2001. The basement of the Northern Apennines: Interpretation of reflection seismics and geodynamics implications, in: FIST (Federazione Italaina Di Scienze Della Terra), GEOITALIA 2001 - 31, Forum Di Scienze Della Terra, Chieti, 5-8 Settembre 2001. pp. 50–51.

Capozzi, R., Artoni, A., Torelli, L., Lorenzini, S., Oppo, D., Mussoni, P., Polonia, A., 2012. Neogene to Quaternary tectonics and mud diapirism in the Gulf of Squillace (Crotone-Spartivento Basin, Calabrian Arc, Italy). Marine and Petroleum Geology 35, 219–234.

Carlini, M., Artoni, A., Bernini, M., Vescovi, P., Aldega, L., Balestrieri, M.L., Corrado, S., Torelli, L., in preparation. Uplift and reshaping of far-travelled/allochthonous tectonic units in mountain belts. New insights for the relationships between compression and coeval extension in the western Northern Apennines (Italy). in preparation.

Carlini, M., Clemenzi, L., Artoni, A., Chelli, A., Vescovi, P., Bernini, M., Tellini, C., Torelli, L., Balestrieri, M.L., 2012. Late orogenic thrust-related antiforms in the western portion of Northern Apennines (Parma Province, Italy): geometries and late Miocene to Recent activity constrained by structural, thermochronological and geomorphologic data. Rendiconti online della Società Geologica Italiana 22, 36–39.

Carlson, W.D., 1990. Mechanisms and kinetics of apatite fission-track annealing. American Mineralogist 75, 1120–1139.

Carmignani, L., Giglia, G., Kligfield, R., 1980. Nuovi dati sulla zona di taglio ensialica delle Alpi Apuane. Memorie della Società Geologica Italiana 21, 93–100.

Carmignani, L., Giglia, Gaetano, Kligfield, R., 1978. Structural Evolution of the Apuane Alps: An Example of Continental Margin Deformation in the Northern Apennines, Italy. The Journal of Geology 86, 487–504.

Carmignani, L., Kligfield, R., 1990. Crustal extension in the Northern Apennines: the transition from compression to extension in the Alpi Apuane core complex. Tectonics 9, 1275–1303.

Carr, A.D., Williamson, J.E., 1990. The relationship between aromaticity, vitrinite reflectance and maceral composition of coals: implications for the use of vitrinite reflectance as a maturation parameter. Organic Geochemistry 16, 313–323.

Carslaw, H.S., Jaeger, C.J., 1959. Conduction of Heat in Solids. Clarendon Press, Oxford.

Castellarin, A., Eva, C., Giglia, C., Vai, G.B., 1986. Analisi strutturale del Fronte Appenninico Padano. Giornale di Geologia 47, 47–75.

Catanzariti, R., Cerrina Feroni, A., Marroni, M., Ottria, G., Pandolfi, L., 2003. Ophiolites Debris In The Aveto Unit (Trebbia Valley, Northern Apennines, Italy): A Record Of The Early Oligocene Apenninic Foredeep? Ofioliti 28, 71.

Catanzariti, R., Cerrina Feroni, A., Ottria, G., Levi, N., 2008. The contribution of calcareous nannofossil biostratigraphy for solving geological problems: the example of the Oligocene-Miocene foredeep of the Northern Apennines (Italy), in: Demchuk, T.D., Gary, A.C. (Eds.), Geologic Problem Solving with Microfossils. Society for Sedimentary Geology Special Publication, pp. 309–321.

Cavinato, G.P., De Celles, P.G., 1999. Extensional basins in the tectonically bimodal central Apennines fold-thrust belt , Italy : Response to corner flow above a subducting slab in retrograde motion. Geology 27, 955–958.

Cerrina Feroni, A., Martinelli, P., Plesi, G., Giammattei, L., Franceschelli, M., Leoni, L., 1985. La cristallinità dell'illite nelle argille e calcari (unità di Canetolo) tra La Spezia e l'alta Val Parma (Appennino Settentrionale). Bollettino della Società Geologica Italiana 104, 421–427.

Cerrina Feroni, A., Ottria, G., Vescovi, P., 2002. Note Illustrative della Carta Geologica d'Italia alla scala 1:50.000, foglio 217 "Neviano degli Arduini". Servizio Geologico d'Italia-Regione Emilia Romagna 112.

Cerrina Feroni, A., Plesi, G., Fanelli, G., Leoni, L., Martinelli, P., 1983. Contributo alla conoscenza dei processi metamorfici di grado molto basso (anchimetamorfismo) a carico della falda toscana nell'area del ricoprimento apuano. Bollettino della Società Geologica Italiana 102, 269–280.

Channell, J.E.T., Argenio, B.D., Horváth, F., 1979. Adria, the African Promontory, in Mesozoic Mediterranean Palaeogeography. Earth-Science Reviews 15, 213–292.

Chelli, A., Ruffini, A., Vescovi, P., Tellini, C., in press, Tectonics and large landslides in the Northern Apennines (Italy), in: Springer-Verlag (Ed.), II World Landslide Forum.

Chicchi, S., Plesi, G., 1991. Sedimentary and tectonic lineations as markers of regional deformation: an example from the Oligo-Micene arenaceous flysch of the Northern Apennines. Bollettino della Società Geologica Italiana 110, 601–616.

Corrado, S., Aldega, L., Di Leo, P., Giampaolo, C., Invernizzi, C., Mazzoli, S., Zattin, M., 2005. Thermal maturity of the axial zone of the southern Apennines fold-and-thrust belt (Italy) from multiple organic and inorganic indicators. Terra Nova 17, 56–65.

Corrado, S., Invernizzi, C., Aldega, L., D'Errico, M., Di Leo, P., Mazzoli, S., Zattin, M., 2010. Testing the validity of organic and inorganic thermal indicators in different tectonic settings from continental subduction to collision: the case history of the Calabria-Lucania border (southern Apennines, Italy). Journal of the Geological Society 167, 985–999.

Crespi, J., Chan, Y., Swaim, M., 1996. Synorogenic extension and exhumation of the Taiwan hinterland. Geology 24, 247–250.

Cyr, A.J., Granger, D.E., 2008. Dynamic equilibrium among erosion, river incision, and coastal uplift in the northern and central Apennines, Italy. Geology 36, 103.

Dahlen, F.A., 1990. Critical taper model of fold-and-thrust belts and accretionary wedges. Annual Review of Earth and Planetary Sciences 18, 55–99.

Dahlen, F.A., Suppe, J., Davis, D., 1984. Mechanics of fold-and-thrust belts and accretionary wedges: Cohesive Coulomb Theory. Journal of Geophysical Research 89, 10087.

Dalla Torre, M., Ferreiro Mahlmann, R., Ernst, W.G., 1997. Experimental study on the pressure dependence of vitrinite maturation. Geochimica et Cosmochimica Acta 61, 2921–2928.

Davis, D., Suppe, J., Dahlen, F.A., 1983. Mechanics of fold-and-thrust belts and accretionary wedges. Journal of Geophysical research 88, 1153–1172.

De Graciansky, P.-C., Roberts, D.G., Tricart, P., 2011. The Western Alps, from Rift to Passive Margin to Orogenic Belt.

De Vente, J., Poesen, J., Bazzoffi, P., Rompaey, A. Van, Verstraeten, G., 2006. Predicting catchment sediment yield in Mediterranean environments: the importance of sediment sources and connectivity in Italian drainage basins. Earth Surface Processes and Landforms 31, 1017–1034.

Del Castello, M., Cooke, M.L., 2007. Underthrusting-accretion cycle: work budget as revealed by the boundary element method. Journal of Geophysical research 112, doi:10.1029/2007JB004997.

Della Vedova, B., Lucazeu, F., Pasquale, V., Pellis, G., Verdoya, M., 1995. Heat flow in the tectonic provinces crossed by the southern segment of the European Geotraverse. Tectonophysics 244, 57–74.

Dercourt, J., Zonenshain, L.P., Ricou, L.E., Kazmin, V.G., Le Pichon, X., Knipper, A.L., Grandjacquet, C., Sbortshikov, I.M., Geyssant, J., Lepvrier, C., Pechersky, D.H., Boulin, J., Sibuet, J.C., Savostin, L.A., Sorokhtin, O., Westphal, M., Bazhenov, M.L., Lauer, J.P., Biju-Duval, B., 1986. Geological evolution of the tethys belt from the atlantic to the pamirs since the LIAS. Tectonophysics 123, 241–315.

Dewey, J.F., 1988. Extensional collapse of orogens. Tectonics 7, 1123–1139.

Di Dio, G., Lasagna, S., Martini, A., Zanzucchi, G., 2005. Note Illustrative della Carta Geologica d'Italia alla scala 1:50.000, foglio 199 "Parma Sud". Servizio Geologico d'Italia-Regione Emilia Romagna.

Dodson, M.H., 1973. Closure temperature in cooling geochronological and petrological systems. Contr. Mineral. and Petrol. 40, 259–274.

Doglioni, C., 1991. A proposal of kinematic modelling for W-dipping subductions - Possible applications to the Tyrrhenian - Apennines system. Terra Nova 3/4, 423–434.

Doglioni, C., 1994. Foredeeps versus subduction zones. Geology 22, 271–274.

Doglioni, C., Harabaglia, P., Merlini, S., Mongelli, F., Peccerillo, a, Piromallo, C., 1999. Orogens and slabs vs. their direction of subduction. Earth-Science Reviews 45, 167–208.

Donelick, R.A., Ketcham, R.A., Carlson, W.D., 1999. Variability of apatite fission-track annealing kinetics; II, Crystallographic orientation effects. American Mineralogist 84, 1224–1234.

Donelick, R.A., O'Sullivan, P.B., Ketcham, R.A., 2005. Apatite Fission-Track Analysis. Reviews in Mineralogy and Geochemistry 58, 49–94.

D'Anastasio, E., De Martini, P.M., Selvaggi, G., Pantosti, D., Marchioni, a., Maseroli, R., 2006. Short-term vertical velocity field in the Apennines (Italy) revealed by geodetic levelling data. Tectonophysics 418, 219–234.

Elter, P., Lasagna, S., Marroni, M., Pandolfi, L., Vescovi, P., Zanzucchi, G., 2005. Note Illustrative della Carta Geologica d'Italia alla scala 1:50.000, foglio 215 "Bedonia". Servizio Geologico d'Italia-Regione Emilia Romagna 117.

Elter, P., Marroni, M., 1991. Le Unità Liguri dell'Appennino Settentrionale: sintesi dei dati e nuove interpretazioni. Memorie Descrittive della Carta Geologica d'Italia 44, 121–138.

Elter, P., Schwab, K., 1959. Note illustrative alla carta geologica all'1-50000 dell aregione Carro-Zeri-Pontremoli. Bollettino della Società Geologica Italiana 78, 157–187.

England, P., Molnar, P., 1990. Surface uplift, uplift of rocks, and exhumation of rocks. Geology 18, 1173–1177.

Espitalié, J., Laporte, J.L., Madec, M., Marquis, F., Leplat, P., Paulet, J., Boutefeu, A., 1977. Méthode Rapide de Charactérisation des Roches Mères de leur Potentiel Pétrolier et de leur Degré d'Évolution. Revue de l'Institut Français du Pétrole 32, 23–42.

Eva, E., Ferretti, G., Solarino, S., 2005. Superposition of different stress orientations in the western sector of the northern Apennines (Italy). Journal of Seismology 9, 413–430.

Faccenna, C., Piromallo, C., Crespo-Blanc, A., Jolivet, L., Rossetti, F., 2004. Lateral slab deformation and the origin of the western Mediterranean arcs. Tectonics 23, 1012–1033.

Fellin, M.G., Reiners, P.W., Brandon, M.T., Wu, E., Balestrieri, M.L., Molli, G., 2007. Thermochronologic evidence for the exhumational history of the Alpi Apuane metamorphic core complex , northern Apennines , Italy. Tectonics 26.

Fitzgerald, P.G., Sorkhabi, R.B., Redfield, Thomas, F., Stump, E., 1995. Uplift and denudation of the central Alaska Range: a case study in the use of apatite fission track thermochronology to determine absolute uplift parameters. Journal of Geophysical Research 100, 20175–20191.

Fleischer, R.L., Price, P.B., Walker, R.M., 1975. Nuclear Tracks in Solids - Principles and Applications. University of California Press, Los Angeles.

Fox, M., Herman, F., Willett, S.D., 2012. Inferring exhumation rates in space and time from spatially distributed thermochronological data. in preparation.

Gallagher, K., Brown, R., Johnson, C., 1998. FISSION TRACK ANALYSIS AND ITS APPLICATIONS TO GEOLOGICAL PROBLEMS. Annual Review of Earth and Planetary Sciences 26, 519–572.

Gelati, R., Rogledi, S., Rossi, M., 1987. Significance of the Messinian unconformity-bounded sequences in the Apenninic margin of the Padan foreland basin, northern Italy (preliminary results). Memorie della Società Geologica Italiana 39, 319–323.

Ghibaudo, G., 1980. Deep-Sea fan deposits in the Macigno Formation (middle-upper Oligocene) of the Gordana Valley, Northern Apennines, Italy. Journal of Sedimentary Petrology 50, 723–742.

Giampaolo, C., Lo Mastro, S., 2000. Analisi quantitative delle argille mediante diffrazione a raggi X, in: Fiore, S. (Ed.), Incontri Scientifici, Istituto Di Ricerca Sulle Argille. pp. 109–146.

Gleadow, A.J.W., Brown, R.W., 2000. Fission-track thermochronology and the long-ter denudational response to tectonics, in: Summerfield, M.A. (Ed.), Geomorphology and Global Tectonics. pp. 57–76.

Green, P.F., Duddy, I.R., Gleadow, A.J.W., Tingate, P.R., Laslett, G.M., 1986. Thermal annealing of fission tracks in apatite 1. A qualitative description. Chemical Geology 59, 237–253.

Green, P.F., Duddy, I.R., Hegarty, K.A., 2002. Quantifying exhumation from apatite fission-track analysis and vitrinite reflectance data: precision, accuracy and latest results from the Atlantic margin of NW Europe. In: Doré, A.G., Cartwright, J., Stoker, M.S., Turner, J.P. & White, N. (eds) Exhumation of the North Atlantic Margin: Timing, Mechanisms and Implications for Petroleum Exploration. Geological Society, London, Special Publications 196, 331–354.

Green, P.F., Moore, M.E., O'Brien, C., Crowhurst, P.V., 2003. Thermal History Reconstruction In The Ataa-1 , Gane-1 , Gant-1 , Gro-3 And Umiivik-1 Boreholes , Onshore West Greenland , Based On Afta® , Vitrinite Reflectance And Apatite (U-Th)/He Dating. Geotrack Report 883.

Gvirtzman, Z., Nur, A., 2001. Residual topography, lithospheric structure and sunken slabs in the central Mediterranean. Earth and Planetary Science Letters 187, 117–130.

Handy, M.R., M. Schmid, S., Bousquet, R., Kissling, E., Bernoulli, D., 2010. Reconciling plate-tectonic reconstructions of Alpine Tethys with the geological–geophysical record of spreading and subduction in the Alps. Earth-Science Reviews 102, 121–158.

Hodges, K., Walker, J., 1992. Extension in the Cretaceous Sevier orogen, North American Cordillera. Geological Society of America … 104, 560–569.

Hoffman, J., Hower, J., 1979. Clay mineral assemblages as low grade metamorphic geothermometers: Application to the thrust faulted disturbed belt of Montana. In: Aspects of Diagenesis, P. A. Scholle & P. R. Schluger eds. SEPM Speci, 55–79.

Houseman, G.A., McKenzie, D.P., Molnar, P., 1981. Convective instability of a thickened boundary layer and its relevance for the thermal evolution of continental convergent belts. Journal of Geophysical Research 86, 6115–6132.

Hurford, A.J., 1991. Uplift and cooling pathways derived from fission track analysis and mica dating: a review. Geologische Rundschau 80, 349–368.

Iaccarino, S., Papani, G., 1979. Significance of the Messinian unconformity-bounded sequences in the Apenninic margin of the Padan foreland basin, northern Italy (preliminary results). In: Volume dedicato a S. Venzo 15–46.

ISIDe, W.G., 2013. Italian Seismological Instrumental and parametric database.

Japsen, P., Green, P.F., Chalmers, J. a., 2005. Separation of Palaeogene and Neogene uplift on Nuussuaq, West Greenland. Journal of the Geological Society 162, 299–314.

Jolivet, L., Faccenna, C., Goffé, B., Mattei, M., Rossetti, F., Brunet, C., Storti, F., Funiciello, R., Cadet, J.P., D'Agostino, N., Parra, T., 1998. Midcrustal shear zones in postorogenic extension: example from the northern Tyrrhenian Sea. Journal of Geophysical … 103, 12123–12160.

Katz, B.J., 1983. Limitations of "Rock-Eval" pyrolysis for typing organic matter. Organic Geochemistry 4, 195–199.

Kisch, H.J., 1990. Calibration of the anchizone: a critical comparison of illite "crystallinity" scales used for definition. Journal of Metamorphic Geology 8, 31–46.

Kisch, H.J., 1991. Illite crystallinity: recommendations on sample preparation, X-ray diffraction settings and interlaboratory standards. Journal of Metamorphic Geology 9, 665–670.

Kligfield, R., 1979. The Northern Apennines as a collisional orogen. American Journal of Science 279, 676–691.

Kübler, B., 1967. La cristallinité de l`illite et les zones tout à fait supérieures du métamorphisme. In: Étages tectoniques, Colloque de Neuchâtel 1966, A La Baconniere, Neuchâtel 105–121.

Landuzzi, A., 1994. Relationships between the Marnoso-Arenacea fromation of the inner Romagna units and the Ligurids (Italy). Memorie della Società Geologica Italiana 48, 523–534.

Littke, R., Sachsenhofer, R.F., 1994. Organic Petrology of Deep Sea Sediments: A Compilation of Results from the Ocean Drilling Program and the Deep Sea Drilling Project. Energy & Fuels 8, 1498–1512.

Malavieille, J., 1993. Late orogenic extension in mountain belts: insights from the Basin and Range and the Late Paleozoic Variscan Belt. Tectonics 12, 1115–1130.

Malavieille, J., Molli, G., Ferrandini, M., Ferrandini, J., Spella, M.O., Brovarone, A.V., Beyssac, O., Ciancaleoni, L., 2011. Field Trip 2 - General Architecture and tectonic evolution of Alpine Corsica. Insights from a transect between Bastia and the Balagne region, in: Malavieille, J., Molli, G., Brovarone, A.V., Beyssac, O. (Eds.), CorseAlp 2011 - Field Trip Guidebook. pp. 1–27.

Malinverno, A., Ryan, W.B.F., 1986. Extension in the Tyrrhenian Sea and shortening in the Apennines as result of arc migration driven by sinking of the lithosphere. Tectonics 5, 227–245.

Mancin, N., Martelli, L., Barbieri, C., 2006. Foraminiferal Biostratigraphic and Paleobathymetric constraints in Geohistory analysis : the example of the Epiligurian succession of the Secchia

Valley (Northern Apennines, Mid Eocene-Late Miocene). Bollettino della Società Geologica Italiana 125, 163–186.

Mancktelow, N.S., Grasemann, B., 1997. Time-dependent effects of heat advection and topography on cooling histories during erosion. Tectonophysics 1, 167–195.

Marroni, M., Molli, G., Ottria, G., Pandolfi, L., 2001. Tectono-sedimentary evolution of the External Liguride units (Northern Apennines, Italy): insights in the pre-collisional history of a fossil ocean-continent transition. Geodinamica Acta 14, 307–320.

Marshak, S., 2001. Earth 2001, Portrait of a Planet.

Martini, A., Zanzucchi, G., 2000. Note Illustrative della Carta Geologica d'Italia alla scala 1:50.000, foglio 198 "Bardi". Servizio Geologico d'Italia-Regione Emilia Romagna 102.

Mazzoli, S., D'Errico, M., Aldega, L., Corrado, S., Invernizzi, C., Shiner, P., Zattin, M., 2008. Tectonic burial and "young" (<10 Ma) exhumation in the southern Apennines fold-and-thrust belt (Italy). Geology 36, 243.

Merriman, R.J., Frey, M., 1999. Patterns of very low grade metamorphism in metapelitic rocks. In: Frey M. & Robinson D. (eds.), Low-grade metamorphism, Blackwell Science 61–107.

Merriman, R.J., Kemp, S.J., 1996. Clay minerals and sedimentary basin maturity. Mineralogical Society Bulletin 111, 7–8.

Michard, A., Chalouan, A., Feinberg, H., Goffé, B., Montigny, R., 2002. How does the Alpine belt end between Spain and Morocco ? Bullettin de la Societé Géologique de France 173, 3–15.

Molli, G., 2008. Northern Apennine-Corsica orogenic system: an updated overview. Geological Society, London, Special Publications 298, 413–442.

Molli, G., Crispini, L., Mosca, P., Piana, F., Federico, L., 2010. Geology of the Western Alps-Northern Apennine junction area: a regional review. Journal of the Virtual Explorer 36.

Molnar, P., England, P., Martinod, J., 1993. Mantle dynamics, uplift of the Tibetan Plateau, and the Indian monsoon. Reviews of Geophysics 31, 357–396.

Montanari, L., Rossi, M., 1982. Evoluzione delle unita'stratigrafico-strutturali terziarie del nordappennino; 1. L'unita'di Canetolo. Bollettino della Società … 101, 275–289.

Mutti, E., Papani, G., Di Biase, D., Davoli, G., Mora, S., Segadelli, S., Tinterri, R., 1995. Il bacino terziario epimesoalpino e le sue implicazioni sui rapporti su Alpi ed Appennino. Memorie di Scienze Geologiche dell'Università di Padova 47, 217–244.

Mutti, E., Ricci Lucchi, F., Roveri, M., 2002. Revisiting turbidites of the Marnoso-arenacea Formation and their basin-margin equivalents: problems with classic models.

Naeser, C.W., 1979. Thermal History of Sedimentary Basins: fission-track dating of subsurface rocks, in: Scholle, P.A., Schluger, P.R. (Eds.), Aspects of Diagenesis. Society of Economic Paleontologists and Mineralogists, Tulsa, Oklahoma, pp. 109–112.

Panini, F., Bettelli, G., Pizziolo, M., 2002. Note Illustrative della Carta Geologica d'Italia alla scala 1:50.000, foglio 237 "Sasso Marconi". Servizio Geologico d'Italia-Regione Emilia Romagna 176.

Papani, G., Tellini, C., Torelli, L., Vernia, L., Iaccarino, S., 1987. Nuovi dati stratigrafici e strutturali sulla formazione di Bismantova nella "sinclinale" Vetto-Carpineti (Appennino Reggiano-Parmense). Memorie della Società Geologica Italiana 39, 245–275.

Pasquale, V., Chiozzi, P., Verdoya, M., Gola, G., 2012. Heat flow in the Western Po Basin and the surrounding orogenic belts. Geophysical Journal International 190, 8–22.

Pini, G.A., 1999. Tectonosomes and olistostromes in the Argille Scagliose of the Northern Apennines, Italy. Geological Society of America, Special Paper 335, 73 pp.

Pini, G.A., Lucente, C.C., Cowan, D.S., De Libero, C.M., Dellisanti, F., Landuzzi, A., Negri, A., Tateo, F., Del Castello, M., Morrone, M., Cantelli, L., 2004. The role of olistostromes and argille scagliose in the structural evolution of the Northern Apennines. Memorie Descrittive della Carta Geologica d'Italia 63.

Platt, J.P., 1986. Dynamics of orogenic wedges and the uplift of high-pressure metamorphic rocks. Geological Society of America Bulletin 97, 1037–1053.

Platt, J.P., Vissers, R.L.M., 1989. Extensional collapse of thickened continental lithosphere: A working hypothesis for the Alboran Sea and Gibraltar arc. Geology 17, 540–543.

Plesi, G., 1975. La nappe de Canetolo. Bulettin de la Societé Géologique de France 6, 979–983.

Plesi, G., 2002. Note Illustrative della Carta Geologica d'Italia alla scala 1:50.000, foglio 235 "Pievepelago". Servizio Geologico d'Italia-Regione Emilia Romagna 138.

Pollastro, R.M., 1990. The illite/smectite geothermometer-Concepts, methodology, and application to basin history and hydrocarbon generation. In Applications of Thermal Maturity Studies to Energy Exploration. V. F. Nuccio and C. E. Barker eds. 1–18.

Principi, G., Treves, B., 1984. Il sistema Corso-Appenninico come prisma d'accrezione. Riflessi sul problema generale del limite Alpi-Appennini. Memorie della Società Geologica Italiana1 28, 549–576.

Provincia di Parma, 2007, Carta Provinciale del Dissesto Idrogeologico.

Puccinelli, A., D'Amato Avanzi, G., Perilli, N., in press, Note Illustrative della Carta Geologica d'Italia alla scala 1:50.000, foglio 233 "Pontremoli". Servizio Geologico d'Italia-Regione Toscana.

Puccinelli, A., D'Amato Avanzi, G., Perilli, N., in press, Note Illustrative della Carta Geologica d'Italia alla scala 1:50.000, foglio 234 "Fivizzano". Servizio Geologico d'Italia-Regione Toscana.

Ratschbacher, L., Frisch, W., Neubauer, F., Schmid, S.M., Neugebauer, J., 1989. Extension in compressional orogenic belts : The eastern Alps. Geology 17, 404–407.

Ravenhurst, C.E., Donelick, R.A., 1992. Fission track thermochronology, in: Zentilli, M., Reynolds, P.H. (Eds.), Short Course Handbook on Low Temperature Geochronology. Mineralogical Association of Canada, Wolfville, Nova Scotia, Canada, pp. 21–42.

Remitti, F., Bettelli, G., Panini, F., Carlini, M., Vannucchi, P., 2012. Deformation, fluid flow, and mass transfer in the forearc of convergent margins: A two-day field trip in an ancient and exhumed erosive convergent margin in the Northern Apennines. GSA Field Guides 28, 1–33.

Remitti, F., Bettelli, G., Vannucchi, P., 2007. Internal structure and tectonic evolution of an underthrust tectonic melange: the Sestola-Vidiciatico tectonic unit of the Northern Apennines, Italy. Geodinamica Acta 20, 37–51.

Remitti, F., Vannucchi, P., Bettelli, G., Fantoni, L., Panini, F., Vescovi, P., 2011. Tectonic and sedimentary evolution of the frontal part of an ancient subduction complex at the transition from accretion to erosion: The case of the Ligurian wedge of the northern Apennines, Italy. Geological Society of America Bulletin 123, 51–70.

Reutter, K.J., Heinitz, I., Ensslin, R., 1991. Structural and geothermal evolution of the Modino-Cervarola Unit. Memorie Descrittive della Carta Geologica d'Italia 46, 257–266.

Reutter, K.J., Teichmüller, M., Teichmüller, R., Zanzucchi, G., 1980. Le Ricerche Sulla Carbonificazione Dei Frustoli Vegetali Nelle Rocce Clastiche, Come Contributo Ai Problemi Di Paleogeotermia E Tettonica Nell'Appennino Settentrionale. Memorie della Società Geologica Italiana 21, 111–126.

Reutter, K.J., Teichmüller, M., Teichmüller, R., Zanzucchi, G., 1983. The Coalification Pattern In The Northern Apennines And Its Palaeogeothermic And Tectonic Significance. International Journal of Earth Sciences (Geologische Rundschau) 72, 861–894.

Ricci Lucchi, F., 1986. Semiallochthonous sedimentation in Northern Apennines. Memorie della Società Geologica Italiana 31, 119–121.

Ricci Lucchi, F., Colalongo, M.L., Cremonini, G., Gasperi, G., Iaccarino, S., Papani, G., Raffi, S., Rio, D., 1982. Evoluzione sedimentaria e paleogeografica nel margine appenninico. In: Cremonini G, Ricci Lucchi F (eds) Guida alla geologia del margine appenninico-padano. Soc. Geol. It. 17–46.

Rizzini, F., 2007. Il sistema d'avanfossa dell'Appennino Settentrionale durante la crisi di salinità del Messiniano: vincoli tettonostratigrafici per una ricostruzione paleogeografica.

Roca, E., Bessereau, G., Jawor, E., Kotarba, M., Roure, F., 1995. Pre-Neogene evolution of the Western Carpathians: constraints from the Bochnia-Tatra Mountains section (Polish Western Carpathians). Tectonics 14.

Rodgers, J., 1997. Exotic nappes in external parts of orogenic belts. American Journal of Science 297, 174–219.

Rosenbaum, G., Lister, G.S., 2004. Neogene and Quaternary rollback evolution of the Tyrrhenian Sea, the Apennines, and the Sicilian Maghrebides. Tectonics 23.

Roveri, M., Bassetti, M., Ricci Lucchi, F., 2001. The Mediterranean salinity crisis: an Apennine foredeep perspective. Sedimentary Geology 140, 201–214.

Royden, L., 1993a. Evolution of retreating subduction boundaries formed during continental collision. Tectonics1 12, 629–638.

Royden, L., 1993b. The tectonic expression slab pull at continental convergent boundaries. Tectonics 12, 303–325.

Royden, L., Patacca, E., Scandone, P., 1987. Segmentation and configuration of subducted lithosphere in Italy: an important control on thrust-belt and foredeep-basin evolution. Geology 15, 714–717.

Ryan, W.B.F., Carbotte, S.M., Coplan, J.O., O'Hara, S., Melkonian, A., Arko, R., Weissel, R.A., Ferrini, V., Goodwillie, A., Nitsche, F., Bonczkowski, J., Zemsky, R., 2009. Global Multi-Resolution Topography synthesis. Geochemistry, Geophysics, Geosystems 10, doi:10.1029/2008GC002332.

Sambridge, M., 1999a. Geophysical inversion with a neighbourhood algorithm-I. Searching a parameter space. Geophysical Journal International 138, 479–494.

Sambridge, M., 1999b. Geophysical inversion with a neighbourhood algorithm-II . Appraising the ensemble. Geophysical Journal International.

Scrocca, D., Carminati, E., Doglioni, C., Marcantoni, D., 2007. Slab retreat and active shortening along the Central-Northern Apennines, in: Lacombe, O., Roure, F., Lavé, J., Vergés, J. (Eds.), Thrust Belts and Foreland Basins. Springer Berlin Heidelberg, pp. 471–478.

Simoni, A., Elmi, C., Picotti, V., 2003. Late Quaternary uplift and valley evolution in the Northern Apennines. Quaternary International 101-102, 253–267.

Stüwe, K., White, L., Brown, R., 1994. The influence of eroding topography on steady-state isotherms. Application to fission track analysis. Earth and Planetary Science Letters 124, 63–74.

Tagami, T., Galbraith, R.F., Yamada, R., Laslett, G.M., 1999. Revised annealing kinetics of fission tracks in zircon and geological implications, in: Van den Haute, P., De Corte, F. (Eds.), Advances in Fission-Track Geochronology. Kluwer Academic Publishers, pp. 99–112.

Teichmüller, M., 1987. Organic material and very low grade metamorphism. In: Low temperature Metamorphism (ed. M. Frey) 114–161.

Tellini, C., Chelli, A., 2003. Ancient and recent landslide occurrences in the Emilia Apennines (Northern Apennines, Italy), in: Castaldini, D., Gentili, B., Materazzi, M., Pambianchi, G. (Eds.), Workshop on "Geomorphological Sensitivity and System Response". Camerino.

Thomson, S.N., Brandon, M.T., Reiners, P.W., Zattin, M., Isaacson, P.J., Balestrieri, M.L., 2010. Thermochronologic evidence for orogen-parallel variability in wedge kinematics during extending convergent orogenesis of the northern Apennines, Italy. Geological Society of America Bulletin 122, 1160–1179.

Valloni, R., 1978. Provenienza e storia post-deposizionale del Macigno di Pontremoli (Massa). Bollettino della Società Geologica Italiana 97, 317–326.

Van der Meulen, M.., Kouwenhoven, T.., Van der Zwaan, G.., Meulenkamp, J.., Wortel, M.J.., 1999. Late Miocene uplift in the Romagnan Apennines and the detachment of subducted lithosphere. Tectonophysics 315, 319–335.

Vannoli, P., Basili, R., Valensise, G., 2004. New geomorphic evidence for anticlinal growth driven by blind-thrust faulting along the northern Marche coastal belt (central Italy). Journal of Seismology 8, 297–312.

Vannucchi, P., Bettelli, G., 2002. Mechanisms of subduction accretion as implied from the broken formations in the Apennines, Italy. Geology 30, 835.

Vannucchi, P., Remitti, F., Bettelli, G., 2008. Geological record of fluid flow and seismogenesis along an erosive subducting plate boundary. Nature 451, 699–703.

Vannucchi, P., Remitti, F., Bettelli, G., 2012. Lateral variability of the erosive plate boundary in the Northern Apennines, Italy. Italian Journal of … 131, 215–227.

Ventura, B., Pini, G., Zuffa, G., 2001. Thermal history and exhumation of the northern Apennines (Italy): evidence from combined apatite fission track and vitrinite reflectance data from foreland basin sediments. Basin Research 13, 435–448.

Venturelli, G; Frey, M., 1977. Anchizone Metamorphism In Sedimentary Sequences Of The Northern Apennines. Rendiconti della Società Italiana di Mineralogia e Petrologia.

Vescovi, P., 1988. L'assetto strutturale del Flysch di M. Caio nella zona del Passo della Cisa e in alta Val Baganza (Prov. di Parma). Rendiconti della Società Italiana 11, 313–316.

Vescovi, P., 1991. L'assetto strutturale delle Arenarie di M.Gottero tra Borgo Val di Taro e Pontremoli (Provv. di Parma e Massa). Memorie Descrittive della Carta Geologica d'Italia 46, 341–354.

Vescovi, P., 1998. Le Unità Subliguri dell'alta Val Parma (Provincia di Parma). Atti Ticinensi di Scienze della Terra 40, 215–231.

Vescovi, P., 2002. Note Illustrative della Carta Geologica d'Italia alla scala 1:50.000, foglio 216 "Borgo Val Di Taro". Servizio Geologico d'Italia-Regione Emilia Romagna 116.

Vissers, R.L.M., Drury, M.R., Hoogerduijn Strating, E.H., Spiers, C.J., Van der Wal, D., 1995. Mantle shear zones and their effect on lithosphere strength during continental breakup. Tectonophysics 249, 155–171.

Wagner, G.A., 1979. Correction and Interpretation of fission track ages, in: Jäger, E., Hunziker, J.C. (Eds.), Lectures in Isotope Geology. Springer-Verlag, Berlin, pp. 170–177.

Wagner, G.A., Van den Haute, P., 1992. Fission Track Dating. Elsevier, Amsterdam.

Wakeham, S.G., Lee, C., 1993. Production, transport, and alteration of particulate organic matter in the marine water column. In: Organic Geochemistry. Engel, M.H. and Macko, S.A. (eds). Plenum Press 145–169.

Waschbusch, P., Beaumont, C., 1996. Effect of a retreating subduction zone on deformation in simple regions of plate convergence. Journal of Geophysical Research 101, 28133–28148.

Willett, S.D., 1999. Rheological dependence of extension in wedge models of convergent orogens. Tectonophysics 305, 419–435.

Willett, S.D., Brandon, M.T., 2002. On steady states in mountain belts. Geology 30, 175.

Wortel, M.J.R., Spakman, W., 2000. Subduction and slab detachment in the Mediterranean-Carpathian region. Science 290, 1910–1918.

Zattin, M., Landuzzi, A., Picotti, V., Zuffa, G.G., 2000. Discriminating between tectonic and sedimentary burial in a foredeep succession , Northern Apennines. Journal of the Geological Society 157, 629–633.

Zattin, M., Picotti, V., Zuffa, G.G., 2002. Fission-track reconstruction of the front of the Northern Apennine thrust wedge and overlying Ligurian Unit. American Journal of Science 302.

Acknowledgments

A very special thanks goes to Andrea Artoni, who gave me the chance to walk this path and who has been a continuous source of help, incitement and comparison. A special thanks goes also to Paolo Vescovi, Massimo Bernini, Giuseppe Bettelli, Francesca Remitti and Paola Vannucchi, who greatly helped me and sustained me during these three years.

I would like to thank also Maria Laura Balestrieri, Sveva Corrado and Luca Aldega, who did the analyses of our data and with whom I shared many moments of confrontation and discussion.

I thank very much also Luigi Torelli, for the kindness and the experienced shared with us, Luca Clemenzi and Fabrizio Storti.

Finally, last but not least, I would like to especially thank my love and my family, who endlessly sustained me and gave me everything.